Cerebral white matter injury in small vessel and Alzheimer's disease

Naomi Vlegels

ISBN:	978-94-6483-272-3
Cover design:	Publiss | www.publiss.nl
Lay-out:	Publiss | www.publiss.nl
Print:	Ridderprint | www.ridderprint.nl

Financial support by the Dutch Heart Foundation and Alzheimer Nederland (Amersfoort) for the publication of this thesis is gratefully acknowledged.

Cerebral white matter injury in small vessel and Alzheimer's disease

Cerebrale witte stof schade in ziektes van de kleine hersenbloedvaten en de ziekte van Alzheimer
(met een samenvatting in het Nederlands)

Proefschrift

ter verkrijging van de graad van doctor aan de
Universiteit Utrecht
op gezag van de
rector magnificus, prof.dr. H.R.B.M. Kummeling,
ingevolge het besluit van het college voor promoties
in het openbaar te verdedigen op

dinsdag 10 oktober 2023 des middags te 12.15 uur

door

Naomi Vlegels

geboren op 19 juli 1993
te Haarlem

Promotor:	Prof. dr. G.J. Biessels
Copromotor:	Dr. Y.D. Reijmer
Beoordelingscommissie:	Prof. dr. J. Hendrikse (voorzitter)
	Prof. dr. H.E. Hulshoff Pol
	Prof. dr. M.J.P. van Osch
	Prof. dr. J.H. Veldink
	Prof. dr. M.J.E. van Zandvoort

Hold fast to dreams
For if dreams die
Life is a broken-winged bird
That cannot fly.

Hold fast to dreams
For when dreams go
Life is a barren field
Frozen with snow.

Langston Hughes

TABLE OF CONTENTS

Chapter 1	General Introduction	07
Chapter 2	Small vessel disease more than Alzheimer's Disease determines diffusion alterations in memory clinic patients	20
Chapter 3	The relation between small vessel function and white matter integrity in monogenic and sporadic small vessel disease - the ZOOM@SVDs study	62
Chapter 4	Does loss of integrity of the Cingulum bundle link Amyloid Beta accumulation and neurodegeneration in Alzheimer's Disease	82
Chapter 5	The cumulative effect of small vessel disease lesions is reflected in structural brain networks of memory clinic patients	106
Chapter 6	Brain network disruption and cognitive decline: relevance of critical white matter connections	124
Chapter 7	Both Alzheimer's Disease and vascular pathologies affect critical and non-critical white matter connections equally.	144
Chapter 8	General discussion	172
Appendices	Nederlandse samenvatting	192
	About the author	198
	List of publications	200
	Dankwoord	202

CHAPTER 1

General introduction

GENERAL INTRODUCTION

Alzheimer's disease (AD) and small vessel disease (SVD) are the most common causes of ageing-related cognitive impairment and dementia.[1] Both conditions entail a cascade of disease processes leading to cerebral tissue injury and functional deficits. In order to better understand these cascades of events there is a need for sensitive brain injury markers, both for AD and SVD. Recent studies have suggested that measures of white matter integrity derived from diffusion MRI could be an injury marker relevant to both conditions.[2–5]

AD is characterized by the accumulation of amyloid beta (Aβ), aggregation of tau into neurofibrillary tangles and neurodegeneration.[6] Within the AD field there are multiple widely used disease markers for these interrelated processes, well known examples of which are CSF and PET-based levels of Aβ and tau. With regards to neurodegeneration, MRI markers such as atrophy are widely used but they mostly focus on cortical injury. In general, there has been a lack of attention for white matter injury in AD, although there are clear indications that the white matter is affected as well. Studies have shown a loss of subcortical white matter volume [7,8] and there were indications from diffusion MRI studies that the white matter microstructure is affected.[4,5] Yet, when I started this research in 2017, there were still many interesting open questions regarding diffusion-based MRI markers of white matter injury in AD, for example: is there an AD specific diffusion signature of white matter injury? Are there AD specific white matter injury patterns? To what extent does white matter injury explain cognitive deficits?

In contrast to AD, research on SVD has always been particularly interested in subcortical brain regions including the white matter, because both autopsy studies and brain imaging show that this is the place where SVD related injury can most readily be observed.[9–11] SVD primarily affects the microvasculature of the brain and here causes a loss of smooth muscle cells, luminal narrowing in the arterioles and thickening of the vessel walls.[12] These processes in turn lead to progressive tissue injury. SVD-related tissue injury can be visualized on MRI in the form of white matter hyperintensities (WMH), lacunes and cerebral microbleeds.[9] These lesion markers indicate the presence of SVD within the brain and have been shown to relate to clinical outcomes such as cognition. However, this relation to cognition is generally quite weak, in terms of inter-individual explained variance.[13,14]

Furthermore, we know that the damage caused by SVD is more extensive than captured by these MRI visible lesions. Diffusion MRI can capture both the visible and invisible damage within the white matter. Notably, measures of diffusion MRI have been shown to relate to cognition more strongly than lesion markers.[15] Yet there are remaining open question about different aspects of the diffusion signal in SVD, for example: can we differentiate SVD from other pathologies, in particular AD, based on the diffusion signal? Does SVD lead to specific injury patterns of the white matter? Which diffusion alterations best explain cognitive deficits in SVD?

Another factor which is often not sufficiently addressed in AD as well as in SVD research, is that these conditions commonly co-occur in the elderly, so-called mixed disease. In neuropathological studies up to 75% of patients show evidence of both pathologies.[16,17] This also generates questions with regard to diffusion MRI in AD and SVD, for example: what is the contribution of both diseases to diffusion alterations? How specific are previous findings from memory clinic cohorts that may have included mixed pathologies?

In this thesis I will zoom into some of these unknowns on diffusion MRI in AD and SVD. The overarching aim of the work described in this thesis is:

To study the microstructural integrity of the white matter in AD and SVD to get a better understanding of brain tissue injury and cognitive decline in these conditions.

We addressed three specific objectives:

1. To study microstructural white matter injury in pure and mixed forms of AD and SVD, also in relation with disease markers.
2. To evaluate spatial patterns of white matter injury in AD and SVD
3. To assess if white matter injury helps to explain the cognitive impact of AD and SVD.

In this introduction I will first shortly introduce diffusion MRI before briefly reviewing previous work on diffusion MRI in AD and SVD and show which questions will be addressed in the chapters of this thesis.

Background of Diffusion MRI

The human brain can be roughly divided into two tissue types: (1) grey matter which consists of all neuronal cell bodies and makes up the cortex and (2) white matter which consists of all myelinated axons that form the communicating fibers between the different grey matter brain regions. Diffusion MRI, a technique that emerged in the mid-1980's, makes it possible to examine these white matter fibers in-vivo[18,19] Diffusion MRI quantifies the diffusion (i.e., movement) of water molecules [20] and can thereby indirectly measure the integrity of the cerebral white matter. In short, this works via the following principles: If water is free to diffuse, such as in a glass of water or within the ventricles of the brain, water molecules will displace freely and randomly and thus have a high extent of diffusion without a preferred direction (Figure 1A).[20]

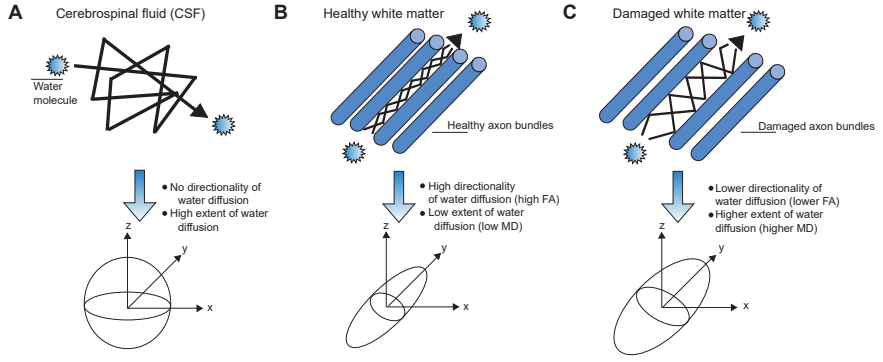

Figure 1. Simplified graphic of diffusion in different situations. The top part of each panel shows the movement of a water molecule. The bottom part of each panel shows how this translates into extent of diffusion and directionality of diffusion. **A)** depicts random diffusion as it would be in a glass of water. The water molecule can diffuse freely without any barriers. This translates in a high extent of diffusion and no preferred direction. **B)** depicts restricted diffusion in healthy white matter tissue. The water molecule is restricted by the axons and will diffuse along the axonal bundle, which leads to a low extent of diffusion and high directionality. **C)** depicts restricted diffusion in damaged white matter tissue. The loss of integrity leads to more space for diffusion which translates into a lower directionality and a higher extent of diffusion as compared to panel B.

Within brain tissue, the diffusion of water molecules is constrained by barriers such as cell membranes. As a result, the displacement of water molecules will be no longer random and there will be a lower extent of diffusion (Figure 1B). The extent of diffusion can be quantified in a measure called Mean Diffusivity (MD).

Next to having a lower extent of diffusion in brain tissue, water molecules will also diffuse in a preferred direction because of the barriers of the tissue. If we look at white matter tissue, diffusion more easily follows the axonal bundles and myelin sheets and their preferred direction will thus be along the direction of the bundles. This preferred direction of diffusion can be measured for each voxel within the brain and can be quantified with fractional anisotropy (FA). By piecing together the estimation of direction of diffusion from each voxel, we can reconstruct the main bundles of axons – which is called tractography. To put it simply, we can reconstruct these bundles of axons for the whole brain with this technique, which is called whole brain tractography. By combining whole brain tractography with a set of brain regions, we can establish which white matter tracts (edges) connect which brain regions (nodes) (Figure 2). This combination of information allows us to reconstruct an individual's structural brain network. This network has a certain organization, of which properties can be quantified with measures based on so called "graph theory".[21] An example of such a measure is "global network efficiency", which reflects the ability to exchange information between brain regions.[21] Furthermore we can define characteristics of the connections such as which connections are most frequently used (critical connections) and characteristics of regions such as which regions connect most regions to each other (hub regions).[22,23]

In case of brain injury, these different measures derived from diffusion MRI can provide important information on damaged white matter tissue. In damaged tissue we typically observe an increase of the extent of diffusion, i.e., an increase in MD, because cell barriers are damaged, and a loss of directionality of diffusion, i.e., decrease in FA, because the tubular structure of the white matter deteriorates (Figure 1C). Such alterations of the diffusion signal are thus assumed to reflect loss of integrity of the white matter. White matter MD and FA can be measured on a whole brain level, which is why tractography is valuable as it allows for the assessment of the integrity of specific bundles individually. Thereby we get a more local assessment of the state of the white matter. Changes in network measures provide further complementary information as they give us the opportunity to assess how network topology is related to for example information processing.

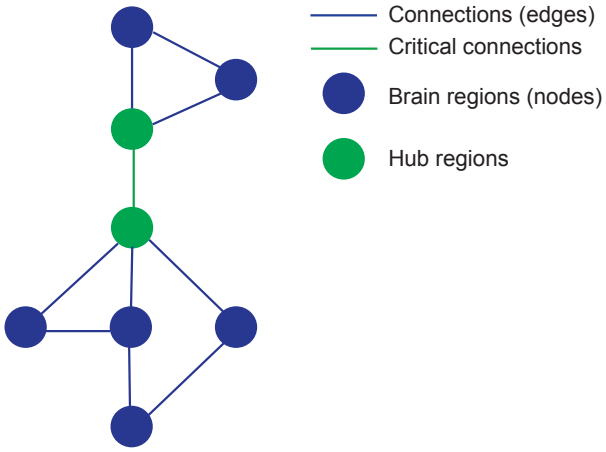

Figure 2. Simplified graphic of a network. The circles represent brain regions and the lines between them represent white matter connections. In this example, the green circles process all communication between the upper and lower part of the network, making them hub regions. The green line is a critical connection, as this connection forms a bridge between the upper and lower part of the network. Without this connection, the two parts of the network would be disconnected.

Diffusion MRI in AD

On post-mortem examination of brains from patients with AD, loss of myelin, axonal degeneration and gliosis have been shown in the white matter.[24] These changes cannot be fully accounted for as processes secondary to cortical degeneration.[24,25] This caught the curiosity of neuroscientists like myself. Diffusion MRI offers an interesting opportunity to further explore white matter changes in AD in vivo. When I started my research in 2017, emerging studies showed diffusion alterations in the white matter of patients with AD. More specifically they reported an increase in the extent of diffusion (i.e., higher MD) and a decrease in directionality of diffusion (i.e., lower FA). It was quickly realized that these injury markers could be of value in tracking disease and to better predict cognitive performance and possibly even be a relevant marker of neurodegeneration. [6]Yet, one of the open questions was whether these injury markers were specific for the AD disease process. Disease specific markers are important for diagnostic purposes and can have potential as an outcome marker in clinical trials. One challenge in answering if diffusion alterations are specific for AD is the frequent co-occurrence of AD and SVD in elderly making it difficult to distinguish any disease specific effects. A systematic study, taking mixed disease into account, was missing.

Questions addressed in this thesis

In the work described in my thesis we tried to disentangle the effects of AD and SVD on diffusion alterations by studying these conditions in pure and in mixed forms. In **chapter 2**, for example, we assessed six cohorts ranging from "pure" genetic AD to "pure" genetic SVD and mixed disease cohorts. We verified the assumption that AD and SVD would have distinct diffusion signatures, that was at that time emerging in the field. It was assumed that these distinct signatures could be detected using a more complex model of the diffusion signal: the free water model which compartmentalizes the diffusion signal into a free water and a restricted diffusion compartment.[26] The hypothesis was that alterations in the free water compartment would be a signature for SVD.[15] while alterations in the restricted compartment would be a signature for AD.[27,28]

My attention was also captured by questions of the effect of AD on white matter tracts and how these changes may affect brain networks. Knowing if tracts are affected in a certain pattern could help us better identify AD as well as provide insights into the disease mechanisms at play. Furthermore, differences in injury patterns of the white matter might help explain the disparity in severity of impairments between patients. When I started this research, emerging tractography studies hinted towards such patterns in white matter tracts injury.[29,30] Especially in later disease stages, major tracts such as the forceps minor and major, the inferior fronto-occipital fasciculus and the posterior cingulum have shown alterations.[31] Yet, there were some open questions. For example, how are white matter tracts affected in earlier stages of the disease? Could it possibly be an early disease marker? Furthermore, it has been hypothesized within the field that tracts are not only essential to transmit information from neurons, but might also form a conduit through which disease processes spread. In **chapter 4** we have assessed this hypothesis in two independent samples of memory clinic patients by assessing if tract integrity was linked to Aβ deposition and neurodegeneration.

The structural brain network has been shown to be disrupted in earlier studies in AD.[5] This can be interpreted as a decrease in overall organization of the network, which might make it less efficient in information processing. This provides some hints as to why for example higher-order cognitive functions are affected. However, as the brain network is a complex construct there were some incompletely tested hypotheses and open questions. One such hypothesis was that hub regions and

critical connections would be more vulnerable to disease in AD than other regions because they consume more energy, which comes at a higher biological cost.[32,33] I was curious if this was the case and therefore tested if critical connections were disproportionally affected by disease first in a pilot study in **chapter 6** and then systematically in **chapter 7.** We explored this both in pure and mixed forms of AD and SVD. As part of the pilot study in **chapter 6** we also examined if damage to critical connections had a disproportional effect on cognition.

Diffusion MRI in SVD

From ex-vivo histopathological studies, it was long known that white matter injury was a part of SVD [10] and MRI made it possible to visualize this injury in-vivo.[9,11] Especially the characteristics of diffusion MRI provide a great opportunity to study the white matter in SVD. For example, to study subtle effects on the white matter and to better understand the injury that is caused by SVD and leading to cognitive impairment.

When I started my research in 2017, it was becoming clear from rapidly emerging diffusion MRI studies that white matter integrity was affected in patients with SVD well beyond the visible lesions on conventional MRI. It became apparent that the so-called normal appearing white matter showed a loss of integrity as well.[2] This sensitivity to subtle alterations to white matter integrity in SVD is an important feature as it could help in improving diagnostics. Moreover, with earlier detection of the disease there might be at least two benefits for patients: 1) a better explanation for the cognitive complaints they may experience and/or 2) identification of people who might benefit most from future treatment.

Questions addressed in this thesis

While diffusion MRI markers showed great potential, there were some unknowns. One of which is that, as in AD, it was unclear whether there was a signature in diffusion alterations that could differentiate between AD and SVD pathology, which would be important for diagnosis. As mentioned before, a challenging factor in this is mixed disease. We therefore assessed and compared the contribution of both AD and SVD to diffusion alterations in **chapter 2** by studying six cohorts of both pure and mixed forms of the disease.

Another challenge in SVD research was the in-vivo imaging of the small vessels themselves. These vessels have diameters well below a millimetre. Until recently the resolution of MRI scanners was not good enough to image them. Conventional MRI markers of SVD are in reality only injury markers, reflecting downstream consequences of the disease, meaning that while they did give us information about the presence of the disease, these markers can only indirectly inform us about the mechanisms at the level of the small vessels. Recently, with the rise of high-resolution imaging on 7T-MRI, it became possible to image the function of the small vessels.[34] This gave us the possibility to better understand how small vessel dysfunction and white matter injury are related to each other in patients with SVD, which is what we have assessed in **chapter 3.**

By causing diffuse white matter injury, SVD is essentially considered to be a disconnection syndrome, meaning that it is thought that cognitive impairment is caused by white matter tract disruption.[35] These tract disruptions affect the structural brain network and both can be measured using diffusion MRI. At the start of my research, there were clear indications that the structural brain network was indeed affected in SVD [36–38] and that these alterations in the network were also related to cognitive impairment. Furthermore, network measures were indicated to outperform individual SVD markers in association to cognition.[2] This is important as cognition is, unfortunately, only weakly related to SVD markers and a better prediction of cognition is needed. Me and my colleagues hypothesized that one reason for the strong association between network efficiency and cognition is probably the sensitivity of network efficiency to the cumulative effect of multiple SVD-related injury on brain connectivity. In **chapter 5** we have assessed the burden of SVD, rather than individual markers, [39–41] in association to the network and cognition to assess if network measures are indeed sensitive to the cumulative effects of disease burden.

Another open question at the start of my research was whether critical connections might be more vulnerable to SVD than non-critical connections, just like in AD. We therefore studied the impact of SVD on these connections in **chapter 7**. With the hypothesis that cognitive deficits in SVD reflect a disconnection syndrome, damage to these same critical connections might have a bigger impact on cognition than others which is what we assess in **chapter 6.**

REFERENCES

1. O'Brien JT, Thomas A. Vascular dementia. *The Lancet* 2015; 386: 1698–1706.
2. Baykara E, Gesierich B, Adam R, et al. A Novel Imaging Marker for Small Vessel Disease Based on Skeletonization of White Matter Tracts and Diffusion Histograms. *Ann Neurol* 2016; 80: 581–592.
3. Pasi M, Van Uden IWM, Tuladhar AM, et al. White Matter Microstructural Damage on Diffusion Tensor Imaging in Cerebral Small Vessel Disease: Clinical Consequences. *Stroke* 2016; 47: 1679–1684.
4. Amlien IK, Fjell AM. Diffusion tensor imaging of white matter degeneration in Alzheimer's disease and mild cognitive impairment. *Neuroscience* 2014; 276: 206–215.
5. Reijmer YD, Leemans A, Caeyenberghs K, et al. Disruption of cerebral networks and cognitive impairment in Alzheimer disease. *Neurology* 2013; 80: 1370–1377.
6. Jack CR, Bennett DA, Blennow K, et al. NIA-AA Research Framework: Toward a biological definition of Alzheimer's disease. *Alzheimer's and Dementia* 2018; 14: 535–562.
7. Lee YW, Lee H, Chung IS, et al. Relationship between postural instability and subcortical volume loss in Alzheimer's disease. *Medicine (United States)* 2017; 96: 1–7.
8. Roh JH, Qiu A, Seo SW, et al. Volume reduction in subcortical regions according to severity of Alzheimer's disease. *J Neurol* 2011; 258: 1013–1020.
9. Wardlaw JM, Smith EE, Biessels GJ, et al. Neuroimaging standards for research into small vessel disease and its contribution to ageing and neurodegeneration. *Lancet Neurol* 2013; 12: 822–838.
10. Pantoni L. Cerebral small vessel disease: from pathogenesis and clinical characteristics to therapeutic challenges. *Lancet Neurol* 2010; 9: 689–701.
11. Gouw AA, Seewann A, van der Flier WM, et al. Heterogeneity of small vessel disease: a systematic review of MRI and histopathology correlations. *Journal of Neurology, Neurosurgery & Psychiatry* 2011; 82: 126 LP – 135.
12. Wardlaw JM, Smith C, Dichgans M. Small vessel disease: mechanisms and clinical implications. *Lancet Neurol* 2019; 18: 684–696.
13. Nitkunan A, Barrick TR, Charlton RA, et al. Multimodal MRI in Cerebral Small Vessel Disease. *Stroke* 2008; 39: 1999–2005.
14. Patel B, Markus HS. Magnetic Resonance Imaging in Cerebral Small Vessel Disease and its Use as a Surrogate Disease Marker. *International Journal of Stroke* 2011; 6: 47–59.
15. Duering M, Finsterwalder S, Baykara E, et al. Free water determines diffusion alterations and clinical status in cerebral small vessel disease. *Alzheimer's and Dementia* 2018; 14: 764–774.
16. Arvanitakis Z, Capuano AW, Leurgans SE, et al. Relation of cerebral vessel disease to Alzheimer's disease dementia and cognitive function in elderly people: a cross-sectional study. *Lancet Neurol* 2016; 15: 934–943.
17. Ossenkoppele R, Jansen WJ, Rabinovici GD, et al. Prevalence of Amyloid PET Positivity in Dementia Syndromes: A Meta-analysis. *JAMA* 2015; 313: 1939–1950.
18. Le Bihan D, Breton E. In vivo magnetic resonance imaging of diffusion. *Comptes Rendus des Seances de l'Academie des Sciences Serie 2* 1985; 301: 1109–1112.
19. Basser PJ, Mattiello J, LeBihan D. MR diffusion tensor spectroscopy and imaging. *Biophys J* 1994; 66: 259–267.
20. Le Bihan D, Iima M. Diffusion magnetic resonance imaging: What water tells us about biological tissues. *PLoS Biol* 2015; 13: 1–13.

21. Rubinov M, Sporns O. Complex network measures of brain connectivity: Uses and interpretations. *Neuroimage* 2010; 52: 1059–1069.
22. Reijmer YD, Fotiadis P, Piantoni G, et al. Small vessel disease and cognitive impairment: The relevance of central network connections. *Hum Brain Mapp* 2016; 37: 2446–2454.
23. van den Heuvel MP, Sporns O. Rich-Club Organization of the Human Connectome. *Journal of Neuroscience* 2011; 31: 15775–15786.
24. Brun A, Englund E. A white matter disorder in dementia of the Alzheimer type: A pathoanatomical study. *Ann Neurol* 1986; 19: 253–262.
25. Agosta F, Pievani M, Sala S, et al. White Matter Damage in Alzheimer Disease and Its Relationship to Gray Matter Atrophy. *Radiology* 2011; 258: 853–863.
26. Pasternak O, Sochen N, Gur Y, et al. Free water elimination and mapping from diffusion MRI. *Magn Reson Med* 2009; 62: 717–730.
27. Maier-Hein KH, Westin C-F, Shenton ME, et al. Widespread white matter degeneration preceding the onset of dementia. *Alzheimer's & Dementia* 2015; 11: 485-493.e2.
28. Hoy AR, Ly M, Carlsson CM, et al. Microstructural white matter alterations in preclinical Alzheimer's disease detected using free water elimination diffusion tensor imaging. *PLoS One* 2017; 12: e0173982.
29. Raj A, Kuceyeski A, Weiner M. A Network Diffusion Model of Disease Progression in Dementia. *Neuron* 2012; 73: 1204–1215.
30. Jagust W. Imaging the evolution and pathophysiology of Alzheimer disease. *Nat Rev Neurosci* 2018; 19: 687–700.
31. Mito R, Raffelt D, Dhollander T, et al. Fibre-specific white matter reductions in Alzheimer's disease and mild cognitive impairment. *Brain* 2018; 141: 888–902.
32. Griffa A, Van den Heuvel MP. Rich-club neurocircuitry: function, evolution, and vulnerability. *Dialogues Clin Neurosci* 2018; 20: 121–132.
33. de Haan W, Mott K, van Straaten ECW, et al. Activity Dependent Degeneration Explains Hub Vulnerability in Alzheimer's Disease. *PLoS Comput Biol*; 8. Epub ahead of print 2012. DOI: 10.1371/journal.pcbi.1002582.
34. Zwanenburg JJM, Van Osch MJP. Targeting cerebral small vessel disease with MRI. *Stroke* 2017; 48: 3175–3182.
35. Ter Telgte A, Van Leijsen EMC, Wiegertjes K, et al. From a Focal To a Global Perspective. *Nat Rev Neurol* 2018; 14: 387–398.
36. Lawrence AJ, Chung AW, Morris RG, et al. Structural network efficiency is associated with cognitive impairment in small-vessel disease. *Neurology* 2014; 83: 304 LP – 311.
37. Tuladhar AM, van Dijk E, Zwiers MP, et al. Structural network connectivity and cognition in cerebral small vessel disease. *Hum Brain Mapp* 2016; 37: 300–310.
38. Reijmer YD, Fotiadis P, Martinez-Ramirez S, et al. Structural network alterations and neurological dysfunction in cerebral amyloid angiopathy. *Brain* 2015; 138: 179–188.
39. Huijts M, Duits A, Van Oostenbrugge R, et al. Accumulation of MRI Markers of Cerebral Small Vessel Disease is Associated with Decreased Cognitive Function. A Study in First-Ever Lacunar Stroke and Hypertensive Patients . *Frontiers in Aging Neuroscience* ; 5.
40. Staals J, Makin SDJ, Doubal FN, et al. Stroke subtype, vascular risk factors, and total MRI brain small-vessel disease burden. *Neurology* 2014; 83: 1228 LP – 1234.
41. Staals J, Booth T, Morris Z, et al. Total MRI load of cerebral small vessel disease and cognitive ability in older people. *Neurobiol Aging* 2015; 36: 2806–2811.

CHAPTER 2

Small vessel disease more than Alzheimer's disease determines diffusion MRI alterations in memory clinic patients

Sofia Finsterwalder,* Naomi Vlegels,* Benno Gesierich, Miguel Á. Araque Caballero, Nick A. Weaver, Nicolai Franzmeier, Marios K. Georgakis, Marek J. Konieczny, Huiberdina L. Koek, Dominantly Inherited Alzheimer Network (DIAN), Celeste M. Karch, Neill R. Graff-Radford, Stephen Salloway, Hwamee Oh, Ricardo F. Allegri, Jasmeer P. Chhatwal, DELCODE study group, Frank Jessen, Emrah Düzel, Laura Dobisch, Coraline Metzger, Oliver Peters, Enise I. Incesoy, Josef Priller, Eike J. Spruth, Anja Schneider, Klaus Fließbach, Katharina Buerger, Daniel Janowitz, Stefan J. Teipel, Ingo Kilimann, Christoph Laske, Martina Buchmann, Michael T. Heneka, Frederic Brosseron, Annika Spottke, Nina Roy, Birgit Ertl-Wagner, Klaus Scheffler, Alzheimer's Disease Neuroimaging Initiative (ADNI), Utrecht VCI study group, Sang Won Seo, Yeshin Kim, Duk L. Na, Hee Jin Kim, Hyemin Jang, Michael Ewers, Johannes Levin, Reinhold Schmidt, Ofer Pasternak, Martin Dichgans, Geert Jan Biessels, and Marco Duering

* These authors contributed equally to this work

Alzheimer's and Dementia. 2020;16:1504–1514.
DOI: 10.1002/alz.12150

ABSTRACT

Background. Microstructural alterations as assessed by diffusion tensor imaging (DTI) are key findings in both Alzheimer's disease (AD) and small vessel disease (SVD). We determined the contribution of each of these conditions to diffusion alterations.

Methods. We studied six samples (N=365 participants) covering the spectrum of AD and SVD, including genetically-defined samples. We calculated diffusion measures from DTI and free water imaging. Simple linear, multivariable random forest, and voxel-based regressions were used to evaluate associations between AD biomarkers (amyloid-beta, tau), SVD imaging markers, and diffusion measures.

Results. SVD markers were strongly associated with diffusion measures and showed a higher contribution than AD biomarkers in multivariable analysis across all memory clinic samples. Voxel-wise analyses between tau and diffusion measures were not significant.

Conclusion. In memory clinic patients, the effect of SVD on diffusion alterations largely exceeds the effect of AD, supporting the value of diffusion measures as markers of SVD.

INTRODUCTION

Alzheimer's disease (AD) and cerebral small vessel disease (SVD) are the two leading causes of cognitive decline and dementia.[1] Altered white matter microstructure is considered a key finding in both conditions[2,3] and has consistently been associated with cognitive deficits.[4-6] The most commonly used method to study white matter microstructure *in vivo* is diffusion tensor imaging (DTI), which quantifies diffusion properties of water molecules in brain tissue.[7,8] The typical finding described in both AD and SVD is an increase in the extent of water diffusion (mean diffusivity) and a decrease in diffusion directionality (fractional anisotropy), which can be detected both globally and regionally.[4,5] Despite the wide use of diffusion alterations as efficient disease markers and their strong associations with clinical deficits, little is known about their underlying pathology.

In memory clinic patients, AD and SVD often co-exist.[9] The extent to which each of these conditions contribute to diffusion MRI alterations is largely elusive. Free water imaging, an advanced diffusion model, improves the specificity of the DTI model and could therefore provide additional insight into the origin of diffusion MRI alterations.[10] As such, free water imaging might be able to disentangle the effects of AD and SVD.[11-14] Previous studies using DTI or free water imaging were limited by the lack of biomarker evidence of AD pathology or insufficient consideration of mixed pathology. Assessing the individual contributions of AD and SVD towards diffusion MRI alterations requires a systematic study covering the entire spectrum of "pure AD", mixed disease, and "pure SVD".

The uncertainty regarding the origin and interpretation of diffusion alterations in memory clinic patients impedes widespread implementation in research and clinical practice. Therefore, the aim of this study was to determine the effect of AD and SVD on diffusion MRI in a memory clinic setting. We examined associations between biomarkers of AD, MRI markers of SVD, and diffusion measures from both conventional DTI and free water imaging. Six study samples (N=365 participants) were included to systematically cover the entire spectrum of AD, mixed disease, and SVD, and to account for both cerebrospinal fluid (CSF) and positron emission tomography (PET) markers. In addition to the common memory clinic setting with predominantly mixed disease, our analysis also included patient samples with pure, genetically-defined AD or SVD. This enabled us to examine effects of both

diseases on diffusion measures without confounding pathology. Analyses were performed separately within each sample in order to validate results and address generalizability using the six independently recruited samples.

METHODS

Participants

We studied six independent samples (N=365 participants) covering the spectrum of AD, mixed disease, and SVD: four memory clinic samples with mixed disease with a recruitment focus on either AD or SVD, one sample each of genetically-defined AD and SVD. Memory clinic samples were drawn from single or multi-center studies, which were selected based on availability of (diffusion) MRI sequences and CSF or PET data. The compilation of samples, subject selection criteria, and exclusions are shown in Fig. 1, and further elaborated in *Alzheimer's disease focused samples, small vessel disease focused samples* and *genetically-defined samples*. MRI, CSF, and PET data from subjects of the included samples were obtained within one year. Diagnostic criteria used in the AD and SVD focused memory clinic samples are summarized in Supplementary Table 1. All studies were approved by the ethics committees of the respective institutions and all subjects provided written informed consent.

Alzheimer's disease focused samples

We included 89 participants from the German multicentric DZNE-Longitudinal Cognitive Impairment and Dementia Study (DELCODE; downloaded in December 2018) with available CSF amyloid-beta$_{1\text{-}40}$ (Aβ 40), amyloid-beta$_{1\text{-}42}$ (Aβ 42), total-tau (t-tau), and phosphorylated- tau$_{181}$ (p-tau) data. The sample consisted of Aβ 42-positive healthy controls (Aβ 42 cut-off see Supplementary Text 1) and patients with subjective cognitive decline, amnestic mild cognitive impairment, and mild dementia.[15]

We further included 53 participants from the multicentric Alzheimer's disease Neuroimaging Initiative (ADNI, phase 3; downloaded in December 2018 at http://adni.loni.usc.edu) with available Aβ [^{18}F]-florbetapir and tau [^{18}F]AV-1451 flortaucipir (PET). The sample consisted of amyloid-positive (cut-off see Supplementary Text 1) healthy controls and patients with amnestic mild cognitive impairment and mild dementia (http://adni.loni.usc.edu).

Small vessel disease focused samples

We included 39 participants from the University Medical Center Utrecht, Netherlands (prospective Utrecht Vascular Cognitive Impairment study, UVCI) with available CSF data for Aβ 42, t-tau, and p-tau. The sample consisted of patients with subjective cognitive decline, mild cognitive impairment, and dementia and with no evidence of a primary etiology other than neurodegenerative disease or sporadic SVD and a high burden of SVD on MRI.[16]

We further included 39 participants from the Samsung Medical Center, Seoul, Republic of Korea (Seoul Vascular Cognitive Impairment study, SVCI) with available Aβ [^{18}F]-florbetaben and tau [^{18}F]AV-1451 flortaucipir (PET). The sample consisted of patients with objective cognitive impairment and a high burden of SVD on MRI.[17,18]

Genetically-defined samples

As a genetically-defined AD sample, we included 77 participants from the multicentric Dominantly Inherited Alzheimer Network (DIAN, data freeze 11; downloaded in August 2018).[19] DIAN is a longitudinal cohort study of individuals at risk of developing autosomal dominant AD. Here we included *PSEN1* (n=59), *PSEN2* (n=5), and *APP* (n=13) mutation carriers with available Aβ 40, Aβ 42, t-tau, and p-tau CSF data. In our study, subjects had to be less than 15 years from estimated symptom onset in order to increase sensitivity to detect AD and SVD marker alterations in proximity to the onset of AD symptoms.[5,20]

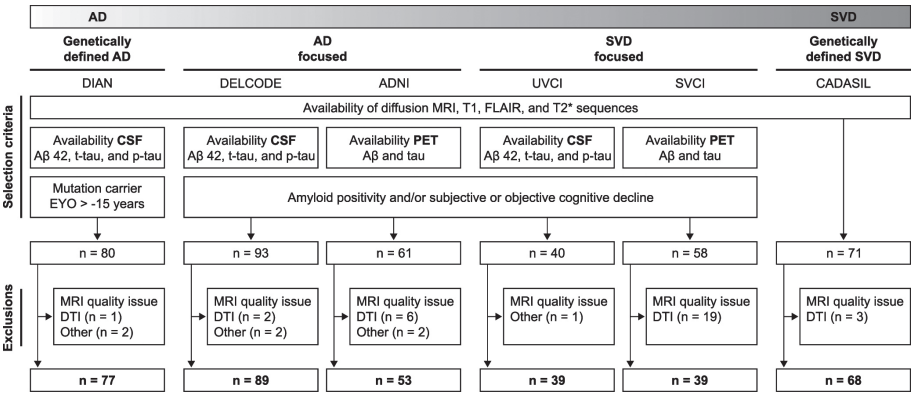

Figure 1. Study concept and participant selection flowchart. Samples cover the entire spectrum of AD, mixed disease, and SVD. AD, Alzheimer's disease; DTI, diffusion tensor imaging; EYO, estimated years from symptom onset; FLAIR, fluid-attenuated inversion recovery; p-tau, phosphorylated-tau$_{181}$; SVD, small vessel disease; t-tau, total tau.

As a genetically-defined SVD sample, we included 68 patients with Cerebral Autosomal Dominant Arteriopathy with Subcortical Infarcts and Leukoencephalopathy (CADASIL) recruited from a single-center study in Munich.[4] Although CSF or PET data were not available in this dataset, we included CADASIL to judge the effect sizes of SVD markers in genetically-defined SVD.

MRI

All MRI data were obtained on 3 Tesla systems. All samples included diffusion MRI, T1-weighted, fluid-attenuated inversion recovery (T2-weighted), and gradient echo (T2*-weighted) sequences. While each study used a standardized protocol, acquisition parameters differed across studies. The MRI protocols have been published previously for DIAN,[5] DELCODE,[21] ADNI,[22] UVCI,[23] SVCI,[17] and CADASIL.[11] Diffusion MRI sequence parameters for all samples are summarized in Supplementary Table 2. All diffusion images were processed with the same pipeline as described in Supplementary Text 2. Global diffusion measures were calculated as mean of all voxels within a white matter skeleton. Regional analyses were based on voxel-wise diffusion measures.

Alzheimer's disease markers

We used Aβ and tau (CSF or PET) as biomarkers of AD. Details on CSF assays, PET tracers, and calculations of PET standardized uptake value ratio (SUVR) scores have previously been published for DIAN,[5] DELCODE,[15] ADNI (http://adni.loni.usc.edu), UVCI,[24] and SVCI.[18]

For the main analyses we used continuous CSF and PET measures. For a subgroup analysis in amyloid-positive individuals, we used study specific Aβ cut-off values. See Supplementary Text 1 for details.

Small vessel disease markers

We used an established total SVD score (ordinal variable)[25] and white matter hyperintensity (WMH) volume (continuous variable) as MRI markers of SVD. The total SVD score summarizes the presence or severity of SVD lesions on an ordinal scale, i.e. WMH, lacunes, microbleeds, and enlarged perivascular spaces.[25] Two trained raters (SF, NV) assessed these lesions according to the STRIVE consensus

criteria:[2] WMHs were rated using the Fazekas scale,[26] the number of lacunes was determined on fluid-attenuated inversion recovery and T1-weighted images, the number of cerebral microbleeds on T2*-weighted gradient echo images, and the number of enlarged perivascular spaces in the basal ganglia on a single T1-weighted axial image slice with the highest number of perivascular spaces.[27] WMH volume was calculated from a previously described semi-automated segmentation pipeline.[4]

Statistical analyses

All statistical analyses were performed in R (version 3.5.1).[28] The statistical significance level was set at $\alpha < 0.05$.

Associations between AD biomarkers, SVD markers, age, sex (independent variables), and global diffusion measures (dependent variables) were first assessed by simple linear regression analyses within each sample. Variables were power transformed in case of non-normal distribution (Shapiro-Wilk test).

To perform multivariable analysis in the presence of multicollinearity (i.e. intercorrelations among disease markers, Supplementary Fig. 1), we used random forest regressions (R package 'party'; version 1.3-2).[29] This method allows to assess the contribution of each AD biomarker, SVD marker, age, and sex to diffusion alterations, while accounting for all other variables. For each sample, we calculated 1501 conditional inference trees with unbiased variable selection and default parameters as previously described.[11] We calculated conditional variable importance together with a 95% confidence interval from 100 repetitions.

An effect of Aβ on diffusion measures might be mediated by vascular pathology, in particular cerebral amyloid angiopathy, i.e. Aβ accumulation in perforating vessels.[30] To address this possibility, we performed a post-hoc mediation analysis (R package 'lavaan'; version 0.6-4)[31] in samples where simple regression analysis showed an effect of Aβ on diffusion measures. Diffusion measures were entered as dependent variables, Aβ as independent variable, WMH volume as mediator, and age as covariate. Standard errors were based on bootstrapping (1000 iterations).

Because amyloid pathology has been shown to strengthen the association between tau accumulation and structural tract alterations as assessed by diffusion

measures,[32] we performed two additional analyses within each sample. First, we conducted a sensitivity analysis restricted to amyloid-positive individuals by repeating simple regression analyses. Second, we assessed the interaction effect of tau * Aβ on diffusion measures.

Finally, since tau is a localized pathology starting in the entorhinal cortex,[33] we also performed regional analyses between voxel-wise diffusion measures and tau in the PET samples, i.e. ADNI and SVCI. We used permutation test theory with a standard general linear model as implemented in 'randomise' (FSL). We assessed associations between both global tau PET SUVR scores as well as regional tau PET SUVR scores in the entorhinal cortex and voxel-wise diffusion measures. The number of permutations was set at 5000. Significant voxels within the skeletonized diffusion measure maps were identified using threshold-free cluster enhancement with 2D optimization and $P < 0.05$, corrected for multiple comparisons.

RESULTS

Sample characteristics are summarized in Table 1. As expected, patients with genetically-defined AD or SVD were considerably younger than memory clinic patients.

Small vessel disease shows stronger associations than Alzheimer's disease with diffusion alterations in simple regression analyses

In simple regressions, both SVD markers, i.e., WMH volume and total SVD score, were consistently and strongly associated with conventional DTI measures (FAu, MDu; range of $R^2_{adj.}$ [0.08–0.79]) and FW (range of $R^2_{adj.}$ [0.18–0.76]) across all six samples (Fig. 2, Supplementary Tables 3-5). In contrast, AD biomarkers, i.e., CSF and PET data, were not or only weakly associated with conventional DTI measures and FW (range of $R^2_{adj.}$ [0.04–0.18]; Fig. 2, Supplementary Tables 3-5). Results were largely consistent across study samples, with a notable exception in the sample of genetically-defined AD (DIAN). Here, effect sizes for Aβ 42 (CSF) were similar to the effect sizes of WMH volume (Fig. 2, Supplementary Table 5). Associations between Aβ 42, WMH volume and diffusion measures in DIAN and DELCODE were further addressed in a post-hoc mediation analysis (see *White matter hyperintensities partially mediate the effect of Aβ on diffusion alterations in genetically defined Alzheimer's disease*).

Table 1. Sample characteristics

	Genetically defined AD	AD focused		SVD focused		Genetically defined SVD
	DIAN (n=77)	**DELCODE (n=89)**	**ADNI (n=53)**	**UVCI (n=39)**	**SVCI (n=39)**	**CADASIL (n=68)**
Age, years	42 (14)	72 (9)	78 (13)	74 (12)	79 (10)	55 (11)
Female, n (%)	40 (52)	36 (40)	25 (47)	13 (33)	28 (72)	44 (65)
Diagnosis, n (%) HC, SCD, MCI, dementia	na	4 (4), 37 (42), 33 (37), 15 (17)	22 (42), na, 23 (43), 8 (15)	0 (0), 3 (8), 18 (46), 18 (46)	0 (0), na, 22 (56), 17 (44)	na
CDR, n (%) 0, 0.5, 1, 2, 3	38 (49), 29 (38), 9 (12), 1 (1), 0 (0)	29 (33), 52 (59), 7 (8), 0 (0), 0 (0)[a]	22 (42), 23 (43), 6 (11), 2 (4), 0 (0)	1 (3), 30 (77), 8 (20), 0 (0), 0 (0)	0 (0), 26 (67), 7 (18), 6 (15), 0 (0)	57 (84), 9 (13), 1 (1), 1 (1), 0 (0)
Aβ-positive, n (%)	46 (60)	44 (49)	37 (70)	22 (56)	19 (49)	na
DTI						
FAu, mm^2/s	0.45 (0.03) [0.38, 0.49]	0.46 (0.03) [0.36, 0.52]	0.45 (0.04) [0.38, 0.50]	0.44 (0.04) [0.36, 0.48]	0.42 (0.04) [0.35, 0.50]	0.40 (0.06) [0.27, 0.49]
MDu, 10^{-4} mm^2/s	7.84 (0.64) [7.27, 9.31]	7.68 (0.59) [6.71, 9.72]	8.21 (0.63) [7.35, 9.77]	8.05 (0.82) [7.23, 9.72]	9.66 (0.76) [8.48, 11.0]	9.40 (1.61) [7.79, 12.89]
FAt, mm^2/s	0.55 (0.02) [0.52, 0.58]	0.56 (0.02) [0.52, 0.60]	0.57 (0.02) [0.54, 0.60]	0.56 (0.02) [0.52, 0.57]	0.59 (0.01) [0.56, 0.63]	0.55 (0.02) [0.50, 0.59]
MDt, 10^{-4} mm^2/s	5.92 (0.07) [5.80, 6.01]	5.97 (0.10) [5.51, 6.14]	6.01 (0.63) [5.94, 6.09]	5.82 (0.15) [5.63, 5.99]	6.00 (0.04) [5.91, 6.12]	5.97 (0.03) [5.89, 6.03]
FW, mm^2/s	0.18 (0.05) [0.14, 0.28]	0.16 (0.04) [0.11, 0.29]	0.20 (0.05) [0.13, 0.31]	0.22 (0.06) [0.16, 0.35]	0.25 (0.04) [0.17, 0.31]	0.29 (0.11) [0.17, 0.51]
AD markers						
CSF						
Aβ 40, ng/L	7634 (4516) [2215, 15622]	7942 (3229) [3721, 13358]	-	na	-	-
Aβ 42, ng/L	436 (332) [174, 1424]	498 (380) [183, 1317]	-	619 (279) [363, 1641]	-	-
T-tau, ng/L	97 (132) [8, 563]	425 (369) [98, 1477]	-	524 (368) [140, 1274]	-	-
P-tau, ng/L	56 (66) [14, 163]	51 (39) [16, 192]	-	67 (47) [19, 166]	-	-
PET						
[^{18}F]-florbetapir SUVR	-	-	1.18 (0.36) [0.90, 1.70]	-	na	-
[^{18}F]-florbetaben SUVR	-	-	na	-	1.38 (0.49) [1.11, 2.17]	-
[^{18}F]AV-1451 SUVR	-	-	1.10 (0.13) [0.86, 1.67]	-	1.11 (0.16) [0.89, 1.60]	-

	Genetically defined AD	AD focused		SVD focused		Genetically defined SVD
	DIAN (n=77)	**DELCODE (n=89)**	**ADNI (n=53)**	**UVCI (n=39)**	**SVCI (n=39)**	**CADASIL (n=68)**
SVD markers						
WMHvol, ml	2.22 (3.05) [0.00, 30.47]	2.78 (5.36) [0.03, 34.50]	3.35 (8.29) [0.00, 77.24]	15.72 (1.85) [1.34, 67.27]	32.19 (21.03) [10.48, 71.20]	71.27 (73.74) [1.09, 257.74]
SVD score, n (%) 0, 1, 2, 3, 4	67 (87), 9 (12), 1 (1), 0 (0), 0 (0)	23 (26), 33 (37), 28 (31), 3 (3), 2 (2)	8 (15), 17 (32), 18 (34), 8 (15), 2 (4)	4 (10), 15 (39), 11 (28), 6 (15), 3 (8)	0 (0), 0 (0), 0 (0), 0 (0), 39 (100)	0 (0), 16 (24), 19 (28), 17 (25), 16 (24)

For numeric variables median (interquartile range) [min, max] is shown, except for age. [a] DELCODE: CDR of 1 subject missing;
AD, Alzheimer's disease; CDR, clinical dementia rating; DTI, diffusion tensor imaging; FAu, uncorrected fractional anisotropy; FAt, free water corrected tissue compartment of fractional anisotropy; FW, free water content; HC, healthy control; MCI, mild cognitive impairment; MDu, uncorrected mean diffusivity; MDt, free water corrected tissue compartment of mean diffusivity; na, not available; p-tau, phosphorylated- tau_{181}; SCD, subjective cognitive decline; SUVR, standardised uptake value ratio; SVD, small vessel disease; SVD score, total small vessel disease score; t-tau, total tau; WMHvol, white matter hyperintensity volume.

Small vessel disease and age contribute most to diffusion alterations in multivariable analyses

Using random forest regression as a multivariable method, we assessed the contribution of each AD biomarker and SVD marker to diffusion measures, while accounting for multicollinearity. In all memory clinic samples, SVD markers showed higher variable importance than AD biomarkers for alterations of conventional DTI measures (FAu and MDu; Fig. 3) and FW (data not shown; nearly identical to MDu). The opposite was found only in DIAN, where AD biomarkers showed higher variable importance. For tissue measures (FAt and MDt), interpretation of random forest regressions was not feasible, because variable importances were zero or almost zero in all samples (data not shown).

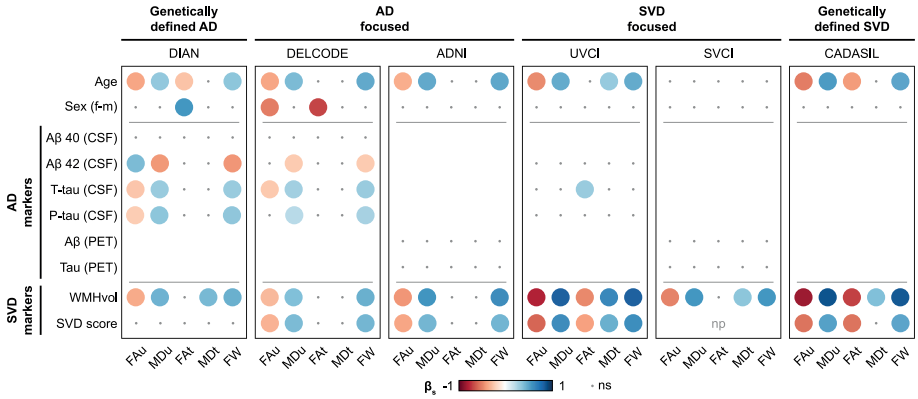

Figure 2. Simple regression analyses. Simple linear regression analyses between diffusion measures and AD biomarkers or SVD markers. Standardized β is represented by color. AD, Alzheimer's disease; β_s, standardized beta; FAu, uncorrected fractional anisotropy; FAt, free water corrected tissue compartment of fractional anisotropy; FW, free water content; MDu, uncorrected mean diffusivity; MDt, free water corrected tissue compartment of mean diffusivity; np, not possible (all patients had the maximum score); ns, not significant; p-tau, phosphorylated- tau_{181}; SVD, small vessel disease; SVD score, total small vessel disease score; t-tau, total tau; WMHvol, white matter hyperintensity volume.

White matter hyperintensities partially mediate the effect of Aβ on diffusion alterations in genetically-defined Alzheimer's disease

For diffusion measures significantly associated with Aβ 42 (CSF) in the simple regression analysis, i.e., in DIAN and DELCODE, we performed a post-hoc mediation analysis to explore whether these associations might be mediated by vascular pathology, such as cerebral amyloid angiopathy. In DIAN, the effect of Aβ 42 on MDu and FW was indeed partially mediated by WMH volume (MDu: β_s=-0.06,

SE=0.03, *P*=0.030; FW: β_s=-0.06, SE=0.03, *P*=0.026). However, we also found a direct effect of Aβ 42 on MDu and FW (MDu: β_s=-0.30, SE=0.12, *P*=0.005; FW: β_s=-0.30, SE=0.11, *P*=0.005). For FAu, mediation analysis was not significant. As a further indication for the presence of cerebral amyloid angiopathy, most (8 out of 9) DIAN participants with cerebral microbleeds showed a strictly lobar distribution, and one participant had disseminated cortical superficial siderosis.

In DELCODE, where simple regression analysis showed only weak effects of Aβ 42, none of the mediation analyses were significant (all *P* > 0.136).

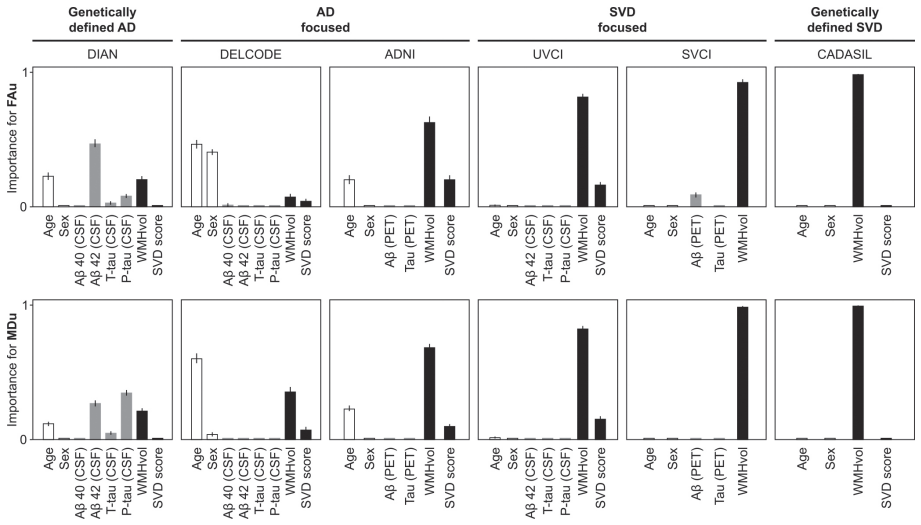

Figure 3. Multivariable analyses. Random forest regression analyses for estimating the relative variable importance of AD biomarkers (grey bars), SVD markers (black bars), age and sex (white bars) with regard to conventional DTI measures (FAu, MDu) while accounting for all other variables (conditional importance). Lines indicate the 95% confidence interval for the conditional variable importance. AD, Alzheimer's disease; FAu, uncorrected fractional anisotropy; MDu, uncorrected mean diffusivity; p-tau, phosphorylated-tau181; SVD, small vessel disease; SVD score, total small vessel disease score; T-tau, total tau; WMHvol, white matter hyperintensity volume.

Tau is not associated with diffusion alterations in amyloid-positive individuals

It was recently reported that Aβ might strengthen the association between tau accumulation and diffusion alterations.[32] We addressed this aspect in a sensitivity analysis restricted to amyloid-positive individuals (Supplementary Tables 6-8, Supplementary Fig. 2). Simple linear regressions between tau and diffusion measures in amyloid-positive individuals were not significant, except for DIAN (n=46; p-tau and MDu, β_s=0.32, $R^2_{adj.}$=0.08, *P*=0.031; p-tau and FW, β_s=0.31, $R^2_{adj.}$=0.07, *P*=0.038). In correspondence with the full DIAN sample, tau showed effect sizes comparable to those found for WMH volume (WMH volume and MDu, β_s=0.35, $R^2_{adj.}$=0.10, *P*=0.017; WMH volume and FW, β_s=0.37, $R^2_{adj.}$=0.12, *P*=0.011). None of the tau * Aβ interaction models with diffusion measures as dependent variables were significant in any of the samples (all $P > 0.051$).

Regional tau is not associated with diffusion alterations

Tau is a localized pathology starting in the entorhinal cortex[33] and previous literature suggests localized effects of tau on white matter microstructure.[32,34,35] We therefore performed regional analyses in the PET samples, i.e., ADNI and SVCI, which allow to assess local tau load. Associations between regional tau PET SUVR scores in the entorhinal cortex or global tau PET SUVR scores and voxel-wise diffusion measures were not significant.

DISCUSSION

We investigated the effect of AD and SVD on brain microstructure assessed by diffusion measures. As a unique feature, our study included six independently recruited samples covering the entire spectrum of AD, mixed disease, and SVD. The main finding is that in memory clinic patients, diffusion MRI alterations are largely determined by SVD. Results were consistent across all memory clinic samples, illustrating the robustness and generalizability of our findings. Our study facilitates the interpretation of diffusion MRI alterations and the development towards clinical application.

The strong effect of SVD on diffusion measures was evident in all of the six study samples. In contrast, an association between AD and diffusion measures was only

detectable in DELCODE and DIAN. While in DELCODE effect sizes of AD biomarkers were considerably smaller than those of SVD markers, effect sizes of Aβ 42 and WMH volume were similar in DIAN. Multivariable analyses using random forest regression showed a higher importance of SVD markers for diffusion alterations in all memory clinic samples. The only sample in which AD biomarkers had a higher variable importance was DIAN. As expected for a genetically-defined sample, these patients are considerably younger than typical memory clinic patients and less likely to show age-related comorbidities, such as SVD. Still, mediation analysis in DIAN suggested a vascular contribution to diffusion alterations also in this population, as the effect of Aβ on diffusion alterations was partly mediated by WMH volume. This might indicate a contribution of cerebral amyloid angiopathy, a specific subtype of SVD caused by deposition of Aβ in perforating vessels.[30] Since the DIAN sample also included asymptomatic mutation carriers up to 15 years before estimated symptom onset, another explanation is that the association between Aβ and diffusion measures is strongest in early, preclinical AD. This view is supported by a recent study demonstrating an association between Aβ and diffusion measures over the adult lifespan in cognitively healthy participants.[36] Overall, we conclude that while the effect of AD on diffusion measures is apparent in DIAN patients with pure and early AD, the presence of SVD in the memory clinic samples masks the effect of AD on diffusion measures.

Seemingly in contrast with our results, associations between AD biomarkers and alterations of white matter microstructure as assessed by DTI have been previously reported in memory clinic patients,[13,14,32,34,37-39] although some studies found no association.[40,41] Importantly, however, only one of these studies accounted for SVD. Hence, the effect of AD on diffusion alterations might have been overestimated. Only Strain and colleagues[34] considered biomarkers of both diseases and found an association between tau PET (but not Aβ PET) in temporal regions and diffusion measures in temporal white matter projections, independently of WMHs. In line with our results, the effect size for WMH volume was larger than effect sizes of AD biomarkers. By considering both diseases, we conclude that SVD determines diffusion alterations to a much larger extent than AD, even in samples where AD was the clinically predominant disease. The strong effect of SVD has implications for future studies, which will need to take SVD into account as an important confounder, as well as for the interpretation of diffusion MRI alterations in clinical routine.

In the current study, neither the regional analysis nor the analysis in amyloid-positive individuals, where the effect of tau was expected to be stronger,[32] indicated a significant association between tau and diffusion measures. In post-mortem studies, white matter alterations in AD patients have been attributed to axonal degeneration secondary to cortical deposition of hyperphosphorylated tau.[42,43] Yet, post-mortem studies by design examine patients in very late stages of AD, while our memory clinic patients were mostly in earlier disease stages. Thus, it is conceivable that our patients have not yet reached the disease stage where associations between tau and axonal degeneration can be detected.

By design, our memory clinic samples were heterogeneous, which in our view accurately reflects a real-life memory clinic setting. To study pure forms of AD and SVD, we included genetically defined samples. Furthermore, the sensitivity analysis in subgroups with amyloid-positive individuals allowed to study memory clinic patients who met the biological definition of AD. Although statistical power was reduced, the strong effect of SVD on diffusion measures was also confirmed in these subgroups.

Our finding that diffusion alterations are predominantly driven by SVD is also supported by a genome-wide association study in the population-based UK Biobank. Polygenic risk scores for altered DTI measures were associated with SVD-related stroke and major depressive disorder, but not with AD.[44] The study thus provided genetic evidence that mechanisms underlying diffusion alterations are shared with cerebrovascular disease.

Another aim of this study was to investigate whether free water imaging allows to disentangle the contribution of SVD and AD. The finding that SVD markers showed strongest associations with FW corroborates previous results indicating that diffusion alterations in SVD patients are predominantly driven by an increase in the free water content.[11] However, our current analysis did not provide evidence that AD biomarkers are reflected in the tissue compartment. The latter result is in contrast to studies suggesting that AD-related neurodegeneration of the white matter might be specifically represented in free water corrected tissue measures: Tissue measures were associated with conversion from mild cognitive impairment to dementia in AD patients[12] and showed Aβ-related longitudinal changes.[14] It should be noted that the current study was cross-sectional and thus we cannot

exclude that the tissue compartment holds valuable information for longitudinal studies.[12,14] Furthermore, multi-shell diffusion data, which would be necessary for more complex parametrization of the fluid compartments,[45-47] was not available in the study samples. This would have allowed to control for the effects of capillary blood flow (intravoxel incoherent motion) in the free water estimation.[47]

A limitation of our study is that elevated tau (especially in CSF) is not specific for AD as it could also indicate other tauopathies, such as Pick's disease, corticobasal degeneration, or progressive supranuclear palsy. However, the tau PET tracer ([^{18}F] AV-1451) employed mostly binds to tau deposits specific for AD.[48] Also, the focus on recruitment of clinical AD, e.g., by including amnestic mild cognitive impairment in DELCODE and ADNI, clearly enriched for AD rather than other tauopathies. Another limitation is the lack of AD biomarkers in the CADASIL sample. Yet, the purpose of the CADASIL sample was to judge the effect sizes of SVD markers in genetically-defined disease, i.e., in young patients with pure SVD. Interestingly, we found similar effect sizes as in SVD focused samples with mixed pathology, in particular the UVCI sample. While we also included voxel-based analyses to identify regional associations, our study mostly focused on global, whole-brain averages of diffusion measures. Thus, we cannot exclude that analyses in specific subregions will yield different results. Because of limitations in the diffusion MRI acquisition protocols (no reversed phase-encoding, directions not sampled on entire sphere), we were not able to correct for susceptibility-induced distortions or to employ a more modern approach for correction of eddy current-induced distortions, motion, and outlier slices.[49] Finally, the lack of pathological confirmation of the presence and extent of AD and SVD pathology originates from the paucity of autopsy studies with high quality, standardized antemortem diffusion MRI.

The main strength of our analysis is the inclusion of multiple samples from different countries and ethnicities, covering the entire spectrum of AD, mixed disease, and SVD. This has enabled us to independently validate results and to assess both CSF and PET biomarkers of AD in a robust manner. The differences in study protocols among the six samples, such as MRI acquisition, biomarker assessment techniques, and recruitment strategies indicate that our results might be generalizable to other populations along the spectrum of AD and SVD. We also included younger individuals with genetically-defined disease to minimize confounding by other age-related pathologies. Finally, the state-of-the art

diffusion imaging analysis pipeline included modern pre-processing techniques and rigorous control for confounding by CSF partial volume effects, which is crucial in patients with atrophy and therefore enlarged CSF spaces.

In conclusion, we demonstrate that the effect of SVD on diffusion alterations largely exceeds the effect of AD. Our systematic analysis contributes to the interpretation of diffusion MRI in memory clinic patients and further advances its application in clinical practice. We validate diffusion measures as markers for SVD and as valuable tools to assess the vascular contribution to AD and dementia, which still needs to be adequately explored.[50] Building upon our findings, future studies could assess if more advanced parameterization of diffusion processes, such as biophysical diffusion models, further increases the sensitivity in earlier or even asymptomatic stages.

REFERENCES

1. O'Brien JT, Thomas A. Vascular dementia. *The Lancet*. 2015;386(10004):1698-1706.
2. Wardlaw JM, Smith EE, Biessels GJ, et al. Neuroimaging standards for research into small vessel disease and its contribution to ageing and neurodegeneration. *The Lancet Neurology*. 2013;12(8):822-838.
3. Nasrabady SE, Rizvi B, Goldman JE, Brickman AM. White matter changes in Alzheimer's disease: a focus on myelin and oligodendrocytes. *Acta neuropathologica communications*. 2018;6(1):22.
4. Baykara E, Gesierich B, Adam R, et al. A novel imaging marker for small vessel disease based on skeletonization of white matter tracts and diffusion histograms. *Annals of neurology*. 2016;80(4):581-592.
5. Araque Caballero MÁ, Suárez-Calvet M, Duering M, et al. White matter diffusion alterations precede symptom onset in autosomal dominant Alzheimer's disease. *Brain*. 2018;141(10):3065-3080.
6. Mito R, Raffelt D, Dhollander T, et al. Fibre-specific white matter reductions in Alzheimer's disease and mild cognitive impairment. *Brain*. 2018;141(3):888-902.
7. Amlien IK, Fjell AM. Diffusion tensor imaging of white matter degeneration in Alzheimer's disease and mild cognitive impairment. *Neuroscience*. 2014;276:206-215.
8. Pasi M, van Uden IWM, Tuladhar AM, de Leeuw F-E, Pantoni L. White matter microstructural damage on diffusion tensor imaging in cerebral small vessel disease: clinical consequences. *Stroke*. 2016;47(6):1679-1684.
9. Kapasi A, DeCarli C, Schneider JA. Impact of multiple pathologies on the threshold for clinically overt dementia. *Acta neuropathologica*. 2017;134(2):171-186.
10. Pasternak O, Sochen N, Gur Y, Intrator N, Assaf Y. Free water elimination and mapping from diffusion MRI. *Magnetic Resonance in Medicine: An Official Journal of the International Society for Magnetic Resonance in Medicine*. 2009;62(3):717-730.
11. Duering M, Finsterwalder S, Baykara E, et al. Free water determines diffusion alterations and clinical status in cerebral small vessel disease. *Alzheimer's & dementia: the journal of the Alzheimer's Association*. 2018;14(6):764-774.
12. Maier-Hein KH, Westin C-F, Shenton ME, et al. Widespread white matter degeneration preceding the onset of dementia. *Alzheimer's & Dementia*. 2015;11(5):485-493.
13. Hoy AR, Ly M, Carlsson CM, et al. Microstructural white matter alterations in preclinical Alzheimer's disease detected using free water elimination diffusion tensor imaging. *PloS one*. 2017;12(3)
14. Vipin A, Ng KK, Ji F, et al. Amyloid burden accelerates white matter degradation in cognitively normal elderly individuals. *Human brain mapping*. 2019;
15. Jessen F, Spottke A, Boecker H, et al. Design and first baseline data of the DZNE multicenter observational study on predementia Alzheimer's disease (DELCODE). *Alzheimer's research & therapy*. 2018;10(1):15.

16. Aalten P, Ramakers IHGB, Biessels GJ, et al. The Dutch Parelsnoer Institute-Neurodegenerative diseases; methods, design and baseline results. *BMC neurology*. 2014;14(1):254.

17. Kim HJ, Yang JJ, Kwon H, et al. Relative impact of amyloid-β, lacunes, and downstream imaging markers on cognitive trajectories. Brain. 2016;139(9):2516-2527.

18. Kim HJ, Park S, Cho H, et al. Assessment of extent and role of tau in subcortical vascular cognitive impairment using 18F-AV1451 positron emission tomography imaging. JAMA neurology. 2018;75(8):999-1007.

19. Moulder KL, Snider BJ, Mills SL, et al. Dominantly Inherited Alzheimer Network: facilitating research and clinical trials. Alzheimer's research & therapy. 2013;5(5):48.

20. Fleisher AS, Chen K, Quiroz YT, et al. Associations between biomarkers and age in the presenilin 1 E280A autosomal dominant Alzheimer disease kindred: a cross-sectional study. JAMA neurology. 2015;72(3):316-324.

21. Franzmeier N, Ren J, Damm A, et al. The BDNF Val66Met SNP modulates the association between beta-amyloid and hippocampal disconnection in Alzheimer's disease. Molecular psychiatry. 2019:1-15.

22. Jiaerken Y, Luo X, Yu X, et al. Microstructural and metabolic changes in the longitudinal progression of white matter hyperintensities. Journal of Cerebral Blood Flow & Metabolism. 2018:1613-22.

23. Heinen R, Vlegels N, de Bresser J, et al. The cumulative effect of small vessel disease lesions is reflected in structural brain networks of memory clinic patients. NeuroImage: Clinical. 2018;19:963-969.

24. de Wilde A, van Maurik IS, Kunneman M, et al. Alzheimer's Biomarkers In Daily Practice (ABIDE) project: rationale and design. Alzheimer's & Dementia: Diagnosis, Assessment & Disease Monitoring. 2017;6:143-151.

25. Staals J, Makin SDJ, Doubal FN, Dennis MS, Wardlaw JM. Stroke subtype, vascular risk factors, and total MRI brain small-vessel disease burden. Neurology. 2014;83(14):1228-1234.

26. Fazekas F, Chawluk JB, Alavi A, Hurtig HI, Zimmerman RA. MR signal abnormalities at 1.5 T in Alzheimer's dementia and normal aging. American journal of roentgenology. 1987;149(2):351-356.

27. Potter GM, Chappell FM, Morris Z, Wardlaw JM. Cerebral perivascular spaces visible on magnetic resonance imaging: development of a qualitative rating scale and its observer reliability. Cerebrovascular diseases. 2015;39(3-4):224-231.

28. R Core Team. R: A language and environment for statistical computing. R Foundation for Statistical Computing, Vienna, Austria. 2013.

29. Strobl C, Boulesteix A-L, Zeileis A, Hothorn T. Bias in random forest variable importance measures: Illustrations, sources and a solution. BMC bioinformatics. 2007;8(1):25.

30. Charidimou A, Boulouis G, Gurol ME, et al. Emerging concepts in sporadic cerebral amyloid angiopathy. Brain. 2017;140(7):1829-1850.

31. Rosseel Y. Lavaan: An R package for structural equation modeling and more. Version 0.5–12 (BETA). Journal of statistical software. 2012;48(2):1-36.

32. Jacobs HIL, Hedden T, Schultz AP, et al. Structural tract alterations predict downstream tau accumulation in amyloid-positive older individuals. Nature neuroscience. 2018;21(3):424.

33. Cho H, Choi JY, Hwang MS, et al. In vivo cortical spreading pattern of tau and amyloid in the Alzheimer disease spectrum. Annals of neurology. 2016;80(2):247-258.

34. Strain JF, Smith RX, Beaumont H, et al. Loss of white matter integrity reflects tau accumulation in Alzheimer disease defined regions. Neurology. 2018;91(4):e313-e318.

35. Kantarci K, Murray ME, Schwarz CG, et al. White-matter integrity on DTI and the pathologic staging of Alzheimer's disease. Neurobiology of aging. 2017;56:172-179.

36. Araque Caballero MÁ, Song Z, Rubinski A, et al. Age□dependent amyloid deposition is associated with white matter alterations in cognitively normal adults during the adult life span. Alzheimer's & Dementia. 2020.

37. Melah KE, Lu SY-F, Hoscheidt SM, et al. CSF markers of Alzheimer's pathology and microglial activation are associated with altered white matter microstructure in asymptomatic adults at risk for Alzheimer's disease. Journal of Alzheimer's disease: JAD. 2016;50(3):873.

38. Racine AM, Merluzzi AP, Adluru N, et al. Association of longitudinal white matter degeneration and cerebrospinal fluid biomarkers of neurodegeneration, inflammation and Alzheimer's disease in late-middle-aged adults. Brain imaging and behavior. 2019;13(1):41-52.

39. Racine AM, Adluru N, Alexander AL, et al. Associations between white matter microstructure and amyloid burden in preclinical Alzheimer's disease: a multimodal imaging investigation. NeuroImage: Clinical. 2014;4:604-614.

40. Kantarci K, Schwarz CG, Reid RI, et al. White matter integrity determined with diffusion tensor imaging in older adults without dementia: influence of amyloid load and neurodegeneration. JAMA neurology. 2014;71(12):1547-1554.

41. Pietroboni AM, Scarioni M, Carandini T, et al. CSF β-amyloid and white matter damage: a new perspective on Alzheimer's disease. J Neurol Neurosurg Psychiatry. 2018;89(4):352-357.

42. McAleese KE, Firbank M, Dey M, et al. Cortical tau load is associated with white matter hyperintensities. Acta neuropathologica communications. 2015;3(1):60.

43. McAleese KE, Walker L, Graham S, et al. Parietal white matter lesions in Alzheimer's disease are associated with cortical neurodegenerative pathology, but not with small vessel disease. *Acta neuropathologica*. 2017;134(3):459-473.

44. Rutten-Jacobs LCA, Tozer DJ, Duering M, et al. Genetic study of white matter integrity in UK Biobank (N= 8448) and the overlap with stroke, depression, and dementia. *Stroke*. 2018;49(6):1340-1347.

45. Hoy AR, Koay CG, Kecskemeti SR, Alexander AL. Optimization of a free water elimination two-compartment model for diffusion tensor imaging. *Neuroimage*. 2014;103:323-333.

46. Sepehrband F, Cabeen RP, Choupan J, et al. Perivascular space fluid contributes to diffusion tensor imaging changes in white matter. *NeuroImage*. 2019;197:243-254.

47. Rydhög AS, Szczepankiewicz F, Wirestam R, et al. Separating blood and water: perfusion and free water elimination from diffusion MRI in the human brain. *Neuroimage*. 2017;156:423-434.

48. Lowe VJ, Curran G, Fang P, et al. An autoradiographic evaluation of AV-1451 Tau PET in dementia. *Acta neuropathologica communications*. 2016;4(1):58.

49. Andersson JLR, Graham MS, Zsoldos E, Sotiropoulos SN. Incorporating outlier detection and replacement into a non-parametric framework for movement and distortion correction of diffusion MR images. *Neuroimage*. Nov 1 2016;141:556-572. doi:10.1016/j.neuroimage.2016.06.058

50. Sweeney MD, Montagne A, Sagare AP, et al. Vascular dysfunction—The disregarded partner of Alzheimer's disease. *Alzheimer's & Dementia*. 2019;15(1):158-167.

SUPPLEMENTARY MATERIAL

Supplementary Table 1. Diagnostic criteria in memory clinic samples

	AD focused		SVD focused	
	DELCODE[a]	ADNI, phase 3[b]	UVCI[c]	SVCI[d,e]
HC	No subjective/ objective cognitive decline	MMSE ≥24; CDR=0	na	na
SCD	Subjectively reported cognitive worsening; age-, sex-, and education-adjusted CERAD neuropsychological test battery > -1.5 SD	na	Subjective cognitive decline; no objective cognitive impairment on a standardized neuropsychological test battery	na
MCI	Age-, sex-, and education-adjusted performance CERAD episodic memory tests < -1.5 SD	Subjective memory complaints without significant functional impairment; MMSE ≥ 24; objective memory impairment on the revised Wechsler Memory Scale; CDR=0.5; memory CDR ≥ 0.5.	Subjective and objective cognitive decline in at least one cognitive domain without significant functional impairment	Objective memory decline below the 16th percentile (- 1.0 SD) of age- and education-matched norms in at least one cognitive domain tested by the Seoul Neuropsychological Screening Battery; Petersen's criteria
Dementia	NIA-AA for probable AD; MMSE ≥18	NINCDS-ADRDA criteria	NINCDS-ADRDA criteria	NIA-AA for probable AD

[a] Jessen F, Spottke A, Boecker H, et al. Design and first baseline data of the DZNE multicenter observational study on predementia Alzheimer's disease (DELCODE). Alzheimer's research & therapy. 2018;10(1):15;
[b] http://adni.loni.usc.edu
[c]Aalten P, Ramakers IHGB, Biessels GJ, et al. The Dutch Parelsnoer Institute-Neurodegenerative diseases; methods, design and baseline results. BMC neurology. 2014;14(1):254.
[d] Kim HJ, Yang JJ, Kwon H, et al. Relative impact of amyloid-β, lacunes, and downstream imaging markers on cognitive trajectories. Brain. 2016;139(9):2516-27
[e] Kim HJ, Park S, Cho H, et al. Assessment of extent and role of tau in subcortical vascular cognitive impairment using 18F-AV1451 positron emission tomography imaging. JAMA neurology. 2018;75(8):999-1007.
AD, Alzheimer's disease; CERAD, Consortium to Establish a Registry for Alzheimer's disease; CDR, clinical dementia rating; CSF, cerebrospinal fluid; ELISA, enzyme-linked immunosorbent assays; HC, cognitively healthy control; MCI, mild cognitive impairment; MMSE, Mini-Mental-State Examination; na, not available; NIA-AA, National Institute on Aging research criteria for probable Alzheimer's disease; NINCDS-ADRDA, National Institute of Neurological and Communicative Disorders and Stroke and the Alzheimer's Disease and Related Disorders Association; PET, positron emission tomography; SCD, subjective cognitive decline; SUVR, standardized uptake value ratio; SD, standard deviation; SVD, small vessel disease.

Supplementary Table 2. Diffusion parameters

	DIAN	DELCODE	ADNI	UVCI	SVCI	CADASIL
Scanner	Siemens systems	Siemens systems	GE Healthcare systems	Philips Achieva	Philips Achieva	Siemens Verio
TR [ms]	11000	12100	7200	6600	7696	12700
TE [ms]	87	88	56	73	60	81
Slice [mm]	2.50	2.00	2.00	2.50	2.00	2.00
In-plane [mm]	2.50 x 2.50	2.00 x 2.00	2.00 x 2.00	1.72 x 1.72	1.72 x 1.72	2.00 x 2.00
b-value [s/mm^2]	1000	700, 1000	1000	1200	600	1000
Directions	64	30, 30	48	45	45	30

TE, echo time; TR, repetition time.

Supplementary Table 3. Simple regression models in Alzheimer's disease focused samples

	FAu			MDu			FAt			MDt			FW		
	β_s	$R^2_{adj.}$	*P*	β_s	$R^2_{adj.}$	*P*	β_s	$R^2_{adj.}$	*P*	β_s	$R^2_{adj.}$	*P*	β_s	$R^2_{adj.}$	*P*
DELCODE (n=89)															
Age	-0.38	0.13	**0.000**	0.42	0.17	**0.000**	-0.21	0.03	0.051	0.15	0.01	0.171	0.49	0.23	**0.000**
Sex (f-m)	-0.52	0.05	**0.016**	0.28	0.01	0.198	-0.69	0.11	**0.001**	0.11	-0.01	0.599	0.23	0.00	0.279
Aβ 40 (CSF)	0.04	-0.01	0.745	-0.03	-0.01	0.770	0.07	-0.01	0.492	0.00	-0.01	0.963	0.00	-0.01	0.969
Aβ 42 (CSF)	0.17	0.02	0.102	-0.23	0.04	**0.029**	0.09	0.00	0.386	-0.11	0.00	0.314	-0.24	0.05	**0.025**
T-tau (CSF)	-0.25	0.05	**0.019**	0.29	0.07	**0.005**	-0.14	0.01	0.201	0.16	0.02	0.123	0.33	0.10	**0.002**
P-tau (CSF)	-0.20	0.03	0.063	0.23	0.04	**0.033**	-0.09	0.00	0.405	0.13	0.00	0.238	0.27	0.06	**0.009**
WMHvol	-0.30	0.08	**0.004**	0.40	0.15	**0.000**	-0.05	-0.01	0.631	0.14	0.01	0.206	0.47	0.21	**0.000**
SVD score	-0.32	0.09	**0.002**	0.41	0.16	**0.000**	-0.14	0.01	0.206	0.18	0.02	0.088	0.44	0.18	**0.000**
ADNI (n=53)															
Age	-0.35	0.10	**0.011**	0.49	0.23	**0.000**	0.10	-0.01	0.464	0.10	-0.01	0.476	0.51	0.24	**0.000**
Sex (f-m)	-0.21	-0.01	0.460	0.42	0.03	0.125	0.28	0.00	0.322	0.29	0.00	0.301	0.39	0.02	0.158
Aβ (PET)	0.14	0.00	0.312	-0.07	-0.02	0.635	0.23	0.04	0.091	-0.19	0.02	0.164	-0.05	-0.02	0.744
Tau (PET)	0.05	-0.02	0.745	-0.04	-0.02	0.777	0.02	-0.02	0.875	0.14	0.00	0.323	-0.05	-0.02	0.702
WMHvol	-0.43	0.17	**0.001**	0.58	0.32	**0.000**	0.12	0.00	0.376	0.10	-0.01	0.490	0.62	0.38	**0.000**
SVD score	-0.38	0.12	**0.006**	0.43	0.17	**0.001**	-0.02	-0.02	0.863	0.26	0.05	0.061	0.45	0.19	**0.001**

P < 0.05 in bold. β_s, standardized beta; FAu, uncorrected fractional anisotropy; FAt, free water corrected tissue compartment of fractional anisotropy; FW, free water content; MDu, uncorrected mean diffusivity; MDt, free water corrected tissue compartment of mean diffusivity; P-tau, phosphorylated-tau_{181}; $R^2_{adj.}$, adjusted explained variance; SVD score, total small vessel disease score; T-tau, total tau; WMHvol, white matter hyperintensity volume.

Supplementary Table 4. Simple regression models in small vessel disease focused samples

	FAu			MDu			FAt			MDt			FW		
	β_s	$R^2_{adj.}$	*P*	β_s	$R^2_{adj.}$	*P*	β_s	$R^2_{adj.}$	*P*	β_s	$R^2_{adj.}$	*P*	β_s	$R^2_{adj.}$	*P*
UVCI (n=39)															
Age	-0.46	0.19	**0.003**	0.49	0.22	**0.002**	-0.32	0.08	0.050	0.33	0.09	**0.039**	0.49	0.22	**0.002**
Sex (f-m)	0.15	0.00	0.363	-0.08	-0.02	0.607	0.22	0.02	0.177	-0.21	0.02	0.199	-0.11	-0.02	0.518
Aβ 42 (CSF)	0.02	-0.03	0.923	-0.18	0.01	0.262	-0.24	0.03	0.135	-0.03	-0.03	0.850	-0.18	0.01	0.262
T-tau (CSF)	0.21	0.02	0.207	-0.07	-0.02	0.678	0.32	0.08	**0.044**	-0.08	-0.02	0.632	-0.05	-0.02	0.743
P-tau (CSF)	0.16	0.00	0.334	-0.07	-0.02	0.651	0.23	0.03	0.159	-0.08	-0.02	0.604	-0.05	-0.02	0.760
WMHvol	-0.80	0.62	**0.000**	0.85	0.72	**0.000**	-0.50	0.23	**0.001**	0.62	0.37	**0.000**	0.85	0.71	**0.000**
SVD score	-0.59	0.33	**0.000**	0.62	0.37	**0.000**	-0.39	0.13	**0.013**	0.46	0.19	**0.003**	0.62	0.36	**0.000**
SVCI (n=39)															
Age	-0.16	0.00	0.333	0.11	-0.02	0.521	-0.18	0.01	0.279	0.08	-0.02	0.616	0.11	-0.01	0.490
Sex (f-m)	0.05	-0.03	0.894	-0.03	-0.03	0.943	0.04	-0.03	0.902	0.36	0.00	0.323	-0.05	-0.03	0.888
Aβ (PET)	-0.27	0.05	0.093	0.30	0.06	0.068	-0.11	-0.01	0.505	0.19	0.01	0.244	0.30	0.06	0.064
Tau (PET)	-0.11	-0.01	0.499	0.09	-0.02	0.572	-0.06	-0.02	0.729	0.10	-0.02	0.529	0.09	-0.02	0.579
WMHvol	-0.49	0.22	**0.001**	0.58	0.32	**0.000**	-0.17	0.00	0.288	0.37	0.11	**0.022**	0.57	0.31	**0.000**
SVD score	np	np	np	np	np	np	np	np	np	np	np	np	np	np	np

P < 0.05 in bold. β_s, standardized beta; FAu, uncorrected fractional anisotropy; FAt, free water corrected tissue compartment of fractional anisotropy; FW, free water content; MDu, uncorrected mean diffusivity; MDt, free water corrected tissue compartment of mean diffusivity; np, not possible (all patients had the maximum score); P-tau, phosphorylated-tau_{181}; $R^2_{adj.}$, adjusted explained variance; SVD score, total small vessel disease score; T-tau, total tau; WMHvol, white matter hyperintensity volume.

Supplementary Table 5. Simple regression models in genetically-defined samples

	FAu			MDu			FAt			MDt			FW		
	β_s	$R^2_{adj.}$	*P*	β_s	$R^2_{adj.}$	*P*	β_s	$R^2_{adj.}$	*P*	β_s	$R^2_{adj.}$	*P*	β_s	$R^2_{adj.}$	*P*
DIAN (n=77)															
Age	-0.38	0.13	**0.001**	0.35	0.11	**0.002**	-0.27	0.06	**0.018**	0.05	-0.01	0.669	0.37	0.12	**0.001**
Sex (f-m)	0.25	0.00	0.267	0.06	-0.01	0.805	0.58	0.07	**0.010**	0.44	0.04	0.055	0.05	-0.01	0.821
Aβ 40 (CSF)	0.08	-0.01	0.468	-0.08	-0.01	0.468	0.07	-0.01	0.564	-0.07	-0.01	0.555	-0.07	-0.01	0.522
Aβ 42 (CSF)	0.41	0.16	**0.000**	-0.43	0.17	**0.000**	0.22	0.03	0.057	-0.18	-0.01	0.053	-0.43	0.18	**0.000**
T-tau (CSF)	-0.26	0.05	**0.024**	0.33	0.10	**0.003**	-0.09	0.00	0.427	0.14	0.01	0.228	0.32	0.09	**0.004**
P-tau (CSF)	-0.23	0.04	**0.047**	0.37	0.12	**0.001**	0.01	-0.01	0.918	0.21	0.04	0.056	0.36	0.12	**0.001**
WMHvol	-0.35	0.11	**0.002**	0.45	0.20	**0.000**	-0.08	-0.01	0.484	0.42	0.17	**0.000**	0.47	0.21	**0.000**
SVD score	-0.18	0.02	0.113	0.16	0.01	0.157	-0.11	0.00	0.345	0.13	0.00	0.255	0.18	0.02	0.115
CADASIL (n=68)															
Age	-0.51	0.25	**0.000**	0.56	0.30	**0.000**	-0.42	0.16	**0.000**	0.02	-0.01	0.888	0.52	0.26	**0.000**
Sex (f-m)	-0.19	-0.01	0.450	0.28	0.00	0.267	-0.03	-0.01	0.900	-0.47	0.04	0.064	0.25	0.00	0.322
WMHvol	-0.84	0.71	**0.000**	0.89	0.79	**0.000**	-0.71	0.49	**0.000**	0.39	0.14	**0.001**	0.87	0.76	**0.000**
SVD score	-0.55	0.29	**0.000**	0.54	0.28	**0.000**	-0.54	0.28	**0.000**	0.02	-0.01	0.878	0.52	0.26	**0.000**

P < 0.05 in bold. β_s, standardized beta; FAu, uncorrected fractional anisotropy; FAt, free water corrected tissue compartment of fractional anisotropy; FW, free water content; MDu, uncorrected mean diffusivity; MDt, free water corrected tissue compartment of mean diffusivity; P-tau, phosphorylated-tau_{181}; $R^2_{adj.}$, adjusted explained variance; SVD score, total small vessel disease score; T-tau, total tau; WMHvol, white matter hyperintensity volume.

Supplementary Table 6. Simple regression models in Alzheimer's disease focused samples in amyloid-positive individuals

	FAu			MDu			FAt			MDt			FW		
	β_s	$R^2_{adj.}$	*P*	β_s	$R^2_{adj.}$	*P*	β_s	$R^2_{adj.}$	*P*	β_s	$R^2_{adj.}$	*P*	β_s	$R^2_{adj.}$	*P*
DELCODE (n=44)															
Age	-0.44	0.17	**0.003**	0.43	0.17	**0.003**	-0.31	0.08	**0.040**	0.18	0.01	0.246	0.49	0.22	**0.001**
Sex (f-m)	-0.88	0.18	**0.003**	0.48	0.04	0.114	-0.99	0.23	**0.001**	0.03	-0.02	0.929	0.64	0.08	**0.033**
Aβ 40 (CSF)	-0.03	-0.02	0.827	0.04	-0.02	0.784	-0.01	-0.02	0.966	0.06	-0.02	0.716	0.06	-0.02	0.722
Aβ 42 (CSF)	0.04	-0.02	0.813	0.00	-0.02	0.998	0.00	-0.02	0.981	0.06	-0.02	0.719	-0.05	-0.02	0.742
T-tau (CSF)	-0.17	0.00	0.277	0.15	0.00	0.323	-0.16	0.00	0.309	0.07	-0.02	0.641	0.18	0.01	0.234
P-tau (CSF)	-0.16	0.00	0.307	0.15	0.00	0.319	-0.10	-0.01	0.504	0.08	-0.02	0.608	0.20	0.02	0.203
WMHvol	-0.28	0.05	0.070	0.35	0.11	**0.018**	-0.09	-0.01	0.546	0.13	-0.01	0.406	0.40	0.14	**0.007**
SVD score	-0.26	0.05	0.085	0.32	0.08	**0.033**	-0.17	0.00	0.279	0.13	-0.01	0.384	0.34	0.10	**0.022**
ADNI (n=37)															
Age	-0.35	0.10	**0.032**	0.54	0.27	**0.001**	0.12	-0.01	0.485	0.03	-0.03	0.853	0.53	0.26	**0.001**
Sex (f-m)	0.10	-0.03	0.778	0.24	-0.01	0.483	0.57	0.05	0.088	0.12	-0.02	0.716	0.18	-0.02	0.588
Aβ (PET)	-0.09	-0.02	0.614	0.12	-0.01	0.495	0.05	-0.03	0.782	0.10	-0.02	0.566	0.12	-0.01	0.492
Tau (PET)	-0.06	-0.02	0.708	0.01	-0.03	0.935	-0.19	0.01	0.271	0.24	0.03	0.156	-0.04	-0.03	0.807
WMHvol	-0.49	0.22	**0.002**	0.58	0.32	**0.000**	-0.01	-0.03	0.946	0.09	-0.02	0.612	0.63	0.38	**0.000**
SVD score	-0.30	0.06	0.074	0.43	0.17	**0.007**	0.07	-0.02	0.663	0.29	0.06	0.080	0.42	0.15	**0.010**

P < 0.05 in bold. β_s, standardized beta; FAu, uncorrected fractional anisotropy; FAt, free water corrected tissue compartment of fractional anisotropy; FW, free water content; MDu, uncorrected mean diffusivity; MDt, free water corrected tissue compartment of mean diffusivity; P-tau, phosphorylated-tau_{181}; $R^2_{adj.}$, adjusted explained variance; SVD score, total small vessel disease score; T-tau, total tau; WMHvol, white matter hyperintensity volume.

Supplementary Table 7. Simple regression models in small vessel disease focused samples in amyloid-positive individuals

	FAu			MDu			FAt			MDt			FW		
	β_s	$R^2_{adj.}$	*P*	β_s	$R^2_{adj.}$	*P*	β_s	$R^2_{adj.}$	*P*	β_s	$R^2_{adj.}$	*P*	β_s	$R^2_{adj.}$	*P*
UVCI (n=22)															
Age	-0.33	0.07	0.129	0.35	0.08	0.105	-0.23	0.01	0.305	0.24	0.01	0.281	0.37	0.09	0.091
Sex (f-m)	0.34	0.07	0.121	-0.33	0.07	0.130	0.28	0.03	0.205	-0.42	0.13	0.054	-0.36	0.09	0.101
Aβ 42 (CSF)	-0.05	-0.05	0.827	-0.05	-0.05	0.833	-0.13	-0.03	0.568	0.01	-0.05	0.954	-0.04	-0.05	0.870
T-tau (CSF)	0.32	0.06	0.151	-0.24	0.01	0.292	0.31	0.05	0.159	-0.09	-0.04	0.687	-0.22	0.00	0.336
P-tau (CSF)	0.31	0.05	0.163	-0.24	0.01	0.278	0.28	0.03	0.205	0.01	-0.05	0.981	-0.23	0.00	0.310
WMHvol	-0.73	0.51	**0.000**	0.79	0.61	**0.000**	-0.45	0.16	**0.036**	0.54	0.26	**0.010**	0.81	0.63	**0.000**
SVD score	-0.47	0.18	**0.028**	0.51	0.22	**0.016**	-0.29	0.04	0.191	0.42	0.14	0.051	0.50	0.22	**0.017**
SVCI (n=19)															
Age	-0.18	-0.02	0.456	0.16	-0.03	0.522	-0.11	-0.05	0.646	0.18	-0.02	0.454	0.17	-0.03	0.482
Sex (f-m)	0.66	0.01	0.305	-0.50	-0.02	0.441	0.78	0.03	0.227	0.55	-0.01	0.395	-0.57	-0.01	0.383
Aβ (PET)	-0.11	-0.05	0.657	0.20	-0.02	0.409	0.11	-0.05	0.664	0.30	0.04	0.215	0.19	-0.02	0.433
Tau (PET)	0.02	-0.06	0.925	-0.04	-0.06	0.870	0.03	-0.06	0.898	0.16	-0.03	0.513	-0.05	-0.06	0.853
WMHvol	-0.54	0.25	**0.016**	0.58	0.30	**0.009**	-0.43	0.14	0.065	0.44	0.14	0.063	0.57	0.28	**0.011**
SVD score	np	np	np	np	np	np	np	np	np	np	np	np	np	np	np

P < 0.05 in bold. β_s, standardized beta; FAu, uncorrected fractional anisotropy; FAt, free water corrected tissue compartment of fractional anisotropy; FW, free water content; MDu, uncorrected mean diffusivity; MDt, free water corrected tissue compartment of mean diffusivity; np, not possible (all patients had the maximum score); P-tau, phosphorylated-tau_{181}; $R^2_{adj.}$, adjusted explained variance; SVD score, total small vessel disease score; T-tau, total tau; WMHvol, white matter hyperintensity volume.

Supplementary Table 8. Simple regression models in genetically-defined samples in amyloid-positive individuals

	FAu			MDu			FAt			MDt			FW		
	β_s	$R^2_{adj.}$	*P*	β_s	$R^2_{adj.}$	*P*	β_s	$R^2_{adj.}$	*P*	β_s	$R^2_{adj.}$	*P*	β_s	$R^2_{adj.}$	*P*
DIAN (n=46)															
Age	-0.10	-0.01	0.495	0.08	-0.02	0.579	-0.11	-0.01	0.483	0.07	-0.02	0.620	0.09	-0.02	0.571
Sex (f-m)	0.32	0.00	0.284	-0.09	-0.02	0.768	0.71	0.11	**0.015**	0.37	0.01	0.212	-0.09	-0.02	0.769
Aβ 40 (CSF)	0.01	-0.02	0.940	-0.01	-0.02	0.966	0.04	-0.02	0.806	-0.04	-0.02	0.808	0.00	-0.02	0.998
Aβ 42 (CSF)	0.27	0.05	0.074	-0.23	0.03	0.127	0.22	0.02	0.150	-0.20	0.02	0.183	-0.24	0.04	0.111
T-tau (CSF)	-0.24	0.03	0.114	0.26	0.04	0.086	-0.16	0.00	0.284	0.05	-0.02	0.730	0.24	0.04	0.102
P-tau (CSF)	-0.25	0.04	0.090	0.32	0.08	**0.031**	-0.08	-0.02	0.609	0.13	-0.01	0.401	0.31	0.07	**0.038**
WMHvol	-0.28	0.06	0.056	0.35	0.10	**0.017**	0.02	-0.02	0.919	0.39	0.13	**0.008**	0.37	0.12	**0.011**
SVD score	-0.03	-0.02	0.861	0.03	-0.02	0.854	0.00	-0.02	0.985	0.13	-0.01	0.405	0.04	-0.02	0.810
CADASIL															
Age	na	na	na	na	na	na	na	na	na	na	na	na	na	na	na
Sex (f-m)	na	na	na	na	na	na	na	na	na	na	na	na	na	na	na
WMHvol	na	na	na	na	na	na	na	na	na	na	na	na	na	na	na
SVD score	na	na	na	na	na	na	na	na	na	na	na	na	na	na	na

P < 0.05 in bold. β_s, standardized beta; FAu, uncorrected fractional anisotropy; FAt, free water corrected tissue compartment of fractional anisotropy; FW, free water content; MDu, uncorrected mean diffusivity; MDt, free water corrected tissue compartment of mean diffusivity; na, not available; P-tau, phosphorylated-tau_{181}; $R^2_{adj.}$, adjusted explained variance; SVD score, total small vessel disease score; T-tau, total tau; WMHvol, white matter hyperintensity volume.

Supplementary Table 9. DIAN consortium

Last Name	First	Affiliation
Allegri	Ricardo	FLENI Institute of Neurological Research (Fundacion para la Lucha contra las Enfermedades Neurologicas de la Infancia)
Bateman	Randy	Washington University in St. Louis School of Medicine
Bechara	Jacob	Neuroscience Research Australia
Benzinger	Tammie	Washington University in St. Louis School of Medicine
Berman	Sarah	University of Pittsburgh
Bodge	Courtney	Brown University-Butler Hospital
Brandon	Susan	Washington University in St. Louis School of Medicine
Brooks	William (Bill)	Neuroscience Research Australia
Buck	Jill	Indiana University
Buckles	Virginia	Washington University in St. Louis School of Medicine
Chea	Sochenda	Mayo Clinic Jacksonville
Chhatwal	Jasmeer	Brigham and Women's Hospital–Massachusetts General Hospital
Chrem	Patricio	FLENI Institute of Neurological Research (Fundacion para la Lucha contra las Enfermedades Neurologicas de la Infancia)
Chui	Helena	University of Southern California
Cinco	Jake	University College London
Clifford	Jack	Mayo Clinic Jacksonville
Cruchaga	Carlos	Washington University in St. Louis School of Medicine
Donahue	Tamara	Washington University in St. Louis School of Medicine
Douglas	Jane	University College London
Edigo	Noelia	FLENI Institute of Neurological Research (Fundacion para la Lucha contra las Enfermedades Neurologicas de la Infancia)
Erekin-Taner	Nilufer	Mayo Clinic Jacksonville
Fagan	Anne	Washington University in St. Louis School of Medicine
Farlow	Marty	Indiana University
Fitzpatrick	Colleen	Brigham and Women's Hospital-Massachusetts
Flynn	Gigi	Washington University in St. Louis School of Medicine
Fox	Nick	University College London
Franklin	Erin	Washington University in St. Louis School of Medicine
Fujii	Hisako	Osaka City University
Gant	Cortaiga	Washington University in St. Louis School of Medicine
Gardener	Samantha	Edith Cowan University, Perth
Ghetti	Bernardino	Indiana University
Goate	Alison	Icahn School of Medicine at Mount Sinai
Goldman	Jill	Columbia University
Gordon	Brian	Washington University in St. Louis School of Medicine
Graff-Radford	Neill	Mayo Clinic Jacksonville
Gray	Julia	Washington University in St. Louis School of Medicine

Last Name	First	Affiliation
Groves	Alexander	Washington University in St. Louis School of Medicine
Hassenstab	Jason	Washington University in St. Louis School of Medicine
Hoechst-Swisher	Laura	Washington University in St. Louis School of Medicine
Holtzman	David	Washington University in St. Louis School of Medicine
Hornbeck	Russ	Washington University in St. Louis School of Medicine
Houeland DiBari	Siri	German Center for Neurodegenerative Diseases (DZNE) Munich
Ikeuchi	Takeshi	Niigata University
Ikonomovic	Snezana	University of Pittsburgh
Jerome	Gina	Washington University in St. Louis School of Medicine
Jucker	Mathias	German Center for Neurodegnerative Diseases (DZNE) Tubingen
Karch	Celeste	Washington University in St. Louis School of Medicine
Kasuga	Kensaku	Niigata University
Kawarabayashi	Takeshi	Hirosaki University
Klunk	William (Bill)	University of Pittsburgh
Koeppe	Robert	University of Michigan
Kuder-Buletta	Elke	German Center for Neurodegnerative Diseases (DZNE) Tubingen
Laske	Christoph	German Center for Neurodegnerative Diseases (DZNE) Tubingen
Lee	Jae-Hong	Asan Medical Center
Levin	Johannes	German Center for Neurodegnerative Diseases (DZNE) Munich
Martins	Ralph	Edith Cowan University
Mason	Neal Scott	University of Pittsburgh Medical Center
Masters	Colin	University of Melbourne
Maue-Dreyfus	Denise	Washington University in St. Louis School of Medicine
McDade	Eric	Washington University in St. Louis School of Medicine
Mori	Hiroshi	Osaka City University
Morris	John	Washington University in St. Louis School of Medicine
Nagamatsu	Akem	Tokyo University
Neimeyer	Katie	Columbia University
Noble	James	Columbia University
Norton	Joanne	Washington University in St. Louis School of Medicine
Perrin	Richard	Washington University in St. Louis School of Medicine
Raichle	Marc	Washington University in St. Louis School of Medicine
Renton	Alan	Icahn School of Medicine at Mount Sinai
Ringman	John	University of Southern California
Roh	Jee Hoon	Asan Medical Center
Salloway	Stephen	Brown University-Butler Hospital
Schofield	Peter	Neuroscience Research Australia

Last Name	First	Affiliation
Shimada	Hiroyuki	Osaka City University
Sigurdson	Wendy	Washington University in St. Louis School of Medicine
Sohrabi	Hamid	Edith Cowan University
Sparks	Paige	Brigham and Women's Hospital-Massachusetts
Suzuki	Kazushi	Tokyo University
Taddei	Kevin	Edith Cowan University
Wang	Peter	Washington University in St. Louis School of Medicine
Xiong	Chengjie	Washington University in St. Louis School of Medicine
Xu	Xiong	Washington University in St. Louis School of Medicine

Supplementary Table 10. DELCODE study group

Last Name	First	Affiliation
Fuentes	Manuel	German Center for Neurodegenerative Diseases (DZNE), Berlin, Germany; Charité – Universitätsmedizin Berlin, corporate member of Freie Universität Berlin, Humboldt-Universität zu Berlin, and Berlin Institute of Health, Institute of Psychiatry and Psychotherapy, Hindenburgdamm 30, 12203 Berlin, Germany
Hauser	Dietmar	Charité – Universitätsmedizin Berlin, corporate member of Freie Universität Berlin, Humboldt-Universität zu Berlin, and Berlin Institute of Health, Institute of Psychiatry and Psychotherapy, Hindenburgdamm 30, 12203 Berlin, Germany
Lindner	Katja	Charité – Universitätsmedizin Berlin, corporate member of Freie Universität Berlin, Humboldt-Universität zu Berlin, and Berlin Institute of Health, Institute of Psychiatry and Psychotherapy, Hindenburgdamm 30, 12203 Berlin, Germany
Megges	Herlind	German Center for Neurodegenerative Diseases (DZNE), Berlin, Germany; Charité – Universitätsmedizin Berlin, corporate member of Freie Universität Berlin, Humboldt-Universität zu Berlin, and Berlin Institute of Health, Institute of Psychiatry and Psychotherapy, Hindenburgdamm 30, 12203 Berlin, Germany
Menne	Felix	German Center for Neurodegenerative Diseases (DZNE), Berlin, Germany; Charité – Universitätsmedizin Berlin, corporate member of Freie Universität Berlin, Humboldt-Universität zu Berlin, and Berlin Institute of Health, Institute of Psychiatry and Psychotherapy, Hindenburgdamm 30, 12203 Berlin, Germany

Last Name	First	Affiliation
Peters	Oliver	German Center for Neurodegenerative Diseases (DZNE), Berlin, Germany; Charité – Universitätsmedizin Berlin, corporate member of Freie Universität Berlin, Humboldt-Universität zu Berlin, and Berlin Institute of Health, Institute of Psychiatry and Psychotherapy, Hindenburgdamm 30, 12203 Berlin, Germany
Amthauer	Holger	Charité – Universitätsmedizin Berlin, corporate member of Freie Universität Berlin, Humboldt-Universität zu Berlin, and Berlin Institute of Health, Department of Nuclear Medicine, Augustenburger Platz 1, 13353 Berlin
Kainz	Christian	Center for Cognitive Neuroscience Berlin (CCNB), Department of Education and Psychology, Freie Universität Berlin, Berlin, Germany
Ehrlich	Marie	Charité – Universitätsmedizin Berlin, corporate member of Freie Universität Berlin, Humboldt-Universität zu Berlin, and Berlin Institute of Health, Institute of Psychiatry and Psychotherapy, Hindenburgdamm 30, 12203 Berlin, Germany
Altenstein	Slawek	German Center for Neurodegenerative Diseases (DZNE), Berlin, Germany
Beuth	Markus	Department of Psychiatry and Psychotherapy, Charité, Charitéplatz 1, 10117 Berlin, Germany
Langenfurth	Anika	Department of Psychiatry and Psychotherapy, Charité, Charitéplatz 1, 10117 Berlin, Germany
Priller	Josef	German Center for Neurodegenerative Diseases (DZNE), Berlin, Germany; Department of Psychiatry and Psychotherapy, Charité, Charitéplatz 1, 10117 Berlin, Germany
Spruth	Eike	Department of Psychiatry and Psychotherapy, Charité, Charitéplatz 1, 10117 Berlin, Germany
Villar Munoz	Irene	German Center for Neurodegenerative Diseases (DZNE), Berlin, Germany
Konstantina	Kafali	Department of Psychiatry and Psychotherapy, Charité, Charitéplatz 1, 10117 Berlin, Germany
Barkhoff	Miriam	German Center for Neurodegenerative Diseases (DZNE), Bonn, Venusberg-Campus 1, 53127 Bonn, Germany
Boecker	Henning	German Center for Neurodegenerative Diseases (DZNE), Bonn, Venusberg-Campus 1, 53127 Bonn, Germany
Daamen	Marcel	German Center for Neurodegenerative Diseases (DZNE), Bonn, Venusberg-Campus 1, 53127 Bonn, Germany
Faber	Jennifer	German Center for Neurodegenerative Diseases (DZNE), Bonn, Venusberg-Campus 1, 53127 Bonn, Germany
Fließbach	Klaus	German Center for Neurodegenerative Diseases (DZNE), Bonn, Venusberg-Campus 1, 53127 Bonn, Germany
Frommann	Ingo	German Center for Neurodegenerative Diseases (DZNE), Bonn, Venusberg-Campus 1, 53127 Bonn, Germany

Last Name	First	Affiliation
Hennes	Guido	German Center for Neurodegenerative Diseases (DZNE), Bonn, Venusberg-Campus 1, 53127 Bonn, Germany
Herrmann	Gabi	German Center for Neurodegenerative Diseases (DZNE), Bonn, Venusberg-Campus 1, 53127 Bonn, Germany
Kalbhen	Pascal	German Center for Neurodegenerative Diseases (DZNE), Bonn, Venusberg-Campus 1, 53127 Bonn, Germany
Kobeleva	Xenia	German Center for Neurodegenerative Diseases (DZNE), Bonn, Venusberg-Campus 1, 53127 Bonn, Germany
Kofler	Barbara	German Center for Neurodegenerative Diseases (DZNE), Bonn, Venusberg-Campus 1, 53127 Bonn, Germany
Miebach	Lisa	German Center for Neurodegenerative Diseases (DZNE), Bonn, Venusberg-Campus 1, 53127 Bonn, Germany
Müller	Anna	German Center for Neurodegenerative Diseases (DZNE), Bonn, Venusberg-Campus 1, 53127 Bonn, Germany
Polcher	Alexandra	German Center for Neurodegenerative Diseases (DZNE), Bonn, Venusberg-Campus 1, 53127 Bonn, Germany
Röske	Sandra	German Center for Neurodegenerative Diseases (DZNE), Bonn, Venusberg-Campus 1, 53127 Bonn, Germany
Schneider	Christine	German Center for Neurodegenerative Diseases (DZNE), Bonn, Venusberg-Campus 1, 53127 Bonn, Germany
Schneider	Anja	German Center for Neurodegenerative Diseases (DZNE), Bonn, Venusberg-Campus 1, 53127 Bonn, Germany; Department for Neurodegenerative Diseases and Geriatric Psychiatry, University Hospital Bonn, Venusberg-Campus 1, 53127 Bonn, Germany
Spottke	Annika	German Center for Neurodegenerative Diseases (DZNE), Bonn, Venusberg-Campus 1, 53127 Bonn, Germany; Department of Neurology, University of Bonn, Venusberg-Campus 1, 53127 Bonn, Germany
Vogt	Ina	German Center for Neurodegenerative Diseases (DZNE), Bonn, Venusberg-Campus 1, 53127 Bonn, Germany
Wagner	Michael	German Center for Neurodegenerative Diseases (DZNE), Bonn, Venusberg-Campus 1, 53127 Bonn, Germany; Department for Neurodegenerative Diseases and Geriatric Psychiatry, University Hospital Bonn, Venusberg-Campus 1, 53127 Bonn, Germany
Westerteicher	Christine	Department of Psychiatry and Psychotherapy, University of Bonn, Venusberg-Campus 1, 53127 Bonn, Germany
Widmann	Catherine	Department of Psychiatry and Psychotherapy, University of Bonn, Venusberg-Campus 1, 53127 Bonn, Germany
Wolfsgruber	Steffen	German Center for Neurodegenerative Diseases (DZNE), Bonn, Venusberg-Campus 1, 53127 Bonn, Germany
Yilmaz	Sagik	German Center for Neurodegenerative Diseases (DZNE), Bonn, Venusberg-Campus 1, 53127 Bonn, Germany
Brosseron	Frederic	German Center for Neurodegenerative Diseases (DZNE), Bonn, Venusberg-Campus 1, 53127 Bonn, Germany

Last Name	First	Affiliation
Jessen	Frank	German Center for Neurodegenerative Diseases (DZNE), Bonn, Venusberg-Campus 1, 53127 Bonn, Germany; Department of Psychiatry, University of Cologne, Medical Faculty, Kerpener Strasse 62, 50924 Cologne, Germany
Bürger	Katharina	German Center for Neurodegenerative Diseases (DZNE, Munich), Feodor-Lynen-Strasse 17, 81377 Munich, Germany; Institute for Stroke and Dementia Research (ISD), University Hospital, LMU Munich, Feodor-Lynen-Strasse 17, 81377 Munich, Germany
Catak	Cihan	Institute for Stroke and Dementia Research (ISD), University Hospital, LMU Munich, Feodor-Lynen-Strasse 17, 81377 Munich, Germany
Coloma Andrews	Lisa	German Center for Neurodegenerative Diseases (DZNE, Munich), Feodor-Lynen-Strasse 17, 81377 Munich, Germany
Dichgans	Martin	Institute for Stroke and Dementia Research (ISD), University Hospital, LMU Munich, Feodor-Lynen-Strasse 17, 81377 Munich, Germany German Center for Neurodegenerative Diseases (DZNE, Munich), Feodor-Lynen-Strasse 17, 81377 Munich, Germany Munich Cluster for Systems Neurology (SyNergy), Munich, Germany
Dörr	Angelika	Institute for Stroke and Dementia Research (ISD), University Hospital, LMU Munich, Feodor-Lynen-Strasse 17, 81377 Munich, Germany
Ertl-Wagner	Birgit	Department of Radiology, University Hospital, LMU Munich, Germany
Frimmer	Daniela	Institute for Stroke and Dementia Research (ISD), University Hospital, LMU Munich, Feodor-Lynen-Strasse 17, 81377 Munich, Germany
Huber	Brigitte	Institute for Stroke and Dementia Research (ISD), University Hospital, LMU Munich, Feodor-Lynen-Strasse 17, 81377 Munich, Germany
Janowitz	Daniel	Institute for Stroke and Dementia Research (ISD), University Hospital, LMU Munich, Feodor-Lynen-Strasse 17, 81377 Munich, Germany
Kreuzer	Max	Institute for Stroke and Dementia Research (ISD), University Hospital, LMU Munich, Feodor-Lynen-Strasse 17, 81377 Munich, Germany
Markov	Eva	Institute for Stroke and Dementia Research (ISD), University Hospital, LMU Munich, Feodor-Lynen-Strasse 17, 81377 Munich, Germany
Müller	Claudia	German Center for Neurodegenerative Diseases (DZNE, Munich), Feodor-Lynen-Strasse 17, 81377 Munich, Germany
Rominger	Axel	Department of Nuclear Medicine, University Hospital, LMU Munich, Munich, Germany Munich Cluster for Systems Neurology (SyNergy), Munich, Germany

Last Name	First	Affiliation
Schmid (form. Spreider)	Jennifer	Institute for Stroke and Dementia Research (ISD), University Hospital, LMU Munich, Feodor-Lynen-Strasse 17, 81377 Munich, Germany
Seegerer	Anna	Institute for Stroke and Dementia Research (ISD), University Hospital, LMU Munich, Feodor-Lynen-Strasse 17, 81377 Munich, Germany
Zollver	Adelgunde	Institute for Stroke and Dementia Research (ISD), University Hospital, LMU Munich, Feodor-Lynen-Strasse 17, 81377 Munich, Germany
Brüggen	Katharina	German Center for Neurodegenerative Diseases (DZNE), Rostock, Germany
Dyrba	Martin	German Center for Neurodegenerative Diseases (DZNE), Rostock, Germany
Heine	Christina	Department of Psychosomatic Medicine, Rostock University Medical Center, Gehlsheimer Str. 20, 18147 Rostock
Henf	Judith	Department of Psychosomatic Medicine, Rostock University Medical Center, Gehlsheimer Str. 20, 18147 Rostock
Kasper	Elisabeth	Department of Psychosomatic Medicine, Rostock University Medical Center, Gehlsheimer Str. 20, 18147 Rostock
Kilimann	Ingo	German Center for Neurodegenerative Diseases (DZNE), Rostock, Germany
Korp	Christin	German Center for Neurodegenerative Diseases (DZNE), Rostock, Germany
Lau	Esther	German Center for Neurodegenerative Diseases (DZNE), Rostock, Germany
Pfaff	Henrike	Department of Psychosomatic Medicine, Rostock University Medical Center, Gehlsheimer Str. 20, 18147 Rostock
Raum	Heike	German Center for Neurodegenerative Diseases (DZNE), Rostock, Germany
Sabik	Petr	German Center for Neurodegenerative Diseases (DZNE), Rostock, Germany
Sänger	Peter	Department of Psychosomatic Medicine, Rostock University Medical Center, Gehlsheimer Str. 20, 18147 Rostock
Schmidt	Monika	German Center for Neurodegenerative Diseases (DZNE), Rostock, Germany
Szagarus	Anna	German Center for Neurodegenerative Diseases (DZNE), Rostock, Germany
Teipel	Stefan	German Center for Neurodegenerative Diseases (DZNE), Rostock, Germany; Department of Psychosomatic Medicine, Rostock University Medical Center, Gehlsheimer Str. 20, 18147 Rostock
Weschke	Sarah	Department of Psychosomatic Medicine, Rostock University Medical Center, Gehlsheimer Str. 20, 18147 Rostock

Last Name	First	Affiliation
Janecek-Meyer	Heike	Department of Psychosomatic Medicine, Rostock University Medical Center, Gehlsheimer Str. 20, 18147 Rostock
Schulz	Heike	German Center for Neurodegenerative Diseases (DZNE), Rostock, Germany
Weber	Marc-Andre	Institut für Diagnostische und Interventionelle Radiologie, Universitätsmedizin Rostock
Buchmann	Martina	Section for Dementia Research, Hertie Institute for Clinical Brain Research and Department of Psychiatry and Psychotherapy, University of Tübingen, Tübingen, Germany
Hinderer	Petra	German Center for Neurodegenerative Diseases (DZNE), Tübingen, Germany
Kuder-Buletta	Elke	German Center for Neurodegenerative Diseases (DZNE), Tübingen, Germany
Laske	Christoph	German Center for Neurodegenerative Diseases (DZNE), Tübingen, Germany; Section for Dementia Research, Hertie Institute for Clinical Brain Research and Department of Psychiatry and Psychotherapy, University of Tübingen, Tübingen, Germany
Mychajliw	Christian	German Center for Neurodegenerative Diseases (DZNE), Tübingen, Germany

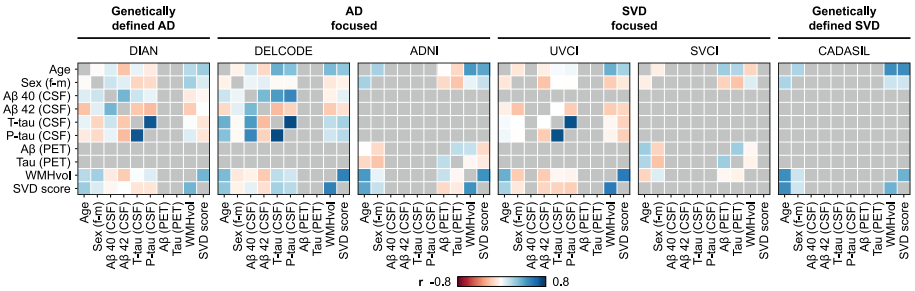

Supplementary Figure 1. Correlation matrices. Intercorrelations (multicollinearity between AD biomarkers, SVD markers, age, and sex. Grey boxes indicate "not available". AD, Alzheimer's disease; P-tau, phosphorylated-tau$_{181}$; SVD, small vessel disease; SVD score, total small vessel disease score; T-tau, total tau; WMHvol, white matter hyperintensity volume.

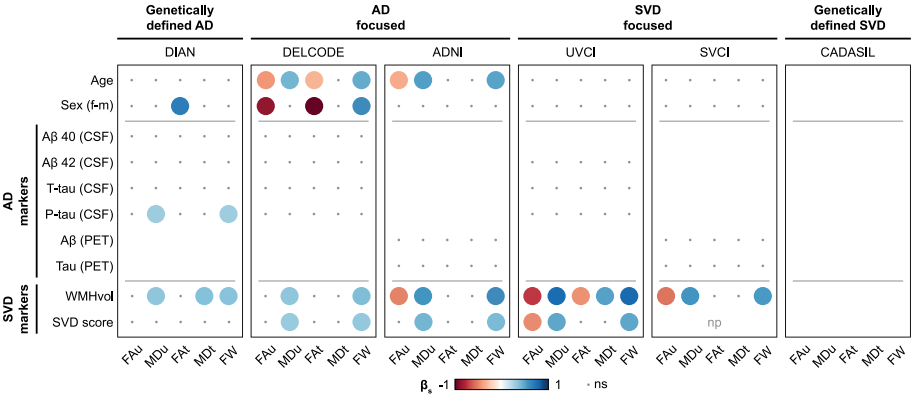

Supplementary Figure 2. Simple regression analyses in amyloid-positive individuals. Simple linear regression analyses between diffusion measures and AD biomarkers or SVD markers in amyloid-positive individuals (sensitivity analysis). Standardized β is represented by color. AD, Alzheimer's disease; β_s, standardized beta; FAu, uncorrected fractional anisotropy; FAt, free water corrected tissue compartment of fractional anisotropy; FW, free water content; MDu, uncorrected mean diffusivity; MDt, free water corrected tissue compartment of mean diffusivity; np, not possible (all patients had the maximum score); ns, not significant; p-tau, phosphorylated- tau$_{181}$; SVD, small vessel disease; SVD score, total small vessel disease score; t-tau, total tau; WMHvol, white matter hyperintensity volume.

Supplementary Text 1. CSF and PET markers

CSF markers

Aβ 40, Aβ 42, t-tau, and p-tau CSF measurements were analyzed locally (within each study) with study specific assays for DIAN,[1] DELCODE,[2] and UVCI.[3] For the subgroup analysis we used the following cut-offs for Aβ 42 (CSF) abnormality: < 496 pg/ml (DELCODE)[2] and < 640 pg/ml (UVCI).[4] For DIAN no study-specific cut-off was available, thus we applied the more restrictive DELCODE threshold (< 496 pg/ml).

PET markers

Aβ [^{18}F]-florbetapir (ADNI) or Aβ [^{18}F]-florbetaben (SVCI) and tau [^{18}F]AV-1451 PET measures were obtained. Details on PET acquisition and analysis are available for ADNI (http://adni.loni.usc.edu) and SVCI.[5] For ADNI, we used the freesurfer-derived global Aβ (PET) SUVR scores across the frontal, anterior-posterior cingulate, lateral-parietal, and lateral-temporal gray matter regions with whole cerebellum as the reference region (provided by the ADNI-PET Core). For SVCI we used locally calculated global Aβ PET SUVR scores across 25 cerebral cortex regions with cerebellar grey matter as the reference region.[5] For the subgroup analysis we used the following Aβ (PET) cut-offs for abnormality: Aβ [^{18}F]-florbetapir > 1.11 (ADNI)[6] and Aβ [^{18}F]-florbetaben > 1.45 (SVCI).[7] For both PET samples, we calculated an established global mean tau PET SUVR score.[8]

Supplementary Text 2. Processing of diffusion measures

All diffusion images were processed with the same pipeline. After visual inspection to exclude major artefacts, raw diffusion images were pre-processed using the MRtrix v3.0 package (http://www.mrtrix.org) and the Functional Magnetic Resonance Imaging of the Brain software library (FSL), v5.0.10.[9] Noise and Gibbs ringing artefacts were removed ('dwidenoise', 'mrdegibbs';[10] MRtrix) and images were corrected for subject motion and eddy current induced distortions ('eddy_correct'; FSL). Conventional DTI measures, i.e., uncorrected fractional anisotropy (FAu) and mean diffusivity (MDu), as well as free water imaging measures, i.e., the free water corrected tissue measures, FAt and MDt, and the free water content (FW), were calculated as previously described.[11] Global and voxel-wise alterations of diffusion measures were assessed on the skeleton of main white matter tracts, which was calculated using the tract-based spatial statistics pipeline[12] within FSL. For all samples, an FAt threshold ≥ 0.3 and a custom-made mask[13] were used to exclude areas prone to CSF contamination, a crucial aspect in patient samples with brain atrophy.[14]

The number of diffusion MRI scans excluded from analysis are reported in Figure 1. Main reasons for exclusion were a cropped field-of-view, uncorrectable motion artefacts and uncorrectable registration errors within the tract-based spatial statistics pipeline.

REFERENCES SUPPLEMENTARY TEXT 1 AND 2

1. Araque Caballero MÁ, Suárez-Calvet M, Duering M, et al. White matter diffusion alterations precede symptom onset in autosomal dominant Alzheimer's disease. Brain. 2018;141(10):3065-80.
2. Jessen F, Spottke A, Boecker H, et al. Design and first baseline data of the DZNE multicenter observational study on predementia Alzheimer's disease (DELCODE). Alzheimer's research & therapy. 2018;10(1):15.
3. de Wilde A, van Maurik IS, Kunneman M, et al. Alzheimer's Biomarkers In Daily Practice (ABIDE) project: rationale and design. Alzheimer's & Dementia: Diagnosis, Assessment & Disease Monitoring. 2017;6:143-51.
4. Zwan M, van Harten A, Ossenkoppele R, et al. Concordance between cerebrospinal fluid biomarkers and [11C] PIB PET in a memory clinic cohort. Journal of Alzheimer's Disease. 2014;41(3):801-7.
5. Kim HJ, Park S, Cho H, et al. Assessment of extent and role of tau in subcortical vascular cognitive impairment using 18F-AV1451 positron emission tomography imaging. JAMA neurology. 2018;75(8):999-1007.
6. Landau SM, Mintun MA, Joshi AD, et al. Amyloid deposition, hypometabolism, and longitudinal cognitive decline. Annals of neurology. 2012;72(4):578-86.
7. Bullich S, Seibyl J, Catafau AM, et al. Optimized classification of 18F-Florbetaben PET scans as positive and negative using an SUVR quantitative approach and comparison to visual assessment. NeuroImage: Clinical. 2017;15:325-32.
8. Maass A, Landau S, Baker SL, et al. Comparison of multiple tau-PET measures as biomarkers in aging and Alzheimer's disease. Neuroimage. 2017;157:448-63.
9. Smith SM, Jenkinson M, Woolrich MW, et al. Advances in functional and structural MR image analysis and implementation as FSL. Neuroimage. 2004;23:S208-S19.
10. Kellner E, Dhital B, Kiselev VG, Reisert M. Gibbs-ringing artifact removal based on local subvoxel-shifts. Magnetic resonance in medicine. 2016;76(5):1574-81.
11. Duering M, Finsterwalder S, Baykara E, et al. Free water determines diffusion alterations and clinical status in cerebral small vessel disease. Alzheimer's & dementia: the journal of the Alzheimer's Association. 2018;14(6):764-74.
12. Smith SM, Jenkinson M, Johansen-Berg H, et al. Tract-based spatial statistics: voxelwise analysis of multi-subject diffusion data. Neuroimage. 2006;31(4):1487-505.
13. Baykara E, Gesierich B, Adam R, et al. A novel imaging marker for small vessel disease based on skeletonization of white matter tracts and diffusion histograms. Annals of neurology. 2016;80(4):581-92.
14. Berlot R, Metzler-Baddeley C, Jones DK, O'Sullivan MJ. CSF contamination contributes to apparent microstructural alterations in mild cognitive impairment. Neuroimage. 2014;92:27-35.

3

CHAPTER

The relation between small vessel function and white matter microstructure in monogenic and sporadic small vessel disease - the ZOOM@SVDs study

Naomi Vlegels*, Hilde van den Brink*,
Anna Kopczak, Tine Arts, Stanley Pham, Jeroen Siero,
Benno Gesierich, Alberto de Luca, Marco Duering,
Jaco Zwanenburg, Martin Dichgans,
Geert Jan Biessels on behalf of the SVDs@target group

*These authors contributed equally to this work

Manuscript in preparation for submission

ABSTRACT

Background. In cerebral small vessel disease, vascular dysfunction has been associated with widespread tissue injury. Here we further explore these associations and hypothesize that local variation in vascular dysfunction explains regional variance in injury.

Methods. We included 23 patients with monogenic cSVD (i.e., CADASIL) and 46 patients with sporadic cSVD. With whole-brain analyses, we tested if small vessel flow velocity and reactivity measures from 7T-MRI associated with global peak-width-of-skeletonized-mean-diffusivity (PSMD). We also tested voxel-wise correlations between reactivity to hypercapnia and mean diffusivity (MD) in white matter.

Results. Whole-brain analyses showed a negative association between blood flow velocity within perforating arteries and PSMD in the centrum semiovale in CADASIL and in the basal ganglia in sporadic cSVD. Global white matter reactivity to hypercapnia was not associated with PSMD, but we did observe significant voxel-wise negative correlations between BOLD% signal change and MD both in CADASIL and sporadic cSVD.

Conclusion. In conclusion, both in patients with CADASIL and sporadic cSVD small vessel dysfunction is associated with microstructural white matter alterations, also at voxel-level. The latter may reflect a direct causal relationship between local small vessel dysfunction and tissue injury.

INTRODUCTION

Cerebral small vessel disease (cSVD) is a major cause of stroke and dementia among the elderly.[1,2] With MRI, cSVD has mostly been studied through markers of parenchymal injury (e.g., white matter hyperintensities (WMH), lacunes, cerebral microbleeds[3]). The processes that underlie the formation of these lesions likely involve disturbances at the level of the cerebral small vessels. Due to their small size these vessels are difficult to probe *in vivo*. Previous studies on the small vessels in cSVD therefore mostly involved neuropathology of autopsy material, showing loss of smooth muscle cells, thickening of the vessel walls and luminal narrowing in cerebral arterioles, but also abnormalities in capillaries and venules.[2] Over the past years, these observations have been complemented by functional vascular measures using MRI. This included studies at common field strengths (i.e., up to 3T-MRI), showing that decreased vessel function related to increased WMH burden.[4–11] With technological advancements on 7T-MRI we can now assess small vessel flow velocity and pulsatility index as well as (small) vessel reactivity with a sensitivity and temporal and spatial resolution that was not possible before *in vivo* in humans.[12] We recently showed that these measures of small vessel function on 7T-MRI were abnormal in patients with cSVD, indicative of regional abnormalities in arteriolar stiffness and reactivity. There were similarities, but also apparent differences in the way that these measures of small vessel function were altered in patients with monogenic (i.e., CADASIL) versus sporadic cSVD ([13], van den Brink et al. in preparation).

Diffusion MRI-based measures of the white matter microstructure are currently the most sensitive method for studying tissue injury in cSVD.[14,15] Diffusion MRI quantifies the diffusion properties of water molecules in brain tissue and is thereby highly sensitive in detecting subtle tissue alterations. Moreover, cSVD related diffusion alterations are associated with clinical deficits and typically outperform conventional MRI markers in terms of strength of this association.[15,16] Diffusion alterations in cSVD can be assessed locally in the white matter, at voxel level, but also with robust global measures such as *"peak width of skeletonized mean diffusivity"* (PSMD). PSMD is a sensitive and robust measure of white matter microstructure.[15]

In the current study, we tested the association between several complementary novel measures of small vessel dysfunction on 7T-MRI with diffusion MRI measures

of white matter microstructure, both in patients with CADASIL and more common sporadic cSVD. We capitalized on the high spatial resolution of 7T-MRI to also directly relate small vessel function impairment to tissue injury on a voxel-by-voxel level, because we hypothesize that local variation in vascular dysfunction explains regional variance in tissue injury.

METHODS

Participants and study procedure

Patients with cSVD were recruited through the ZOOM@SVDs study, a prospective observational cohort study,[12] at the Institute of Stroke and Dementia Research at Ludwig Maximilian University (LMU) Munich, Germany, and the University Medical Center Utrecht (UMCU) in the Netherlands. Detailed inclusion and exclusion criteria and study procedures are published in the design paper of ZOOM@SVDs[12] but a short description can be found below:

- Monogenic cSVD: At LMU, a tertiary national referral centre for patients with CADASIL in Germany, 23 patients with CADASIL and 13 age- and sex-matched reference participants were recruited. CADASIL was either confirmed by molecular genetic testing (n=20) or by skin biopsy (n=3). Reference participants without cSVD (defined as no history of stroke or of cognitive complaints for which the person has previously sought medical advice, and no so-called "silent" cSVD (Fazekas <2 and no lacunes) on the study MRI) were recruited among partners or relatives of the patients and through advertisement. There were no screen failures. All participants underwent clinical assessment and 3T brain MRI at LMU and travelled to the UMCU to undergo 7T brain MRI.
- Sporadic cSVD: At the stroke and memory clinics of the UMCU and referring centres, 54 patients with symptomatic sporadic cSVD and 28 age- and sex- matched reference participants were recruited. Symptomatic sporadic cSVD was defined as having a history of clinical lacunar stroke in the last 5 years with a corresponding lesion on MRI or CT, or having cognitive impairment with confluent WMH on MRI (Fazekas ≥ 2). Reference participants without cSVD were recruited among partners or relatives of the patients and through advertisement. There were 3 patients for

whom we could not confirm a small subcortical infarct on the study MRI, 3 reference participants were excluded because of signs of silent cSVD on the study MRI and 1 reference participant was excluded because of objective cognitive impairment. This left 51 included patients and 24 included reference participants. These participants underwent clinical assessment, 3T and 7T brain MRI at the UMCU.

For the current study we only included patients and reference participants with at least one available small vessel function measure on 7T-MRI and available diffusion MRI. We could include all patients with CADASIL (n=23) and their reference participants (n=13). We had to exclude 5 patients with sporadic cSVD and 2 of their reference participants due to missing small vessel function measures and 1 of the reference participants due to a failed diffusion scan, leaving 46 patients with sporadic cSVD and 21 reference participants for this study.

The Medical Ethics Review Committees of LMU and UMCU both approved the study, which is conducted in accordance with the declaration of Helsinki and the European law of General Data Protection Regulation. Written informed consent was obtained from all participants prior to enrolment in the study.

Brain MRI acquisition

At LMU, 3T brain MRI was acquired in patients with CADASIL and reference participants on a Siemens Magnetom Skyra 3T scanner with a 64-channel head/neck coil. At UMCU, a Philips Achieva 3T scanner with an 8-channel SENSE head coil was used for the 3T brain MRI in patients with sporadic cSVD and reference participants. The scan protocol and acquisition parameters have been previously published[12] and included a 3D T1-weighted gradient echo, a 3D T2*-weighted gradient echo, a 3D fluid-attenuated inversion recovery (FLAIR), and a diffusion-weighted MRI scan (LMU: voxel size 2x2x2m^3, TR/TE: 3800/104.8 ms, b-values: 0, 1000 and 2000 s/mm^2, 90 diffusion directions (30 for b = 1000 s/mm^2, 60 for b = 2000 s/mm^2); UMCU: voxel size 2.5x2.5x2.5mm^3, TR/TE: 8185/73 ms, b-values 0 and 1200 s/mm^2, 45 diffusion directions).

All participants underwent a 7T brain MRI on a Philips 7T scanner (Philips Healthcare, Best, The Netherlands) using a 32-channel receive head coil in combination with a quadrature transmit coil (Nova Medical, MA, USA). The scan protocol

and acquisition parameters are published elsewhere[12] and included 2D-Qflow sequences to assess blood flow velocity and pulsatility index in perforating arteries in the basal ganglia and centrum semiovale as well as blood oxygen-level dependent (BOLD) sequences to assess vascular reactivity in response to a visual stimulus and hypercapnic challenge.

Conventional cSVD markers and brain volumetrics

Lacunes (on T1-weighted and FLAIR) and microbleeds (on T2*-weighted) were manually rated according to the STRIVE-criteria.[3] Volumetric measures and masks of WMH, intracranial volume, total brain volume, white matter and grey matter were acquired as previously published.[12]

Small vessel function measures

Three complementary measures of small vessel function in different small vessel populations were acquired on 7T brain MRI. A detailed description of these measures,[12] as well as the processing pipelines[13], is provided elsewhere. In short:

1. 2D-Qflow velocity mapping acquisitions were acquired at the level of the basal ganglia and centrum semiovale to assess flow velocity in perforating arteries. Mean blood flow velocity and pulsatility index within perforating arteries of the basal ganglia and centrum semiovale were derived. In these cohorts with known small vessel alterations, we regard pulsatility index in perforating arteries as an indicator of perforating artery stiffness.
2. BOLD data were acquired in the visual cortex to assess endothelial-dependent (via neurovascular coupling) vascular reactivity in response to looking at a short visual stimulus. The average BOLD hemodynamic response function as generated by the short visual stimulus was estimated and the BOLD% signal change and full-width-at-half-maximum (FWHM) were derived.
3. Whole-brain BOLD data were acquired to assess endothelial-independent vascular reactivity in response to a hypercapnic stimulus (i.e., breathing 6% CO_2 in air for 2x2 minutes). The BOLD% signal change in the cortical grey matter, subcortical grey matter and white matter were derived.

Diffusion measures

The diffusion images for both patients with CADASIL and patients with sporadic cSVD were processed with similar pipelines. After visual inspection to exclude major artefacts, raw diffusion images were pre-processed using the MRtrix3 packages (MRtrix3)[17] and the Functional Magnetic Resonance Imaging of the Brain (FMRIB) software library (FSL[18]), v6.0.3. First, noise and Gibbs ringing artefacts were removed ('dwidenoise',[19–21] 'mrdegibbs',[22] MRtrix3), followed by correction of subject motion and distortion correction ('topup' (only for CADASIL), 'eddy',[23–26] FSL). Lastly, we corrected for bias field in the CADASIL group (ANTS[27]). Patients with CADASIL who underwent their 3T brain MRI in Munich, had a multishell diffusion MRI. After preprocessing we only selected volumes with b=0 and b=1000 s/mm^2 ('dwiextract', MRtrix3[17]) and used this single shell for further processing. Using the preprocessed diffusion images, we calculated the diffusion tensors to obtain mean diffusivity (MD) maps (which were used for the voxel-wise analyses as described below) ('dtifit', FSL). As a marker of whole-brain microstructure of the white matter, we calculated PSMD.[15] PSMD is a sensitive and robust measure of white matter microstructure[15] and was calculated using the publicly available script (http://psmd-marker.com). PSMD is an index of the dispersion of mean diffusivity (MD) values across the white matter skeleton and has been described in detail before.[15] In short: to calculate PSMD, the white matter tracts are first skeletonized using tract-based spatial statistics (TBSS[28], FSL), then to avoid CSF contamination by partial volume effects, the skeleton is masked with a custom-made mask designed to exclude regions close to CSF. Lastly, with histogram analysis of MD values within the masked skeleton the peak width is calculated as the difference between the 95th and 5th percentile. PSMD was calculated both for the total white matter and for the normal appearing white matter (NAWM). The NAWM mask was obtained by subtracting lesions (i.e., WMH and lacunes) from the total white matter mask and subsequent erosion of the mask.

Analyses

Differences in baseline characteristics between the patient groups and their respective reference groups were tested with independent sample t-tests for continuous normally distributed data, Mann Whitney U tests for non-parametric continuous data, chi-square tests for categorical data and ANOVA with age and sex correction for 7T small vessel function measures. Statistical analyses on group

differences in pulsatility index were additionally corrected for mean blood flow velocity. BOLD reactivity to hypercapnia analyses were additionally corrected for change in end-tidal CO_2 in response to hypercapnia.

Whole-brain analyses on small vessel function and diffusion alterations

Within the CADASIL patient group and the sporadic cSVD patient group, we tested the association between small vessel function measures and PSMD in total white matter with simple linear regressions. All analyses were repeated with NAWM PSMD. Regression analyses were not adjusted for age. Given that age is not a confounder in CADASIL, we wanted to keep the primary analyses as harmonized as possible. In an additional sensitivity analysis in patients with sporadic cSVD we added age as a covariate in the statistical analyses.

Voxel-wise analyses on small vessel function and diffusion alterations

For these analyses, we first registered the 3T 3D-T1 weighted images to the 7T BOLD images for each participant, using FLIRT (FSL[29–31]). The resulting transformation matrix was then applied to register the 3T MD map to the 7T BOLD image. All registrations were visually checked. Per participant, we then calculated the correlation coefficient between BOLD% signal change and MD across all voxels within the white matter mask (see example in Figure 1).

These within-participant assessments essentially eliminate the influence of possible confounders (i.e., shared risk factors for abnormal small vessel function and cerebral tissue injury). We performed two different analyses with these correlation coefficients. First, we tested for each group if the pooled individual correlation coefficients of the BOLD% signal change with MD significantly deviated from zero using a Wilcoxon rank sum test. Second, we tested if the group-level mean of individual correlation coefficients was different for patients and reference participants in both CADASIL and sporadic cSVD with Wilcoxon rank sum tests. These analyses were repeated for the NAWM. All statistical analyses were performed in R and a significance level of $p < 0.05$ was considered significant.

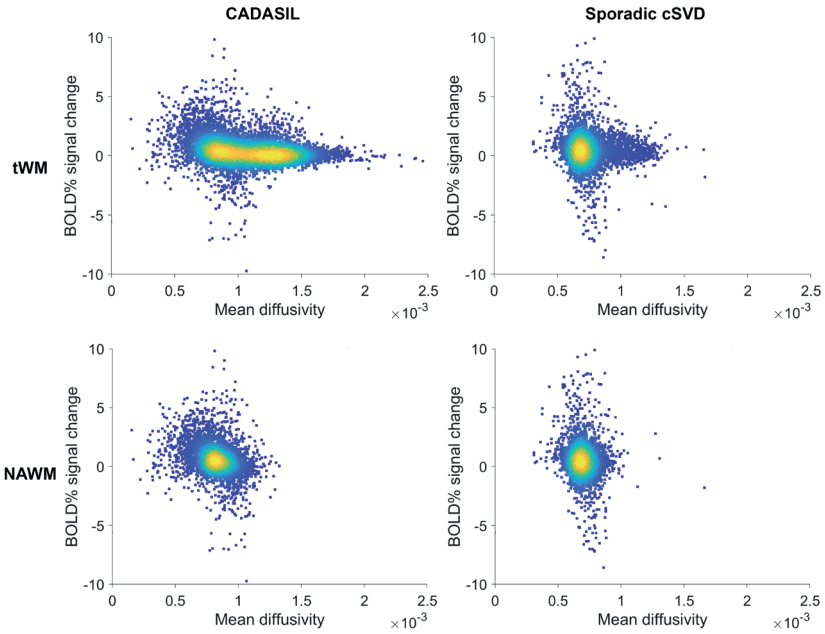

Figure 1. Example density plots for one representative CADASIL and sporadic cSVD patient. Each panel shows the relationship of each voxel in a single patient between BOLD% signal change and mean diffusivity in total white matter (tWM; upper panels) and normal appearing white matter (NAWM; lower panels). From this, we calculated the correlation coefficient between BOLD% signal change and mean diffusivity for each participant.

RESULTS

Characteristics of the patients with CADASIL, patients with sporadic cSVD and both matched reference groups are shown in Table 1. As reported previously ([13], van den Brink et al., in preparation), small vessel function measures, including blood flow velocity, pulsatility, and reactivity, were affected both in patients with CADASIL and sporadic cSVD, but with differences in the affected vessel populations and differences in the way that vascular reactivity was affected (Table 1). As expected, both patients with CADASIL and sporadic cSVD had a higher lesion load and higher PSMD (i.e., loss of white matter microstructure) than their reference groups.

Whole-brain associations between small vessel function measures and PSMD

In both patient groups, perforating artery flow velocity was associated with PSMD, albeit with differences in the arterioles involved. In CADASIL, lower blood flow

velocity in the centrum semiovale was associated with higher PSMD (Table 2). In sporadic cSVD, this negative association was observed for blood flow velocity in the perforating arteries in the basal ganglia instead. Additionally, in this group, higher pulsatility index in the perforating arteries in the basal ganglia associated with increased PSMD (Table 2).

Table 1. Characteristics of patients with CADASIL and sporadic cSVD and their respective reference groups

	CADASIL	**Reference**		**Sporadic cSVD**	**Reference**	
	n = 23	n = 13	*p*	n = 46	n = 21	*p*
Demographics						
Age [years]	51.1±10.1	46.1±12.6	0.20	65.3±9.4	63.3±6.7	0.42
Female sex	12 (52)	6 (46)	1.00	15 (33)	8 (38)	0.87
7T MRI small vessel function						
2D-Qflow centrum semiovale[a]	n=22	n=10		n=46	n=21	
Blood flow velocity [cm/s]	0.54±0.06	0.63±0.13	**0.03**	0.65±0.12	0.65±0.10	0.87
Pulsatility index[b]	0.56±0.19	0.37±0.11	**0.009**	0.35±0.13	0.32±0.11	0.34
2D-Qflow basal ganglia	n=21	n=9		n=44	n=21	
Blood flow velocity [cm/s]	3.07±0.67	4.05±0.83	**0.003**	3.7±0.69	3.9±0.70	0.35
Pulsatility index[b]	0.46±0.12	0.29±0.15	0.06	0.45±0.14	0.36±0.13	**0.005**
BOLD visual stimulus	n=19	n=10		n=35	n=19	
BOLD% signal change	0.61±0.20	0.82±0.25	**0.04**	0.63±0.2	0.66±0.16	0.51
Full width half max [s]	3.82±0.65	3.94±0.36	0.60	3.37±0.97	4.01±0.81	**0.02**
BOLD hypercapnic stimulus[cd]	n=17	n=11		n=36	n=18	
CGM BOLD% signal change	3.66±1.24	3.07±1.20	0.26	3.66±1.38	3.39±1.43	0.51
SGM BOLD% signal change	3.37±0.98	3.44±1.42	0.87	3.91±1.49	3.52±1.50	0.38
tWM BOLD% signal change	0.35±0.33	0.17±0.31	0.31	0.56±0.44	0.55±0.38	0.96
3T MRI cSVD markers						
PSMD [$mm^2/s \times 10^{-4}$]	4.1 [1.87]	2.1 [0.26]	**<0.001**	4.1 [1.97]	2.9 [0.8]	**<0.001**
WMH volume [% of ICV]	4.5 [4.4]	0.01 [0.04]	**<0.001**	1.15 [1]	0.09 [0.08]	**<0.001**
Lacune presence	13 (57)	0 (0)	**0.001**	30 (65)	0 (0)	**<0.001**
Microbleed presence	13 (57)	0 (0)	**0.001**	23 (50)	4 (9)	**0.03**
Brain volume [% of ICV]	78.3±5.2	77.6±3.2	0.76	69.9±6.4	73.3±4.3	**0.04**

Differences were tested with an independent sample t-test for continuous normally distributed data, Mann-Whitney U test for non-parametric continuous data (i.e., PSMD and WMH volume) and chi-square for categorical data. Data presented as M±SD, n(%) or median[IQR].
[a] The ROI is the entire semioval centre and basal ganglia excluding lacunes. Analyses are corrected for age and sex. [b] Additional correction for blood flow velocity. [c] Analyses corrected for age, sex and change in end-tidal CO_2 to hypercapnia. [d] Vascular reactivity to hypercapnia was reduced in WMH

(compared to NAWM in both CADASIL: mean BOLD% change difference -0.29, $p = 0.02$ and sporadic cSVD: mean BOLD% change difference -0.35, $p < 0.001$).
BOLD = Blood oxygenation level-dependent, BP = blood pressure, CGM = cortical grey matter, ICV = intracranial volume, PSMD = peak width of skeletonized mean diffusivity, Qflow = quantitative flow (velocity phase contrast MRI), SGM = subcortical grey matter, tWM = total white matter, WMH = White matter hyperintensity.

Vascular reactivity to hypercapnia in the cortical grey matter was negatively associated with PSMD in patients with sporadic cSVD, but not in CADASIL, although the direction of the effect was the same (Table 2). Of note, in both groups reactivity to hypercapnia in the cortical grey matter tended to be higher in the patients than in the reference groups (Table 1).

Subcortical grey matter and white matter reactivity to hypercapnia did not relate to PSMD (Table 2).

In sensitivity analyses using PSMD in the NAWM only, the above significant associations persisted (Supp. Table 1). We performed additional sensitivity analyses in patients with sporadic cSVD in which we corrected for age. In these age-corrected analyses, only the association between blood flow velocity in the perforating arteries of the basal ganglia and white matter PSMD remained significant (B(CI) = -0.32 (-0.60 – -0.04), $p = 0.03$; Supp. Table 2).

Table 2. Linear regressions between 7T small vessel function measures and PSMD in total white matter

	CADASIL			**Sporadic cSVD**		
	B	CI95	*p*	B	CI95	*p*
2D-Qflow centrum semiovale	N=22			N= 46		
Blood flow velocity [cm/s]	-0.42	-0.83 – -0.03	**0.04**	0.02	-0.28 – 0.33	0.87
Pulsatility Index	-0.18	-0.63 – 0.25	0.38	0.12	-0.19 – 0.42	0.44
2D-Qflow basal ganglia	N=21			N= 44		
Blood flow velocity [cm/s]	-0.23	-0.72 – 0.26	0.33	-0.45	-0.73 – -0.17	**0.002**
Pulsatility index	0.21	-0.28 – 0.70	0.38	0.31	0.01 – 0.60	**0.04**
BOLD visual stimulus	N=19			N=35		
BOLD% signal change	-0.25	-0.67 – 0.18	0.24	-0.04	-0.37 – 0.28	0.78
Full width half max [s]	0.36	-0.05 – 0.76	0.08	-0.23	-0.54 – 0.08	0.14
BOLD hypercapnic stimulus	N=17			N=36		
CGM BOLD% signal change	-0.27	-0.84 – 0.31	0.35	-0.35	-0.68 – -0.03	**0.03**
SGM BOLD% signal change	-0.30	-0.87 – 0.28	0.29	-0.25	-0.59 – 0.08	0.14
NAWM BOLD% signal change	0.26	-0.33 – 0.86	0.36	-0.01	-0.36 – 0.34	0.96

B = standardized beta, BOLD = Blood oxygenation level-dependent, CGM = cortical grey matter, CI95 = 95% confidence interval, NAWM = normal appearing white matter, PSMD = peak width of skeletonized mean diffusivity, Qflow = quantitative flow (velocity phase contrast MRI), SGM = subcortical grey matter.

Voxel-wise correlations between BOLD% signal change to hypercapnia and MD

In the voxel-wise analyses we found a negative correlation between BOLD% signal change to hypercapnia and MD across voxels in the white matter both in patients with CADASIL (mean of individual correlation coefficients (r)±sd: -0.14±0.08; Wilcoxon rank sum test p <. 0001, indicating that a significant proportion of patients showed this negative correlation) and in patients with sporadic cSVD (r = -0.10 ± 0.09; Wilcoxon p < .0001). This, mean negative correlation was stronger in the patient groups than in their respective reference groups, both in the total white matter (mean difference CADASIL and reference group -0.04, p = 0.3; mean difference sporadic cSVD and reference group -0.08, p = 0.003; Figure 2) and NAWM (mean difference CADASIL and reference group 0.01, p = 0.006, mean difference sporadic cSVD and reference group 0.06, p = 0.007; Figure 2).

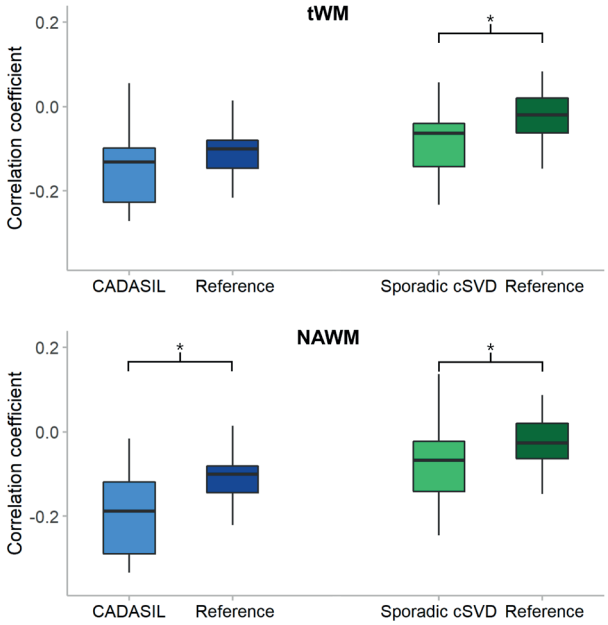

Figure 2. Boxplots showing the correlation coefficients of the voxel-wise relation between BOLD% signal change to hypercapnia and mean diffusivity in total white matter and normal appearing white matter. As mentioned in Figure 1, we calculated a correlation coefficient between BOLD% signal change and mean diffusivity across all voxels for each participant (both patient and reference groups). We tested whether the mean of these individual correlation coefficients was different between the patient groups and their respective reference groups. The negative associations are significantly stronger for the patient groups, except for the difference between CADASIL and the reference group in total white matter (see difference between light coloured and dark coloured boxes). * indicates p < .05.

DISCUSSION

Here we show that small vessel dysfunction is associated with white matter alterations at a whole-brain but also at a voxel-by-voxel level. Whole-brain changes in white matter microstructure mostly related with perforating artery blood flow velocity, but with notable differences between CADASIL and sporadic cSVD in the arterioles involved. Whole-brain changes in white matter microstructure did not consistently relate with endothelial-dependent or independent reactivity, while both in CADASIL and sporadic cSVD a voxel-by-voxel level correlation was found between endothelial-independent white matter reactivity and white matter microstructure. Particularly these voxel-by-voxel level correlations in both patient groups could support a causal relationship between small vessel dysfunction and white matter alterations.

Assessment of perforating artery blood flow velocity and pulsatility index with 7T MRI is a relatively new technique([13], van den Brink et al., in preparation). Consequently, the relation of small vessel function measures with microstructural white matter alterations has not been studied before. In this study we observed a significant association between decreased blood flow velocity and microstructural white matter alterations, with disease-specific patterns. In patients with CADASIL this relation was significant for blood flow velocity in perforating arteries in the centrum semiovale and for patients with sporadic cSVD for blood flow velocity in perforating arteries in the basal ganglia. These findings could reflect differences in the underlying physiology leading to parenchymal injury, varying between small vessel populations and types of cSVD. Even though it is plausible that small vessel dysfunction and white matter injury are causally related, these observed whole-brain associations could also reflect shared risk factors.

The whole-brain relation between endothelial-independent vessel reactivity (to hypercapnia and acetazolamide) and white matter injury has been studied previously with 3T-MRI. Findings indicated that decreased reactivity related to increased WMH burden, both in patients with CADASIL and sporadic cSVD.[4–11] In addition, one earlier study reported an association between reduced vascular reactivity and white matter alterations with diffusion MRI on 3T-MRI.[8] In the present observations from the ZOOM@SVDs study, we extend these earlier findings with detailed reactivity measurements on 7T-MRI. We did not observe a

consistent relation between endothelial-dependent or independent reactivity and white matter alterations, with the exception of a negative relation of endothelial-independent reactivity in the cortex with white matter alterations in patients with sporadic cSVD. The direction of this effect was similar in patients with CADASIL. At first, the direction of the effect may seem counterintuitive, but baseline cortical grey matter reactivity in fact tended to be *higher* in patients than in the reference groups. This might reflect a compensatory mechanism to protect the cortex. *Higher* endothelial-independent reactivity in the cortex thus relates to more microstructural white matter damage, while no relations were observed in the subcortical grey matter or white matter. Interestingly, both in patients with CADASIL and sporadic cSVD, when performing voxel-level within-subject analyses in the white matter, we observed a significant negative correlation between endothelial-independent reactivity and white matter microstructure. This correlation was stronger in patients than in the reference groups, implying that this correlation was driven by cSVD related disease processes. Even though there might be a weak correlation between vascular reactivity and white matter microstructure in healthy tissue, this correlation is apparently stronger in damaged tissue. Furthermore, we found this correlation both in total white matter as well as NAWM which suggests that disease processes are already taking place in tissue that looks healthy on conventional MRI scans. Given that these voxel-level analyses eliminate the influence of confounders, these findings provide a more direct lead towards a possible causal relation between decreased white matter endothelial-independent reactivity and white matter microstructure, both in patients with CADASIL and sporadic cSVD.

The main strength of this study is that we used state-of-the-art 7T measures of small vessel function, which measure complementary aspects of function from distinct vessel populations. These measures provided the opportunity to not only assess whole-brain relationships, voxel-by-voxel ones as well, which are free of confounders (i.e., shared risk factors for abnormal small vessel function and cerebral tissue injury). Furthermore, we were able to study both a genetically-defined and thus pure and a sporadic form of cSVD. A limitation of the study is the relatively small sample size of both patient groups, which might have caused a lack of power in the whole-brain analyses. Furthermore, we have a selection bias in our CADASIL patient group as they were required to travel internationally to be

included in the study, leaving out the more affected patients. However, we would expect disease effects to be more pronounced in more affected patients, meaning that we would expect even stronger relations in more affected patients. In our voxel-wise analyses, we could only assess reactivity to hypercapnia in the white matter in relation to loss of white matter microstructure. Other forms of small vessel function might be differentially related to white matter microstructure and this should be explored in future studies. For the CADASIL patient group, multi-shell diffusion data was acquired, which would have allowed for more complex modelling such as diffusion kurtosis and biophysical diffusion models. However, this data was not available in the sporadic cSVD group and we decided to keep the analysis harmonized between the two groups by using only the tensor model. Lastly, we only had cross-sectional data available for this study and longitudinal data is needed to establish causality in the relationship between small vessel function and tissue injury.

In conclusion, we found that whole-brain changes in white matter microstructure related with perforating artery blood flow velocity, with differences in the arterioles involved between CADASIL and sporadic cSVD. For endothelial-dependent or independent reactivity, despite absence of significant relations with whole-brain changes in white matter microstructure, we did observe local voxel-by-voxel level correlations, both in CADASIL and sporadic cSVD. These findings indicate a possible causal relationship between small vessel function and white matter microstructure that should be studied further in longitudinal studies.

REFERENCES

1. Debette S, Schilling S, Duperron MG, et al. Clinical Significance of Magnetic Resonance Imaging Markers of Vascular Brain Injury: A Systematic Review and Meta-analysis. *JAMA Neurol* 2019; 76: 81–94.
2. Wardlaw JM, Smith C, Dichgans M. Small vessel disease: mechanisms and clinical implications. *Lancet Neurol* 2019; 18: 684–696.
3. Wardlaw JM, Smith EE, Biessels GJ, et al. Neuroimaging standards for research into small vessel disease and its contribution to ageing and neurodegeneration. *Lancet Neurol* 2013; 12: 822–838.
4. Blair GW, Doubal FN, Thrippleton MJ, et al. Magnetic resonance imaging for assessment of cerebrovascular reactivity in cerebral small vessel disease: A systematic review. *Journal of Cerebral Blood Flow and Metabolism* 2016; 36: 833–841.
5. Blair GW, Thrippleton MJ, Shi Y, et al. Intracranial hemodynamic relationships in patients with cerebral small vessel disease. *Neurology* 2020; 94: e2258–e2269.
6. Sam K, Crawley AP, Conklin J, et al. Development of White Matter Hyperintensity Is Preceded by Reduced Cerebrovascular Reactivity. *Ann Neurol* 2016; 80: 277–285.
7. Sam K, Conklin J, Holmes KR, et al. Impaired dynamic cerebrovascular response to hypercapnia predicts development of white matter hyperintensities. *NeuroImage Clin* 2016; 11: 796–801.
8. Reginold W, Sam K, Poublanc J, et al. The efficiency of the brain connectome is associated with cerebrovascular reactivity in persons with white matter hyperintensities. *Hum Brain Mapp* 2019; 40: 3647–3656.
9. Chabriat H, Pappata ; S, Ostergaard ; L, et al. *Cerebral Hemodynamics in CADASIL Before and After Acetazolamide Challenge Assessed With MRI Bolus Tracking*, http://ahajournals.org (2000).
10. Atwi S, Shao H, Crane DE, et al. BOLD-based cerebrovascular reactivity vascular transfer function isolates amplitude and timing responses to better characterize cerebral small vessel disease. *NMR Biomed*; 32. Epub ahead of print 1 March 2019. DOI: 10.1002/nbm.4064.
11. Smith EE, Beaudin AE. New insights into cerebral small vessel disease and vascular cognitive impairment from MRI. *Current Opinion in Neurology* 2018; 31: 36–43.
12. van den Brink H, Kopczak A, Arts T, et al. Zooming in on cerebral small vessel function in small vessel diseases with 7T MRI: Rationale and design of the "ZOOM@SVDs" study. *Cereb Circ - Cogn Behav* 2021; 2: 100013.
13. van den Brink H, Kopczak A, Arts T, et al. CADASIL Affects Multiple Aspects of Cerebral Small Vessel Function on 7T-MRI. *Ann Neurol*; n/a. Epub ahead of print 12 October 2022. DOI: https://doi.org/10.1002/ana.26527.
14. Pasi M, Van Uden IWM, Tuladhar AM, et al. White Matter Microstructural Damage on Diffusion Tensor Imaging in Cerebral Small Vessel Disease: Clinical Consequences. *Stroke* 2016; 47: 1679–1684.
15. Baykara E, Gesierich B, Adam R, et al. A Novel Imaging Marker for Small Vessel Disease Based on Skeletonization of White Matter Tracts and Diffusion Histograms. *Ann Neurol* 2016; 80: 581–592.

16. Low A, Mak E, Stefaniak JD, et al. Peak Width of Skeletonized Mean Diffusivity as a Marker of Diffuse Cerebrovascular Damage. *Front Neurosci* 2020; 14: 1–11.
17. Tournier JD, Smith R, Raffelt D, et al. MRtrix3: A fast, flexible and open software framework for medical image processing and visualisation. *Neuroimage* 2019; 202: 116137.
18. Smith SM, Jenkinson M, Woolrich MW, et al. Advances in functional and structural MR image analysis and implementation as FSL. *Neuroimage* 2004; 23: 208–219.
19. Veraart J, Novikov DS, Christiaens D, et al. Denoising of diffusion MRI using random matrix theory. *Neuroimage* 2016; 142: 394–406.
20. Veraart J, Fieremans E, Novikov DS. Diffusion MRI noise mapping using random matrix theory. *Magn Reson Med* 2016; 76: 1582–1593.
21. Cordero-Grande L, Christiaens D, Hutter J, et al. Complex diffusion-weighted image estimation via matrix recovery under general noise models. *Neuroimage* 2019; 200: 391–404.
22. Kellner E, Dhital B, Kiselev VG, et al. Gibbs-ringing artifact removal based on local subvoxel-shifts. *Magn Reson Med* 2016; 76: 1574–1581.
23. Andersson JLR, Sotiropoulos SN. An integrated approach to correction for off-resonance effects and subject movement in diffusion MR imaging. *Neuroimage* 2016; 125: 1063–1078.
24. Andersson JLR, Graham MS, Zsoldos E, et al. Incorporating outlier detection and replacement into a non-parametric framework for movement and distortion correction of diffusion MR images. *Neuroimage* 2016; 141: 556–572.
25. Andersson JLR, Graham MS, Drobnjak I, et al. Towards a comprehensive framework for movement and distortion correction of diffusion MR images: Within volume movement. *Neuroimage* 2017; 152: 450–466.
26. Andersson JLR, Graham MS, Drobnjak I, et al. Susceptibility-induced distortion that varies due to motion: Correction in diffusion MR without acquiring additional data. *Neuroimage* 2018; 171: 277–295.
27. Tustison NJ, Avants BB, Cook PA, et al. N4ITK: Improved N3 Bias Correction. *IEEE Trans Med Imaging* 2010; 29: 1310–1320.
28. Smith SM, Jenkinson M, Johansen-Berg H, et al. Tract-based spatial statistics: Voxelwise analysis of multi-subject diffusion data. *Neuroimage* 2006; 31: 1487–1505.
29. Jenkinson M, Smith S. A global optimisation method for robust affine registration of brain images. *Med Image Anal* 2001; 5: 143–156.
30. Jenkinson M, Bannister P, Brady M, et al. Improved Optimization for the Robust and Accurate Linear Registration and Motion Correction of Brain Images. *Neuroimage* 2002; 17: 825–841.
31. Greve DN, Fischl B. Accurate and robust brain image alignment using boundary-based registration. *Neuroimage* 2009; 48: 63–72.

SUPPLEMENTARY MATERIAL

Supplementary table 1. Linear regressions between 7T small vessel function measures and PSMD in normal appearing white matter

	CADASIL			Sporadic cSVD		
	B	CI95	*p*	B	CI95	*p*
2D-Qflow centrum semiovale	N=22			N=46		
Blood flow velocity [cm/s]	-0.43	-0.82 – -0.05	**0.03**	-0.018	-0.34 – 0.30	0.91
WM Pulsatility Index	-0.27	-0.69 – 0.14	0.19	0.047	-0.29 – 0.38	0.78
2D-Qflow basal ganglia	N=21			N=44		
Blood flow velocity [cm/s]	-0.04	-0.54 – 0.46	0.86	-0.383	-0.68 – -0.1	**0.01**
Pulsatility index	0.09	-0.40 – 0.59	0.69	0.305	0.01 – 0.61	**0.05**
BOLD visual stimulus	N=19			N=35		
BOLD% signal change	-0.37	-0.79 – 0.05	0.08	0.017	-0.29 – 0.32	0.91
Full width half max [s]	-0.15	-0.41 – 0.11	0.25	-0.154	-0.45 – 0.14	0.30
BOLD hypercapnic stimulus	N=17			N=36		
CGM BOLD% signal change	-0.37	-0.90 – 0.17	0.16	-0.36	-0.69 – -0.03	**0.03**
SGM BOLD% signal change	-0.34	-0.89 – 0.19	0.19	-0.27	-0.56 – 0.13	0.21
NAWM BOLD% signal change	0.04	-0.54 – 0.63	0.88	-0.168	-0.52 – 0.18	0.33

B = standardized beta, BOLD = Blood oxygenation level-dependent, CGM = cortical grey matter, CI95 = 95% confidence interval, NAWM = normal appearing white matter, PSMD = peak width of skeletonized mean diffusivity, Qflow = quantitative flow (velocity phase contrast MRI), SGM = subcortical grey matter.

Supplementary table 2. Linear regressions between 7T small vessel function measures and PSMD corrected for age in patients with sporadic cSVD

	PSMD WM (log transformed)			**PSMD NAWM (log transformed)**		
	B	CI95	*P*	B	CI95	*p*
2D-Qflow centrum semiovale	N= 46			N = 46		
Blood flow velocity [cm/s]	0.07	-0.20 – 0.34	0.61	0.08	-0.20 – 0.36	0.58
WM Pulsatility Index	0.09	-0.18 – 0.36	0.51	0.08	-0.21 – 0.37	0.58
2D-Qflow basal ganglia	N = 44			N = 44		
Blood flow velocity [cm/s]	-0.32	-0.60 – -0.04	**0.03**	-0.23	-0.51 – 0.06	0.12
Pulsatility index	0.19	-0.09 – 0.48	0.18	0.18	-0.10 – 0.46	0.21
BOLD visual stimulus	N = 35			N = 35		
BOLD% signal change	-0.05	-0.36 – 0.25	0.72	0.01	-0.28 – 0.29	0.96
Full width half max [s]	-0.25	-0.54 – 0.05	0.10	-0.17	-0.45 – 0.10	0.21
BOLD hypercapnic stimulus	N = 36			N = 36		
CGM BOLD% signal change	-0.28	-0.59 – 0.03	0.07	-0.28	-0.58 – 0.02	0.07
SGM BOLD% signal change	-0.24	-0.55 – 0.07	0.11	-0.21	-0.51 – 0.10	0.18
NAWM BOLD% signal change	-0.12	-0.43 – 0.20	0.46	-0.07	-0.41 – 0.28	0.69

B = standardized beta, BOLD = Blood oxygenation level-dependent, CGM = cortical grey matter, CI95 = 95% confidence interval, NAWM = normal appearing white matter, PSMD = peak width of skeletonized mean diffusivity, Qflow = quantitative flow (velocity phase contrast MRI), SGM = subcortical grey matter.

4

CHAPTER

Does loss of integrity of the Cingulum bundle link Amyloid Beta accumulation and neurodegeneration in Alzheimer's Disease?

Naomi Vlegels, Rik Ossenkoppele, Wiesje M. van der Flier,
Huiberdina L. Koek, Yael D. Reijmer, Laura EM Wisse,
Geert Jan Biessels and the Alzheimer's Disease Neuroimaging Initiative

Journal of Alzheimer's disease. 2022. DOI: 10.3233/JAD-220024

ABSTRACT

Background. Alzheimer's Disease is characterized by the accumulation of Amyloid Beta (Aβ) into plaques, aggregation of tau into neurofibrillary tangles and neurodegenerative processes including atrophy. However, there is a poorly understood spatial discordance between initial Aβ deposition and local neurodegeneration. Here, we test the hypothesis that the cingulum bundle links Aβ deposition in the cingulate cortex to medial temporal lobe (MTL) atrophy.

Methods. 21 participants with mild cognitive impairment (MCI) from the UMC Utrecht memory clinic (UMCU, discovery sample) and 37 participants with MCI from Alzheimer's Disease Neuroimaging Initiative (ADNI, replication sample) with available Aβ-PET scan, T1-weighted and diffusion-weighted MRI were included. Aβ load of the cingulate cortex was measured by the standardized uptake value ratio (SUVR), white matter integrity of the cingulum bundle was assessed by mean diffusivity (MD) and atrophy of the MTL by normalized MTL volume. Relationships were tested with linear mixed models, to accommodate multiple measures for each participant.

Results. We found at most a weak association between Cingulate Aβ and MTL volume (added R^2<0.06), primarily for the posterior hippocampus. In neither sample, white matter integrity of the cingulum bundle was associated with cingulate Aβ or MTL volume (added R^2<0.01). Various sensitivity analyses (Aβ-positive individuals only, posterior cingulate SUVR, MTL sub region volume) provided similar results.

Conclusion. These findings, consistent in two independent cohorts, do not support our hypothesis that loss of white matter integrity of the cingulum is a connecting factor between cingulate gyrus Aβ deposition and MTL atrophy.

INTRODUCTION

Alzheimer's Disease (AD) is characterized by the accumulation of Amyloid Beta (Aβ) into plaques, aggregation of tau into neurofibrillary tangles and neurodegenerative processes like atrophy.[1] However, there is a notable spatial discordance between typical initial locations of Aβ deposition and neurodegenerative processes. Whereas Aβ deposition typically starts in the precuneus, medial orbitofrontal cortex and the cingulate cortex,[2,3] the aggregation of tau and atrophy mostly start in the medial temporal lobe (MTL),[4–6] Additionally, while Aβ plaques are known to gradually spread throughout the brain, Aβ-PET studies have found relatively little involvement of Aβ in the MTL compared to neocortical regions.[7–9] This spatial discordance between Aβ deposition and neurodegeneration in the MTL in AD is poorly understood[10]. In addition, there is a largely unexplained temporal discordance, as Aβ deposition precedes neurodegeneration processes by a decade.[11,12]

A hypothesis in the AD field is that Aβ deposition and distant neurodegeneration might be interconnected through the functional and structural architecture of the brain.[13] If these two processes are indeed connected via the structural connections of the brain, i.e., the white matter tracts, the cingulum bundle is of particular interest, because it connects the typical starting locations of Aβ deposition (i.e., the cingulate cortex) with that of neurodegenerative processes (the MTL, see Figure 1). The proposed role of the cingulum bundle could be two-fold. First, the cingulum might serve as a conduit for pathology or signals, linking Aβ deposition in the cingulate cortex to spread of tau and neurodegeneration from the MTL to the neocortex. Second, the tracts of the cingulum bundle might degenerate because of Aβ deposition on one end of the bundle, which might increase vulnerability of the MTL on the other end of the bundle and thereby promote local tau aggregation.[14–17] The integrity of the white matter in the cingulum bundle has been shown to be affected in AD[18] and has been implicated in Aβ-facilitated tau spread from the MTL to the posterior cingulate cortex.[19] In the current study, we explore the hypothesis that the cingulum bundle links Aβ deposition in the cingulate cortex to neurodegeneration in the MTL. We tested this hypothesis in early symptomatic disease stages, i.e., patients with mild cognitive impairment (MCI), by assessing whether the relationship between white matter integrity of the cingulum bundle and pathology at either end of the bundle (i.e., Aβ in the cingulate cortex and atrophy in the MTL) is stronger than the relationship between the two pathologies itself.

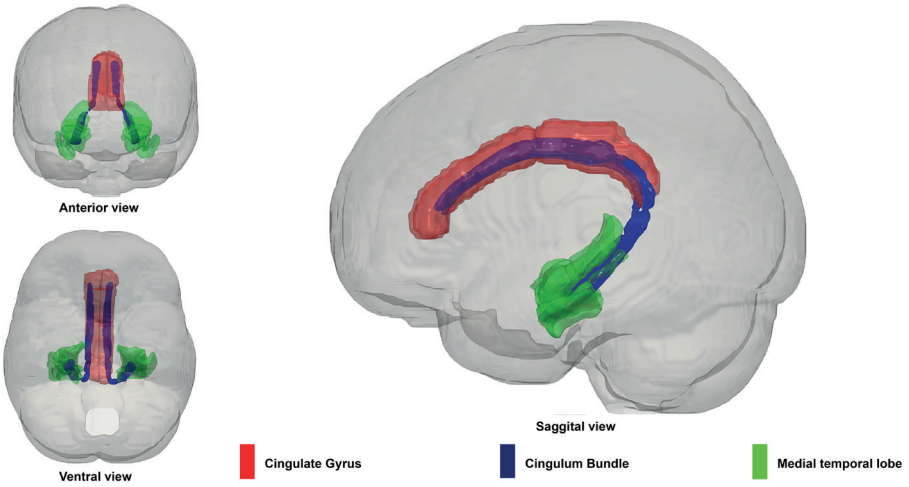

Figure 1. Spatial overview of ROIs. A spatial overview of the cingulate gyrus (in red), the cingulum bundle (in blue) and the medial temporal lobe (in green) in anterior, ventral and sagittal view.

METHODS

Participants

UMCU

21 participants from the ABIDE study,[20] recruited at the memory clinic of the UMC Utrecht (UMCU), were included. All participants underwent a one-day memory clinic evaluation including a physical examination, an interview, brain MRI and neuropsychological assessment. For the present study we selected participants with a diagnosis of MCI, available Aβ [^{18}F]-florbetaben PET scan, diffusion MRI scan and 3D-T1-weighted MRI scan. Clinical diagnosis was established at a multidisciplinary consensus meeting after the one-day memory clinic evaluation. MCI was defined as complaints or deterioration from prior functioning and objective evidence of impairment in at least one cognitive domain. Furthermore, daily living activities had to be normal or mildly impaired.[21,22]

ADNI

As a replication sample, we included 37 participants from the multicentric Alzheimer's Disease Neuroimaging Initiative (ADNI, phase 3, downloaded August

2019 at http://adni.loni.usc.edu). We selected participants with a diagnosis of MCI who had an available Aβ [^{18}F]-florbetapir PET, available diffusion MRI scan and available T1-weighted MRI (flowchart of the selection of participants can be found in Supplementary figure 1). The MRI and PET scan had to be acquired with a maximum of 1 year apart. As diffusion measures are impacted by factors related to scanner and acquisition protocols,[23–25] we selected participants from any center in which MRI was obtained on a Siemens scanner with a harmonized diffusion protocol. MCI diagnosis was based on the visit closest to the MRI scan. ADNI criteria for the diagnosis of MCI can be found on the website (http://adni.loni.usc.edu) and have been previously reported [26].

Neuroimaging

Amyloid PET

For the UMCU sample, Amyloid PET scans were made on a Siemens Biograph 40 MCT. Participants were injected with a tracer dose of approximately 300 MBq ± 20% [^{18}F]-florbetaben (NeuraceqTM). The image acquisition window extended from 90 to 110 minutes (4x5-minute frames) after dose injection. Detailed information on acquisition and processing can be found in Supplementary text 1. To obtain Aβ load for each participant, we first calculated the global cortical standardized uptake value ratio (SUVR) based on the volumes and the standardized uptake value (SUV) of all cortical ROIs with cerebellar gray matter as the reference tissue. For the primary analyses we used a composite score of the cingulate cortex (Cingulate SUVR) based on the Hammers atlas[27]. This composite consisted of the SUVR of the anterior cingulate and the posterior cingulate. In a sensitivity analysis, we've also assessed the SUVR of only the posterior cingulate.

For the ADNI sample, participants were injected with 370 MBq ± 10% [^{18}F]Florbetapir. Images were acquired 50 to 70 min (4x5min frames) after dose injection. Further details on acquisition and processing of [^{18}F]-Florbetapir PET have been described elsewhere and can be found on the website ([28]; http://adni.loni.usc.edu http://adni.loni.usc.edu/). As a global measure of Aβ load, we used the neocortical composite SUVR that comprises an average of frontal, cingulate, lateral-parietal and lateral temporal gray matter regions-of-interest, using whole cerebellum as the reference region. For the primary analyses, we used the composite score of the cingulate regions (Cingulate SUVR) based on the Desikan-Killiany atlas[29] which

consisted of the caudal anterior cingulate, isthmus cingulate, posterior cingulate and rostral anterior cingulate.

MRI Acquisition

For the UMCU sample, brain MRI data was acquired using a Philips 3 T scanner (Achieva, Philips, Best, the Netherlands) with a standardized MRI protocol that included a 3D-T1 weighted sequence (192 continuous slices, voxel size: 1x1x1 mm^3, repetition time (TR)/echo time (TE): 7.9/4.5 ms, flip angle of 8°) and a diffusion-weighted sequence (single-shot echo EPI, 48 contiguous slices, voxel size 1.72x1.72x2.50 mm^3, TR/TE 6600/73 ms, 45 gradient directions with a b-value of 1200 s/mm^2 and one with a b-value of 0 s/mm^2 (number of signal averages = 3)).

For the ADNI sample, brain MRI data for participants included in this study was acquired using a Siemens 3 T scanner (Siemens Healthineers, Erlangen, Germany). The standardized MRI protocol included an MPRAGE (170 sagittal slices, voxel size of 1x1x1 mm^3, TR/TE/Inversion time (TI): 2.98/2300/900 ms, flip angle of 9°) and a diffusion-weighted sequence (voxel size 2x2x2m^3, TR/TE: 7200/56, 41 gradient directions with a b-value of 1000 s/mm^2 and five with a b-value of 0 s/mm^2).

Diffusion preprocessing and tractography

For both the UMCU and ADNI study samples, the diffusion-weighted data was processed with ExploreDTI (version 4.8.6; https://www.exploredti.com/;[30]) running on MATLAB R2018a (MATLAB and Statistics Toolbox Release 2014b, The MathWorks, Inc., Natick, Massachusetts, United States). Preprocessing of the data included correction for subject motion, eddy current and susceptibility artefacts, including rotation of the B-matrix prior to the estimation of the diffusion tensor.[30–32] The diffusion tensors were computed using robust estimators[31] followed by whole-brain tractography. Fiber tracts were reconstructed by starting seed points uniformly throughout the data at 2 mm isotropic resolution with a step size of 1 mm. Each streamline was propagated using integration over fiber orientation distributions. Streamlines were guided by fiber orientations inferred using constrained spherical deconvolution with a maximum harmonic order (*l-max*) of 6. This method allows for the reconstruction of more complex pathways, such as crossing fibers.[33] Streamlines were terminated when they entered a voxel with fiber orientation distributions <0.1 or when the deflection angle between two successive steps was > 45°.

Following preprocessing and tractography, we manually reconstructed the superior part and the parahippocampal part of the cingulum bundle per hemisphere in each participant. For the reconstruction of the tracts we used an earlier described multiple region of interest (ROI) approach.[34,35] In short, ROIs for tract selection and tract exclusion were manually drawn on color coded fiber orientation maps in native space. ROI placement was based on previously defined anatomical landmarks to reduce subjectivity in fiber tracking.[36] Low inter- and intra-rater variability with this method has been demonstrated in previous studies.[37,38] For the reconstructed cingulum bundles, mean diffusivity (MD) was determined for the primary analysis. As a sensitivity analysis, we also performed an along tract analysis. Along tract analysis allows to assess multiple data points throughout the bundle rather than only the mean of the entire bundle, giving a higher sensitivity to subtle changes.[39] With the along tract analysis we assessed 8 different data points along the reconstructed cingulum bundles (4 for the superior part and 4 for the parahippocampal part) and determined MD for each of these data points per hemisphere, per subject.

Medial temporal lobe volume

MTL volume was determined for each participant by using the Automatic Segmentation of Hippocampal Subfields (ASHS) software package. More specifically we used the atlas for the T1-weighted MRI.[40,41] ASHS automatically segments anterior and posterior hippocampus as well as MTL cortical sub regions for both hemispheres. All segmentation results were visually inspected, manual edits were not needed. Following visual inspection, we combined the volumes of the anterior hippocampus, posterior hippocampus, entorhinal cortex, Brodmann area 35 and 36 (perirhinal cortex) and the parahippocampal cortex to obtain MTL volume. MTL volume was normalized by the intracranial volume for each participant. For the UMCU sample intracranial volume was obtained by probabilistic segmentations using MeVisLab (MeVis Medical Solutions AG, Bremen, Germany). For the ADNI sample, intracranial volume was obtained by segmentations using the Computational Anatomical Toolbox (CAT) 12 toolbox (version R1073, C. Gaser, Structural Brain Mapping Group, Jena University Hospital, Jena, Germany) for SPM version 12.

Statistical analysis

All statistical analyses were performed in R (version 3.5.1)[42] and statistical significance level was set at $\alpha = 0.05$. All associations were tested with linear mixed models. Linear mixed models were used (using the "lme4" package;[43]) because they allow for both within- and between-subject factors, thus accommodating the four measurements of the cingulum bundle for each subject (left superior, right superior, left parahippocampal and right parahippocampal), two measurements for both cingulate SUVR and MTL (left and right), as well as considering between-subjects factors such as age and sex. The association between Cingulate SUVR and MTL volume was tested with a model that included Cingulate SUVR, hemisphere (left/right), age and sex. The relationship between Cingulate SUVR and Cingulum MD was tested with a model that included MD of the cingulum, location (superior or parahippocampal), hemisphere, age and sex. For the association between MTL volume and cingulum MD we included MD of the cingulum, location, hemisphere, age and sex. For these main analyses we report the standardized fixed effect (B), the 95% confidence interval, the *p*-value and explained variance (R^2) of the model without and with the variable of interest.

We performed the following post-hoc sensitivity analysis (also with linear mixed models). First, all analyses were repeated in Aβ-positive individuals only, to rule out that findings were confounded by patients without AD pathology. For Aβ load we repeated the analysis with posterior cingulate cortex SUVR only, as this region is part of the posterior MTL network and might be more sensitive. For the integrity of the cingulum bundle we also ran a more fine-grained along tract analysis. For MTL volume, we zoomed in on specific sub regions of the structure as these might be more sensitive than the complete volume. We assessed 1) posterior hippocampus volume, as this is spatially close to the cingulate cortex; 2) entorhinal cortex volume as the cingulum bundle projects mostly on this structure and 3) parahippocampal cortex as this region is part of the posterior MTL network, together with the posterior cingulate. All sensitivity analyses were done in a similar way as described in the preceding paragraph. All tests were performed separately for the UMCU and ADNI sample.

RESULTS

Table 1 shows the characteristics of the participants of both the UMCU and the ADNI sample.

Cingulate SUVR – MTL volume

No association was found between Cingulate SUVR and MTL volume in both the UMCU sample (B (CI): -0.27 (-0.63 – 0.09), p = 0.197, R^2 in model without and with SUVR 0.30 and 0.35, respectively) and the ADNI sample (B(CI)= -0.03 (-0.34 – -.29), p = 0.88, R^2 in model without and with SUVR was 0.013 and 0.014, respectively), see Table 2 and Figure 2 A&B.

In a sensitivity analysis that assessed posterior hippocampus volume, an association was found for the ADNI sample (B (CI) = -0.38 (-0.67 - -0.08), *bonferonni corrected p* = 0.045), but not the UMCU sample (Supplementary table 6). All other sensitivity analyses (in Aβ-positive individuals, using posterior cingulate SUVR and using entorhinal cortex and parahippocampal volume) yielded results similar to the main analysis (Supplementary table 4, 5 and 6).

Table 1. Participant characteristics.

	UMCU (n = 21)	**ADNI (n = 37)**
Age in years	75.9 ± 6.5	75.6 ± 7.9
Female sex	8 (38)	15 (41)
MMSE	26 [3.5] (21 – 29)	27 [2] (23 – 30)
Aβ-positive	14 (67)	22(59)
[^{18}F]-florbetaben global SUVR	1.49 [0.3] (1.17 – 2.34)	NA
[^{18}F]-florbetaben cingulate SUVR	1.68 [0.45] (1.26 – 2.47)	NA
[^{18}F]-florbetapir global SUVR	NA	1.29 [0.57] (0.86 – 2.28)
[^{18}F]-florbetapir cingulate SUVR	NA	1.35 [0.54] (0,92 – 2,31)
ICV in ml	1445 [191] (1101 – 1645)	1482 [217] (1067 – 1774)
TBV, % of ICV	68.7 [4,9] (62.5 – 73.3)	72.1 (6.7) (63.5 – 82.7)
MTL volume, % of ICV	0.89 [0.13] (0.75 – 1.11)	0.96 [0.17] (0.66 – 1.22)
MD Superior Cingulum bundle 10^{-4} mm^2/s	7.61 [0.41] (7.22 – 9.07)	7.77 [0.31] (7.2 – 9.1)
MD Hippocampal Cingulum bundle 10^{-4} mm^2/s	10.1 [1.77] (7.9 –12.6)	9.34 [1.38] (7.7 – 11.9)

Abbreviations: ^{18}F = fluorine-18, Aβ = Amyloid Beta, ICV = Intracranial volume, MD = Mean Diffusivity, mm = millimeter, MMSE = Mini Mental State Exam, MTL = Medial Temporal lobe, NA = Not Applicable, SUVR = Standardized Uptake Value Ratio, TBV = Total Brain Volume.
Data is presented as mean ± standard deviation, n(%) and median[interquartile range] (min – max).

Associations with cingulum MD

The findings in Table 2 and Figure 2 C&D indicate that there was no association between Cingulate SUVR and Cingulum MD for either the UMCU (B(CI) = 0.006 (-0.06 – 0.07), p = 0.86, R^2 for model without or with SUVR was 0.0231 and 0.0232, respectively) or the ADNI sample (B(CI) = 0.013 (-0.03 – 0.01), p = 0.25, R^2 for model without or with SUVR was 0.017 and 0.017, respectively). There were no significant associations for any of the covariates: age, sex, hemisphere and location (Supplementary table 2). We performed sensitivity analyses in which we assessed the relationship between Cingulate SUVR and Cingulum MD in Aβ-positive individuals and in which we used posterior cingulate SUVR rather than Cingulate SUVR but both yielded no difference in results (Supplementary table 4 and 5).

Table 2. Main linear mixed model results

	UMCU			ADNI		
	β (CI)	**F (df)**	***p***	**β (CI)**	**F (df)**	***p***
Cing. SUVR - MTL vol.	-0.27 (-0.63 – 0.09)	1.84 (1, 13.4)	0.2	-0.03 (-0.34 – 0.29)	0.02 (1, 36.8)	0.88
MD - Cing. SUVR	0.01 (-0.06 – 0.07)	0.03 (1, 48.2)	0.86	-0.01 (-0.03 – 0.01)	1.33 (1, 108.2)	0.25
MD - MTL volume	0.06 (-0.16 – 0.28)	0.24 (1, 44.4)	0.62	- 0.01 (-0.10 – 0.08)	0.06 (1, 111.3)	0.80

Table shows the main results for the linear mixed models. Top row shows the results for the relationship between cingulate Aβ and MTL volume, middle row the results for cingulum MD and cingulate Aβ and the bottom row shows the results of the relationship between cingulum MD and MTL volume. Results are displayed as follows: the standardized fixed effects coefficients (β) plus 95% confidence intervals, the F-tests with the degrees of freedom (df) and the *p*-value for both the UMCU and ADNI study samples.

There was no relationship between MTL volume and cingulum MD in either the UMCU (B(CI) = 0.06 (-0.16 – 0.28), p = 0.62, R^2 for model without and with MTL volume was 0.29 and 0.29, respectively) or the ADNI sample (B(CI) = - 0.01(-0.10 – 0.08), p = 0.80, R^2 for model without and with MTL volume was 0.0077 and 0.0078, respectively), see Table 2 and Figure 2E&F. There was no effect from the covariates (Supplementary table 3). The sensitivity analysis in Aβ-positive individuals gave similar results (Supplementary table 4). When we tested the association using volumes of the sub regions of the MTL rather than the complete MTL, results remained non-significant (Supplementary table 6).

As a sensitivity analysis on the white matter integrity of the cingulum we performed a more fine-grained along-tracts analysis of 8 data points of the MD of the cingulum bundle. This analysis did not change the interpretation of the results (data not shown).

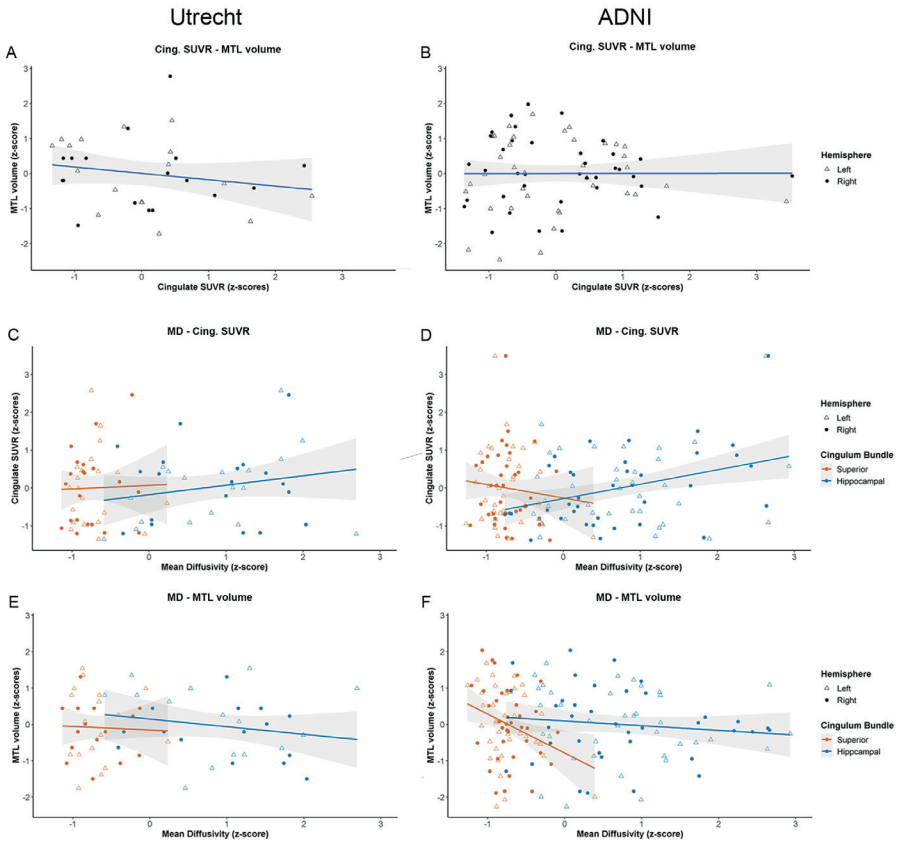

Figure 2. Scatterplots of regression analyses. Scatterplots showing the association for UMCU (left) and ADNI (right) between Cingulate SUVR and MTL volume (panel A and B), for the association between Cingulum MD and Cingulate SUVR (panel C and D) as well as for the association between Cingulum MD and MTL volume. The legends on the outer right side of the figure refer to both panels.

DISCUSSION

We found at most a weak association between Cingulate Aβ and MTL volume, primarily for the posterior hippocampus, in line with earlier findings.[36,37] In neither sample, white matter integrity of the cingulum bundle was associated with Cingulate Aβ on one end of the bundle or MTL volume at the other end. These consistent findings in two independent cohorts of patients with MCI do not support our hypothesis that loss of integrity of the cingulum bundle links Aβ deposition in the cingulate cortex to neurodegeneration of structures in the MTL.

Aβ deposition, tau aggregation and neurodegeneration are all characteristic features of AD, but Aβ deposition has a striking spatiotemporal discordance with tau and neurodegeneration.[17,44] The temporal discordance has been attributed to the sequence in which pathological processes take place. Aβ accumulates first while neurodegeneration starts about a decade later.[11,45] By the time that neurodegeneration starts, Aβ deposition is believed to have reached a plateau level,[44,46] which in part explains the weak correlation between levels of biomarkers for these processes, as we also see in the current study. Here we focused on the discordant starting locations of Aβ deposition compared to tau and neurodegenerative processes and zoomed in on loss of white matter integrity of the cingulum bundle as a connecting factor. The cingulum bundle was primarily chosen because of its anatomical location, directly linking the cingulate gyrus and the MTL, but the bundle is also known to be affected in AD.[18] Microstructural changes in the cingulum bundle, specifically in the parahippocampal cingulum, are well established in MCI and AD.[18,47,48] Mito et al.[48] showed that the posterior cingulum bundle was 1 of 2 bundles affected in patients with MCI when compared to healthy controls. The integrity of the cingulum bundle has also been shown to predict tau deposition in the posterior cingulate cortex in Aβ positive individuals from the MTL to the posterior cingulate cortex.[19]

This study did not find that Aβ deposition was linked to atrophy in the MTL via loss of integrity of the cingulum bundle. For the primary analysis we deliberately looked at the cingulate cortex and the complete MTL. It could however be argued that looking at these ROIs in closer detail would reveal more subtle relationships. Nevertheless, the post hoc sensitivity analyses that we performed did not show such an effect, with the exception of the association between cingulate Aβ and

posterior hippocampus volume. Our findings do not preclude involvement of white matter tracts in the dissemination of AD disease processes across the brain. Aβ in the neocortex might facilitate tau spread via the white matter tracts, without the tracts itself being damaged in that process.[16] A hint towards such a mechanism can be found in functional connectivity studies. It has been established in multiple studies that the default mode network (DMN), which shows reduced connectivity in AD, shows a large overlap with Aβ deposition patterns.[49,50] Furthermore, network analysis has shown that the level of connectivity to an initially affected area is a more important factor for vulnerability to Aβ deposition than proximity to such an affected area.[51–53]

The main strength of our study is that we performed a hypothesis-driven study in two independent cohorts of patients with MCI with high quality MRI and PET data. We used a state-of-the-art diffusion imaging analysis pipeline which included modern preprocessing techniques. One important aspect of diffusion MRI is that it is susceptible for scanner influences. For ADNI, a multicenter study, we tried to limit scanner influences on the diffusion measures by only selecting MRIs obtained on a Siemens scanner with a harmonized protocol. However, they were still obtained on different (types of) scanners which might have influenced our diffusion measures. Furthermore, the voxels of the UMCU diffusion scan were slightly anisotropic, which might have negatively influenced tractography results. However, we found very similar results in the ADNI cohort for which the diffusion scan was isotropic.

Another limitation is that we had no reference group to establish if the integrity of the white matter of the cingulum was indeed affected in this group. However, a number of studies have shown that the white matter,[54] specifically the cingulum bundle,[48] is affected in patients with MCI as compared to controls. Furthermore, we assessed an MCI population and the lack of associations of both MTL atrophy and white matter integrity with Aβ deposition might be because of a plateau effect of this latter biomarker. However, the association between Aβ markers and atrophy is known to be inconsistent, also in early stages of the disease[55,56] as is the association of Aβ markers with white matter integrity[57–59]. Another limitation is that we could only assess Aβ-PET as AD biomarker. Tau, especially in the entorhinal cortex, might have been valuable but this was not available for the UMCU sample. Lastly, in both cohorts sample sizes were modest, which affects

statistical power. However, the results were very consistent across cohorts and point estimates for the tested associations were close to zero, indicating that the null finding is unlikely to be due to low power alone. Furthermore, future studies could use Bayesian models to exclude even small effects.

In conclusion, our results do not support the hypothesis that loss of integrity of the white matter is a connecting factor between Aβ deposition in the cingulate gyrus and local neurodegeneration in the MTL. The hypothesis on involvement of the white matter tracts in the dissemination of AD disease processes should be further explored in future studies with a larger group of Aβ-positive individuals.

REFERENCES

1. Jack CR, Bennett DA, Blennow K, et al. NIA-AA Research Framework: Toward a biological definition of Alzheimer's disease. *Alzheimer's Dement* 2018; 14: 535–562.
2. Iturria-Medina Y, Sotero RC, Toussaint PJ, et al. Epidemic Spreading Model to Characterize Misfolded Proteins Propagation in Aging and Associated Neurodegenerative Disorders. *PLoS Comput Biol*; 10. Epub ahead of print 2014. DOI: 10.1371/journal.pcbi.1003956.
3. Palmqvist S, Schöll M, Strandberg O, et al. Earliest accumulation of β-amyloid occurs within the default-mode network and concurrently affects brain connectivity. *Nat Commun*; 8. Epub ahead of print 2017. DOI: 10.1038/s41467-017-01150-x.
4. Jack CR, Petersen RC, O'brien PC, et al. MR-based hippocampal volumetry in the diagnosis of Alzheimer's disease. *Neurology* 1992; 42: 183–188.
5. Whitwell JL, Petersen RC, Negash S, et al. Patterns of atrophy differ among specific subtypes of mild cognitive impairment. *Arch Neurol* 2007; 64: 1130–1138.
6. Pini L, Pievani M, Bocchetta M, et al. Brain atrophy in Alzheimer's Disease and aging. *Ageing Res Rev* 2016; 30: 25–48.
7. Cho SH, Shin JH, Jang H, et al. Amyloid involvement in subcortical regions predicts cognitive decline. *Eur J Nucl Med Mol Imaging* 2018; 45: 2368–2376.
8. Grothe MJ, Barthel H, Sepulcre J, et al. In vivo staging of regional amyloid deposition. *Neurology* 2017; 89: 2031–2038.
9. Cho H, Choi JY, Hwang MS, et al. In vivo cortical spreading pattern of tau and amyloid in the Alzheimer disease spectrum. *Ann Neurol* 2016; 80: 247–258.
10. van der Kant R, Goldstein LSB, Ossenkoppele R. Amyloid-β-independent regulators of tau pathology in Alzheimer disease. *Nat Rev Neurosci* 2020; 21: 21–35.
11. Jack CR, Knopman DS, Jagust WJ, et al. Hypothetical model of dynamic biomarkers of the Alzheimer's pathological cascade. *Lancet Neurol* 2010; 9: 119–128.
12. Baek MS, Cho H, Lee HS, et al. Temporal trajectories of in vivo tau and amyloid-β accumulation in Alzheimer's disease. *Eur J Nucl Med Mol Imaging* 2020; 47: 2879–2886.
13. Raj A, Kuceyeski A, Weiner M. A Network Diffusion Model of Disease Progression in Dementia. *Neuron* 2012; 73: 1204–1215.
14. Vogel JW, Iturria-Medina Y, Strandberg OT, et al. Spread of pathological tau proteins through communicating neurons in human Alzheimer's disease. *Nat Commun* 2020; 11: 2612.
15. Bennett RE, DeVos SL, Dujardin S, et al. Enhanced Tau Aggregation in the Presence of Amyloid β. *Am J Pathol* 2017; 187: 1601–1612.
16. Raj A, Iturria-Medina Y. Network spread models of neurodegenerative diseases. *Front Neurol* 2019; 9: 1159.
17. Jagust W. Imaging the evolution and pathophysiology of Alzheimer disease. *Nat Rev Neurosci* 2018; 19: 687–700.
18. Metzler-Baddeley C, Jones DK, Steventon J, et al. Cingulum microstructure predicts cognitive control in older age and mild cognitive impairment. *J Neurosci* 2012; 32: 17612–17619.
19. Jacobs HIL, Hedden T, Schultz AP, et al. Structural tract alterations predict downstream tau accumulation in amyloid-positive older individuals. *Nat Neurosci* 2018; 21: 424–431.

20. de Wilde A, van Maurik IS, Kunneman M, et al. Alzheimer's biomarkers in daily practice (ABIDE) project: Rationale and design. *Alzheimer's Dement Diagnosis, Assess Dis Monit* 2017; 6: 143–151.
21. Petersen RC. Mild cognitive impairment as a diagnostic entity. *J Intern Med* 2004; 256: 183–194.
22. Winblad B, Palmer K, Kivipelto M, et al. Mild cognitive impairment - Beyond controversies, towards a consensus: Report of the International Working Group on Mild Cognitive Impairment. *J Intern Med* 2004; 256: 240–246.
23. Jones DK. Precision and accuracy in diffusion tensor magnetic resonance imaging. *Top Magn Reson Imaging* 2010; 21: 87–99.
24. Vollmar C, O'Muircheartaigh J, Barker GJ, et al. Identical, but not the same: Intra-site and inter-site reproducibility of fractional anisotropy measures on two 3.0T scanners. *Neuroimage* 2010; 51: 1384–1394.
25. Grech-Sollars M, Hales PW, Miyazaki K, et al. Multi-centre reproducibility of diffusion MRI parameters for clinical sequences in the brain. *NMR Biomed* 2015; 28: 468–485.
26. Bondi MW, Edmonds EC, Jak AJ, et al. Neuropsychological Criteria for Mild Cognitive Impairment Improves Diagnostic Precision, Biomarker Associations, and Progression Rates. *J Alzheimer's Dis* 2014; 42: 275–289.
27. Hammers A, Allom R, Koepp MJ, et al. Three-dimensional maximum probability atlas of the human brain, with particular reference to the temporal lobe. *Hum Brain Mapp* 2003; 19: 224–247.
28. Landau SM, Fero A, Baker SL, et al. Measurement of longitudinal β-amyloid change with 18F-florbetapir PET and standardized uptake value ratios. *J Nucl Med* 2015; 56: 567–574.
29. Desikan RS, Ségonne F, Fischl B, et al. An automated labeling system for subdividing the human cerebral cortex on MRI scans into gyral based regions of interest. *Neuroimage* 2006; 31: 968–980.
30. Leemans A, Jeurissen B, Sijbers J, et al. ExploreDTI: a graphical toolbox for processing, analyzing, and visualizing diffusion MR data. In: *17th Annual Meeting of Intl Soc Mag Reson Med*. Hawaii, USA, 2009, p. 3537.
31. Tax CMW, Otte WM, Viergever MA, et al. REKINDLE: Robust Extraction of Kurtosis INDices with Linear Estimation. *Magn Reson Med* 2015; 73: 794–808.
32. Veraart J, Sijbers J, Sunaert S, et al. Weighted linear least squares estimation of diffusion MRI parameters: Strengths, limitations, and pitfalls. *Neuroimage* 2013; 81: 335–346.
33. Jeurissen B, Leemans A, Jones DK, et al. Probabilistic fiber tracking using the residual bootstrap with constrained spherical deconvolution. *Hum Brain Mapp* 2011; 32: 461–479.
34. Wisse LEM, Reijmer YD, Ter Telgte A, et al. Hippocampal disconnection in early Alzheimer's disease: A 7 tesla MRI study. *J Alzheimer's Dis* 2015; 45: 1247–1256.
35. Reijmer YD, Leemans A, Heringa SM, et al. Improved Sensitivity to Cerebral White Matter Abnormalities in Alzheimer's Disease with Spherical Deconvolution Based Tractography. *PLoS One* 2012; 7: 1–8.
36. Catani M, Thiebaut de Schotten M. A diffusion tensor imaging tractography atlas for virtual in vivo dissections. *Cortex* 2008; 44: 1105–1132.

37. Danielian LE, Iwata NK, Thomasson DM, et al. Reliability of fiber tracking measurements in diffusion tensor imaging for longitudinal study. *Neuroimage* 2010; 49: 1572–1580.
38. Kristo G, Leemans A, De Gelder B, et al. Reliability of the corticospinal tract and arcuate fasciculus reconstructed with DTI-based tractography: Implications for clinical practice. *Eur Radiol* 2013; 23: 28–36.
39. Colby JB, Soderberg L, Lebel C, et al. Along-tract statistics allow for enhanced tractography analysis. *Neuroimage* 2012; 59: 3227–3242.
40. Yushkevich PA, Pluta JB, Wang H, et al. Automated volumetry and regional thickness analysis of hippocampal subfields and medial temporal cortical structures in mild cognitive impairment. *Hum Brain Mapp* 2015; 36: 258–287.
41. Xie L, Wisse LEM, Das SR, et al. Accounting for the Confound of Meninges in Segmenting Entorhinal and Perirhinal Cortices in T1-Weighted MRI. In: Ourselin S, Joskowicz L, Sabuncu MR, et al. (eds) *Medical Image Computing and Computer-Assisted Intervention -- MICCAI 2016*. Cham: Springer International Publishing, 2016, pp. 564–571.
42. R Core Team. R: A language and environment for statistical computing. R Foundation for Statistical Computing, https://www.r-project.org/ (2018).
43. Bates D, Mächler M, Bolker B, et al. Fitting Linear Mixed-Effects Models Using lme4. *J Stat Softw* 2015; 67: 1–48.
44. Jack CR, Lowe VJ, Weigand SD, et al. Serial PIB and MRI in normal, mild cognitive impairment and Alzheimers disease: Implications for sequence of pathological events in Alzheimers disease. *Brain* 2009; 132: 1355–1365.
45. Caballero MÁA, Suárez-Calvet M, Duering M, et al. White matter diffusion alterations precede symptom onset in autosomal dominant Alzheimer's disease. *Brain* 2018; 141: 3065–3080.
46. Villemagne VL, Burnham S, Bourgeat P, et al. Amyloid β deposition, neurodegeneration, and cognitive decline in sporadic Alzheimer's disease: A prospective cohort study. *Lancet Neurol* 2013; 12: 357–367.
47. Bubb EJ, Metzler-Baddeley C, Aggleton JP. The cingulum bundle: Anatomy, function, and dysfunction. *Neurosci Biobehav Rev* 2018; 92: 104–127.
48. Mito R, Raffelt D, Dhollander T, et al. Fibre-specific white matter reductions in Alzheimer's disease and mild cognitive impairment. *Brain* 2018; 141: 888–902.
49. Buckner RL, Snyder AZ, Shannon BJ, et al. Molecular, structural, and functional characterization of Alzheimer's disease: Evidence for a relationship between default activity, amyloid, and memory. *J Neurosci* 2005; 25: 7709–7717.
50. Elman JA, Madison CM, Baker SL, et al. Effects of Beta-Amyloid on Resting State Functional Connectivity Within and between Networks Reflect Known Patterns of Regional Vulnerability. *Cereb Cortex* 2016; 26: 695–707.
51. Zhou J, Gennatas ED, Kramer JH, et al. Predicting Regional Neurodegeneration from the Healthy Brain Functional Connectome. *Neuron* 2012; 73: 1216–1227.
52. Sepulcre J, Grothe MJ, Sabuncu M, et al. Hierarchical organization of tau and Amyloid deposits in the cerebral cortex. *JAMA Neurol* 2017; 74: 813–820.
53. Pasquini L, Benson G, Grothe MJ, et al. Individual Correspondence of Amyloid-β and Intrinsic Connectivity in the Posterior Default Mode Network Across Stages of Alzheimer's Disease. *J Alzheimer's Dis* 2017; 58: 763–773.

54. Amlien IK, Fjell AM. Diffusion tensor imaging of white matter degeneration in Alzheimer's disease and mild cognitive impairment. *Neuroscience* 2014; 276: 206–215.
55. Becker JA, Hedden T, Carmasin J, et al. Amyloid-β associated cortical thinning in clinically normal elderly. *Ann Neurol* 2011; 69: 1032–1042.
56. Chételat G, Villemagne VL, Bourgeat P, et al. Relationship between atrophy and β-amyloid deposition in Alzheimer disease. *Ann Neurol* 2010; 67: 317–324.
57. Kantarci K, Schwarz CG, Reid RI, et al. White matter integrity determined with diffusion tensor imaging in older adults without dementia: Influence of amyloid load and neurodegeneration. *JAMA Neurol* 2014; 71: 1547–1554.
58. Vipin A, Ng KK, Ji F, et al. Amyloid burden accelerates white matter degradation in cognitively normal elderly individuals. *Hum Brain Mapp* 2019; 40: 2065–2075.
59. Finsterwalder S, Vlegels N, Gesierich B, et al. Small vessel disease more than Alzheimer's disease determines diffusion MRI alterations in memory clinic patients. *Alzheimer's Dement* 2020; 1–11.
60. Svarer C, Madsen K, Hasselbalch SG, et al. MR-based automatic delineation of volumes of interest in human brain PET images using probability maps. *Neuroimage* 2005; 24: 969–979.

SUPPLEMENTARY MATERIAL

Supplementary text 1

Amyloid PET scans are made on a Siemens Biograph 40 MCT scanner. Patients are injected with a tracer dose of approximately 300 MBq ± 20% ^{18}F-florbetaben (Neuraceq™). The image acquisition window extends from 90 to 110 minutes (4 × 5-minute frames) after dose injection. PET scans are collected centrally at the Amsterdam UMC – location VUmc. PET images were reconstructed in 4 frames (of 5 min each) with a matrix size of 200x200x148 and a final voxel size of 2.036x2.036x1.5 mm^3. After checking and correcting for motion, the 4 PET frames were averaged into a single frame. Using PVELAB [60], regions of interest (ROIs) were delineated on the co-registered MRI scan based on the Hammers template [27], and superimposed onto the static average PET scan to obtain gray matter (GM) standardized uptake values (SUV). Finally, we calculated SUV ratio (SUVr), using cerebellar GM as reference tissue, based on the average of the extracted volume-weighted cortical ROIs

Supplementary figure 1. Flowchart of ADNI selection

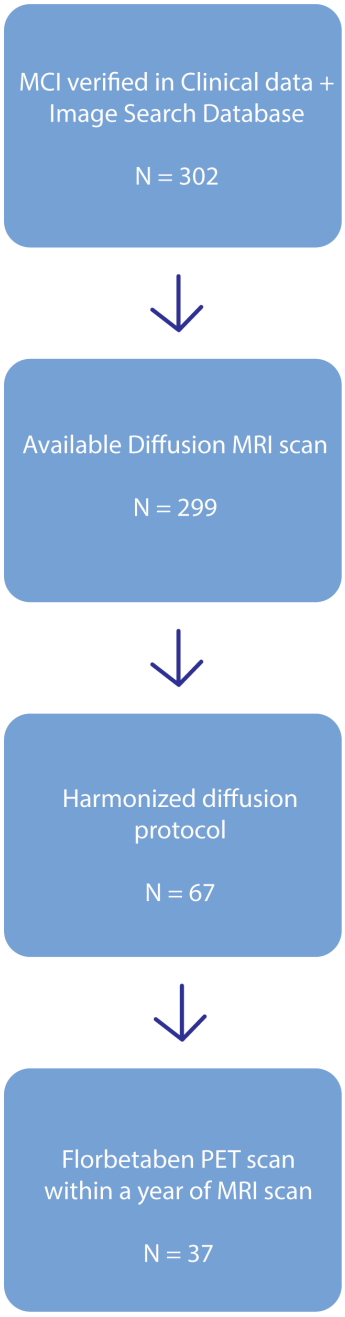

Supplementary table 1 Complete linear mixed model of association between Cingulate SUVR and MTL volume adjusted for hemisphere, age and sex.

	UMCU			ADNI		
	β (CI)	**F (df)**	***p***	**β (CI)**	**F**	***p***
Cing. SUVR	-0.27 (-0.63 – 0.09)	1.84 (1, 13.4)	0.2	-0.03 (-0.34 – 0.29)	0.02 (1, 36.8)	0.88
Hemisphere	-0.04 (-0.2 – 0.13)	0.19 (1, 14.9)	0.67	-0.08 (-0.16 – 0.00)	3.57 (1, 36.2)	0.07
Age	-0.1 (-0.16 – -0.04)	8.58 (1, 12)	**0.01**	-0.01 (-0.05 – 0.04)	0.06 (1, 33)	0.81
Sex	-0.6 (-1.37 – 0.17)	1.99 (1, 12)	0.18	0.16 (-0.81 – 0.49)	0.22 (1, 33)	0.64

Supplementary table 2 Complete linear mixed model of association between cingulum MD and cingulate SUVR adjusted for location, hemisphere, age and sex.

	UMCU			ADNI		
	β (CI)	**F (df)**	***p***	**β (CI)**	**F (df)**	***p***
MD	0.01 (-0.06 – 0.07)	0.03 (1, 48.2)	0.86	-0.01 (-0.03 – 0.01)	1.33 (1, 108.2)	0.25
Location	0.00 (-0.06 – 0.06)	0.00 (1, 48.1)	0.99	-0.01 (-0.03 – 0.01)	0.90 (1, 108.1)	0.34
Hemisphere	-0.00 (-0.03 – 0.02)	0.06 (1, 48)	0.80	-0.00 (-0.01 – 0.01)	0.00 (1, 108)	1.00
Age	-0.03 (-0.10 – 0.05)	0.42 (1, 15)	0.53	0.01 (-0.03 – 0.06)	0.36 (1, 34)	0.55
Sex	-0.04 (-1.02 – 0.93)	0.01 (1, 15)	0.93	-0.2 (-0.87 – 0.47)	0.33 (1, 34)	0.57

Supplementary table 3 Complete linear mixed model of association between cingulum MD and MTL volume adjusted for location, hemisphere, age and sex.

	UMCU			ADNI		
	β (CI)	**F (df)**	***p***	**β (CI)**	**F (df)**	***p***
MD	0.06 (-0.16 – 0.28)	0.24 (1, 44.37)	0.62	-0.01 (-0.10 – 0.08)	0.06 (1, 111.3)	0.80
Location	0.04 (-0.17 – 0.25)	0.11 (1, 43.88)	0.74	-0.01 (0.09 – 0.07)	0.04 (1, 110.2)	0.84
Hemisphere	-0.03 (-0.13 – 0.06)	0.43 (1, 42.11)	0.52	0.00 (-0.05 – 0.05)	0.00 (1, 108)	1.00
Age	-0.09 (-0.16 – -0.03)	7.20 (1, 13.44)	**0.02**	-0.01 (-0.05 – 0.04)	0.07 (1, 34)	0.79
Sex	-0.52 (-1.36 – 0.32)	1.34 (1, 12.97)	0.27	0.15 (-0.8 – 0.5)	0.20 (1, 34)	0.66

Supplementary table 4. Sensitivity analysis in Aβ-positive patients.

	UMCU			ADNI		
	β (CI)	**F (df)**	***p***	**β (CI)**	**F (df)**	***p***
PCC SUVR - MTL vol.	-0.28 (-0.65 – 0.08)	1.91 (1, 12.87)	0.19	-0.02 (-0.33 – 0.29)	0.01 (1, 39.9)	0.91
MD – PCC SUVR	-0.06 (-0.11 – 0.00)	3.81 (1, 48.12)	0.06	-0.01 (-0.04 – 0.02)	0.47 (1, 108.32)	0.57

Top row shows the results for the relationship between cingulate Aβ and MTL volume, middle row the results for cingulum MD and cingulate Aβ and the bottom row shows the results of the relationship between cingulum MD and MTL volume.

Supplementary table 5. Sensitivity analyses with posterior cingulate SUVR.

	UMCU			ADNI		
	β (CI)	**F(df)**	***p***	**β (CI)**	**F(df)**	***p***
ERC vol. – Cing. SUVR	-0.24 (-0.59 – 0.11)	1.53 (1, 18.29)	0.23	0.1 (-0.2 – 0.39)	0.37 (1,40.2)	0.54
ERC vol. – MD	0.19 (-0.02 – 0.39)	3.07 (1, 44.07)	0.09	-0.04 (-0.15 – 0.07)	0.49 (1, 113.6)	0.49
PHC vol. – Cing SUVR	-0.07 (-0.43 – 0.3)	0.12 (1, 13.53)	0.74	0.16 (-0.14 – 0.46)	1.04 (1, 39.6)	0.32
PHC vol. - MD	0.32 (-0.03 – 0.67)	2.94 (1, 48.48)	0.09	-0.05 (-0.16 – 0.06)	0.73 (1, 113.3)	0.39
PHipp. vol. – Cing SUVR	-0.36 (-0.71 – -0.01)	3.34 (1, 24.6)	0.08	-0.38 (-0.67 – 0.07)	6.23 (1, 56.1)	**0.02**
PHipp. vol. - MD	0.11 (-0.05 – 0.27)	1.64 (1, 43.03)	0.21	0.02 (-0.06 – 0.09)	0.19 (1, 110.1)	0.66

Top row shows the results for the relationship between posterior cingulate Aβ and MTL volume and bottom row the results for cingulum MD and posterior cingulate Aβ.

Supplementary table 6. Sensitivity analysis sub regions of the MTL.

	UMCU			**ADNI**		
	β (CI)	**F(df)**	***p***	**β (CI)**	**F(df)**	***p***
ERC vol. – Cing. SUVR	-0.24 (-0.59 – 0.11)	1.53 (1, 18.29)	0.23	0.1 (-0.2 – 0.39)	0.37 (1,40.2)	0.54
ERC vol. – MD	0.19 (-0.02 – 0.39)	3.07 (1, 44.07)	0.09	-0.04 (-0.15 – 0.07)	0.49 (1, 113.6)	0.49
PHC vol. – Cing SUVR	-0.07 (-0.43 – 0.3)	0.12 (1, 13.53)	0.74	0.16 (-0.14 – 0.46)	1.04 (1, 39.6)	0.32
PHC vol. - MD	0.32 (-0.03 – 0.67)	2.94 (1, 48.48)	0.09	-0.05 (-0.16 – 0.06)	0.73 (1, 113.3)	0.39
PHipp. vol. – Cing SUVR	-0.36 (-0.71 – -0.01)	3.34 (1, 24.6)	0.08	-0.38 (-0.67 – 0.07)	6.23 (1, 56.1)	**0.02**
PHipp. vol. - MD	0.11 (-0.05 – 0.27)	1.64 (1, 43.03)	0.21	0.02 (-0.06 – 0.09)	0.19 (1, 110.1)	0.66

Top 2 rows show the results for the relationship with entorhinal cortex volume, middle 2 rows the results for parahippocampal cortex and the bottom 2 rows show the results of posterior hippocampus volume.

5

CHAPTER

The cumulative effect of small vessel disease lesions is reflected in structural brain networks of memory clinic patients

Rutger Heinen*, Naomi Vlegels*, Jeroen de Bresser,
Alexander Leemans, Geert Jan Biessels, Yael D. Reijmer,
on behalf of the Utrecht Vascular Cognitive Impairment study group
* These authors contributed equally to this work

NeuroImage: Clinical 2018;19:963-969.

ABSTRACT

Background. Mechanisms underlying cognitive impairment in patients with small vessel disease (SVD) are still unknown. We hypothesized that cognition is affected by the cumulative effect of multiple SVD-related lesions on brain connectivity. We therefore assessed the relationship between the total SVD burden on MRI, global brain network efficiency, and cognition in memory clinic patients with vascular brain injury.

Methods. 173 patients from the memory clinic of the University Medical Center Utrecht underwent a 3T brain MRI scan (including diffusion MRI sequences) and neuropsychological testing. MRI markers for SVD were rated and compiled in a previously developed total SVD score. Structural brain networks were reconstructed using fiber tractography followed by graph theoretical analysis. The relationship between total SVD burden score, global network efficiency and cognition was assessed using multiple linear regression analyses.

Results. Each point increase on the SVD burden score was associated with .260 [-.404 – -.117] SD units decrease of global brain network efficiency (p < .001). Global network efficiency was associated with information processing speed (standardized B =-.210, p=.004) and attention and executive functioning (B =.164, p =.042), and mediated the relationship between SVD burden and information processing speed (p = .027) but not with executive functioning (p =.12).

Conclusion. Global network efficiency is sensitive to the cumulative effect of multiple manifestations of SVD on brain connectivity. Global network efficiency may therefore serve as a useful marker for functionally relevant SVD-related brain injury in clinical trials.

INTRODUCTION

Small vessel disease (SVD) is a common cause of cognitive decline and dementia.[1] However, the mechanisms underlying cognitive impairment in SVD remain largely unknown. A proposed mechanism is that SVD-related lesions (such as white matter hyperintensities (WMH), lacunes, cerebral microbleeds (CMB), and perivascular spaces (PVS)) affect structural brain connectivity and thereby the efficiency of the brain network to process information. Due to recently developed techniques, we can now estimate the efficiency of the brain network using diffusion MRI and graph theory analyses. Several studies have shown that global network efficiency is related to reduced processing speed and executive functioning in patients with SVD.[2-5] In these studies, associations between network efficiency and cognition were found to be stronger than between individual MRI markers of SVD and cognition.[6] One reason for the strong associations between network efficiency and cognition, could be a sensitivity of network efficiency to the cumulative effect of multiple types of SVD-related injury on brain connectivity.[7] In previous studies a total SVD burden score was used to capture these multiple types of SVD-related injury.[8-10] To date, the association between increasing SVD burden and brain network efficiency has not yet been assessed in memory clinic patients. In the current study, we used a previously developed total SVD score that combines various well-established MRI markers of SVD[8-10] to test the relationship between SVD, global network efficiency, and cognition. We expected that with increasing SVD burden (i.e., a higher SVD burden score), global network efficiency would decrease. Secondly, we hypothesized that global network efficiency mediates the association between total SVD score and cognition (i.e., processing speed and executive functioning).

METHODS

Study population

Patients in the current study were recruited from the memory clinic at the University Medical Center Utrecht (UMC Utrecht) between September 2009 and December 2013. This study sample has been described in detail earlier.[11] In short, all patients that presented with cognitive complaints and vascular brain injury on MRI (i.e., possible VCI) were eligible to participate. In order to capture

the whole spectrum of possible VCI, we defined no threshold for cognitive impairment or specific patterns of vascular brain injury. Vascular brain injury was operationalized as[11]: either (1) WMH with a Fazekas scale grade ≥ 2, (2) Fazekas scale grade 1 combined with two or more vascular risk factors (hypertension, hypercholesterolemia, diabetes mellitus, obesity or current smoking) (3) presence of ≥1 lacunar infarcts, (5) presence of ≥ 1 non-lacunar infarct (5) presence of ≥ 1 cerebral microbleeds or (6) presence of ≥ 1 intracerebral hemorrhage. All markers were rated according to the STRIVE criteria.[12] Absence or presence of possible co-existing neurodegenerative disorders did not play a role in the selection of patients.[11] Patients with a primary etiology other than vascular brain injury or an etiology other than neurodegeneration were excluded. All patients underwent a one-day evaluation consisting of an interview, a physical and a neurological examination, neuropsychological assessment and a brain MRI scan. During the interview and physical examination, information on education, smoking, medical history, use of medication, BMI and blood pressure was collected. In total, 173 patients were included in the analyses. The study was approved by the institutional review board of the UMC Utrecht. All patients provided informed consent prior to any research procedures.

MRI data acquisition

All patients underwent a brain MRI scan using a Philips 3T scanner (Achieva, Philips, Best, the Netherlands). The standardized MRI protocol included the following transversal 2D sequences (48 slices, voxel size: 0.96 x 0.96 x 3.00 mm^3): T2-weighted (repetition time (TR)/ echo time (TE): 3198/140 ms), T2*-weighted (TR/ TE: 1653/20 ms), and fluid-attenuated inversion recovery sequence (FLAIR; TR/ TE/Inversion time: 11000/125/2800 ms). The MRI protocol also included a 3D T1-weighted sequence (192 slices, voxel size: 1.00 x 1.00 x 1.00 mm^3, TR/TE: 7.9/4.5 ms), and a diffusion-weighted sequence (48 slices, voxel size: 1.72 x 1.72 x 2.50 mm^3, TR/TE: 6600/73 ms, 45 gradient directions with a b-value of 1200 s/mm^2 and one with a b value of 0 s/mm^2(number of signal averages = 3).

Small vessel disease burden on MRI

MRI images were rated for the presence of WMH of presumed vascular origin, lacunes of presumed vascular origin, CMB, and basal ganglia PVS by trained and experienced raters (RH under supervision of JdB) according to the STRIVE

criteria.[12] Perivascular and deep WMH were rated using the Fazekas scale on the FLAIR sequence.[13] Lacunes were defined as hypointense areas between 2 and 15 mm on both FLAIR and T1-weighted images with a hyperintense rim on FLAIR images. CMB were defined as small, homogenous, round, focal areas of hypointense areas on T2*-weighted images. Basal ganglia PVS were defined as small linear hyperintensities on T2-weighted images. PVS were rated according to a semi-quantitative scale ranging from 0 to 4.[14] Subsequently, a total SVD score was constructed for each patient according to a previously developed scale, see Figure 1.[8-10] This score summarizes the presence or severity of each of four SVD MRI markers: beginning confluent to confluent deep WMH (deep WMH Fazekas grade ≥ 2) and/or irregular periventricular WMH extending into the deep white matter (periventricular WMH Fazekas grade 3) (one point); presence of lacunes (one point); presence of CMB (one point); and moderate to severe PVS in the basal ganglia (grade 2-4 on semi-quantitative scale)[14] (one point). Due to motion artifacts, CMB and basal ganglia PVS could not be scored for 2 patients. For these 2 patients, CMB and basal ganglia PVS were not included in the calculation of the total SVD score.

Total brain volume

For all patients, segmentations of grey matter, white matter and cerebrospinal fluid were obtained for an earlier study with FreeSurfer version 5.3.0 (http://surfer.nmr.mgh.harvard.edu/)[15] using the 3D T1-weighted sequence. All brain volume segmentations underwent a visual quality check and were manually edited if needed. Manual edits consisted of correcting for large ventricles, correcting the brain mask and correcting for WMH. Total brain volume was defined as the sum of the grey and white matter volumes. To normalize total brain volume for variations in head size, total brain volume was adjusted for intracranial volume. Normalized total brain volumes were generated from linear regression of the residuals.[16]

Diffusion MRI processing and tractography

Brain networks were reconstructed as described previously,[2,3] using *ExploreDTI* version 4.8.6 (http://www.exploredti.com).[17] Preprocessing of the data included correction for subject motion and eddy current induced geometric distortions followed by robust tensor estimation (including adjustment of the B-matrix).[18-20] During the motion-distortion correction, all scans were rigidly registered to

Montreal Neurological Institute space. For each patient, whole-brain white matter tractography was performed using constrained spherical deconvolution (CSD)-based tractography, which allows for the reconstruction of pathways that go through crossing fiber regions.[21-24] Fiber tracts were reconstructed by starting seed samples uniformly distributed throughout the white matter of the brain at a 2 mm isotropic resolution. Fiber tracts were terminated when they deflected in an angle of more than 45° or if they entered a voxel with a fiber orientation distribution threshold of less than 0.1. Brain network nodes were defined using the automated anatomic labeling (AAL) template,[25] resulting in 90 cortical and subcortical brain regions. Two brain regions were considered to be connected if two end points of a reconstructed fiber bundle lay within both regions. This resulted in a 90x90 binary connectivity matrix. For all patients, each connection was multiplied by the mean fractional anisotropy (FA) of that connection which resulted in a 90x90 weighted connectivity matrix. For a graphical representation, see Figure 1.

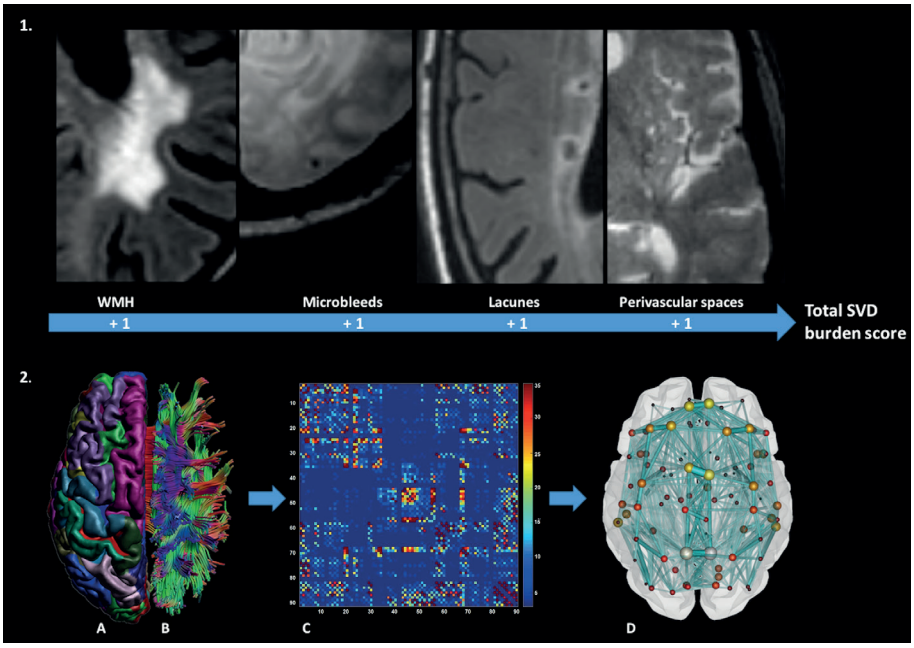

Figure 1 continued on next page.

Figure 1. Flowchart of construction of SVD burden score and structural network reconstruction. Panel 1 depicts the calculation of the total small vessel disease burden score. One point is added to the score for the presence for (1) Deep WMH (Fazekas grade ≥ 2) or perivascular WMH (Fazekas grade 3), (2) Presence of microbleeds, (3) Presence of lacunes, and (4) >10 perivascular spaces. Panel 2 depicts (A) The coregistration of an Automated Anatomical Labeling atlas (AAL) template, consisting of 90 cortical and subcortical brain regions to (B) the whole-brain Constrained Spherical Deconvolution (CSD)-based tractography, (C) For any two regions of the AAL template, it was established if a connection was present. Each connection was multiplied by the mean fractional anisotropy (FA) of that connection, resulting in a 90x90 weighted connectivity matrix. (D) The weighted connectivity matrix can be viewed as a graph composed of nodes (brain regions) and edges (white matter connections). Network measures such as global network efficiency were calculated on individual structural brain networks.

Brain network characteristics

Characteristics of the organization of the reconstructed structural brain networks were computed using the Brain Connectivity Toolbox.[26] First, the degree of the structural brain network was calculated on the binary connectivity matrices. Degree is defined as the number of connections per node.[26] Next global efficiency was computed on the FA-weighted connectivity matrices. Global efficiency reflects the ability to rapidly exchange information between distributed brain regions.[26] Global efficiency was calculated as the inverse of the characteristic path length. The characteristic path length quantifies the average number of connections between regions along the shortest path. The shorter the path length, the higher the efficiency of the network.[26] Global network efficiency was transformed into standardized z-scores to ease interpretation of the results.

Cognitive testing

All patients underwent standardized neuropsychological testing. The present study focused on the domains "information processing speed" and "attention and executive functioning" as these are among the most frequently impaired cognitive domains in patients with VCI.[27] Information processing speed was assessed by completion time of the Trail Making Test (TMT) A[28] and completion time of the Stroop Colour Word test I and II,[29] and the Digit symbol-coding test.[30] Attention and executive functioning was assessed by the ratio of completion time of the TMT-A and TMT-B,[28] and completion time of the Stroop Color Word test part III (adjusted for part I and II),[29] and two verbal fluency tasks: category naming and lexical fluency.[31] Z-scores were calculated for each test using the means and standard deviations of the present sample and averaged for tests comprising one cognitive domain.

Statistical analysis

The relationship between the total SVD score and global brain network efficiency was evaluated with multiple linear regression analysis (resulting in unstandardized betas with a 95% confidence interval and *p*-values (α = 0.05)). Next, correction for possible confounding effects of age, sex, vascular risk factors (hypertension, hypercholesterolemia, diabetes mellitus, and current smoking) and normalized total brain volume was performed by adding those variables as covariates in the model. Correction was also performed for the degree of the network. In a sensitivity analysis, the regression was repeated in patients without a clinical diagnosis of Alzheimer's disease (AD). To verify whether the associations with the total SVD burden score were not driven by WMH, the most common SVD marker in our cohort, we re-calculated SVD-scores without WMH. To check whether the tractography was affected by WMH, we assessed the association between WMH severity and number of network connections.

To assess the association between the total SVD score/global network efficiency and cognition, multiple linear regression analyses were performed. Correction was performed for possible confounding effects of age, sex and education and subsequently for vascular risk factors and normalized total brain volume. Correction was performed for normalized total brain volume and degree of the structural brain network. Finally, a mediation analysis was performed using the PROCESS (v2.16.3) macro[32] in SPSS to test whether the relationship between SVD burden and cognition was mediated by global network efficiency. The indirect effect of the mediation was tested with 5000 bootstrapping samples and 95% confidence interval.

RESULTS

Patient characteristics

Patient characteristics are shown in Table 1. 98% of the patients had some degree of WMH (Fazekas grade 1 or more), with 58% having moderate to severe WMH (Fazekas grade 2-3). Almost all patients (96%) had moderate to severe PVS (PVS score grade 2-4). Mean ± SD total brain volume of the patients was 962 ± 108 (normalized for intracranial volume 959 ± 96 cc). As a reference, non-normalized brain volumes in non-demented elderly controls have been estimated at 1013 ± 96 cc, using the same method.[33]

Table 1. Patient characteristics

	Total SVD score				
	0 **N = 6**	**1** **N = 47**	**2** **N = 65**	**3** **N = 37**	**4** **N = 18**
Age in years	64 ± 10	69 ± 10	73 ± 10	76 ± 11	71 ± 12
Female sex, %	33	47	43	49	39
Level of education*	5 (3 – 7)	5 (1 – 7)	5 (2 – 7)	5 (2 – 7)	6 (2 – 7)
MMSE	27.5 (25 – 28)	26 (7 – 30)	27 (17 – 30)†	26 (21 – 30)	27 (21 – 30)‡
Vascular risk factors					
Hypertension, %	100	96	89	95	100
Hypercholesterolemia, %	100	89	63	62	78
Diabetes Mellitus, %	33	47	25	40.5	44
Current smokers, %	50	32†	9†	8	22
Neuroimaging markers					
Basal ganglia PVS score	1 (1)	2 (2 – 3)	2 (1 – 3)	3 (2 – 4)	3 (2 – 3)
WMH Fazekas scale grade					
Periventricular	1 (1)	1 (0 – 3)	2 (0 – 3)	2 (1 – 3)	2.5 (1 – 3)
Deep	1 (0 – 1)	1 (0 – 3)	1 (0 – 3)	2 (1 – 3)	2.5 (1 – 3)
Total SVD score					
Presence of lacunes, %	-	-	32	59.5	100
Presence of microbleeds, %	-	-	32	57	100
Basal ganglia PVS (grade 2-4)	-	98	98.5	100	100
Moderate to severe WMH (Fazekas: PV=3 or Deep ≥2)	-	2	37	84	100

Data are given as mean ± SD, percentages or median (range). Abbreviations: MMSE = Mini Mental State Exam; PVS = Perivascular Spaces; WMH = White Matter Hyperintensities; PV = periventricular.
*: Verhage scale: (1) less than six years of primary education, (2) finished six years of primary education, (3) six years primary education and less than two years of low level secondary education, (4) four years of low level secondary education, (5) four years of average level secondary education, (6) five years of high level secondary education, (7) university degree. [44]
†: 2 missing
‡: 1 missing

Relationship between total SVD score and global network efficiency

The analysis between total SVD score and structural brain network measures showed that with each point increase in total SVD burden on MRI, there was a decrease in global network efficiency (regression coefficient: B [95% CI] = -.260 [-.406 – -.114], p = .001, see Figure 2). In other words, there was a dose-response relationship between the cumulative effect of SVD markers and global network efficiency. After controlling for age, sex, vascular risk factors (hypertension, hypercholesterolemia, diabetes mellitus and current smoking) and normalized total brain volume this association remained significant (B = -.239 [-.390 – -.089], p

= .002). The association between total SVD burden and global network efficiency was not changed by controlling for degree of the network (B = -.285 [-.366 – -.204], p < .001), indicating that the association with network efficiency was not driven by variations in the network density.

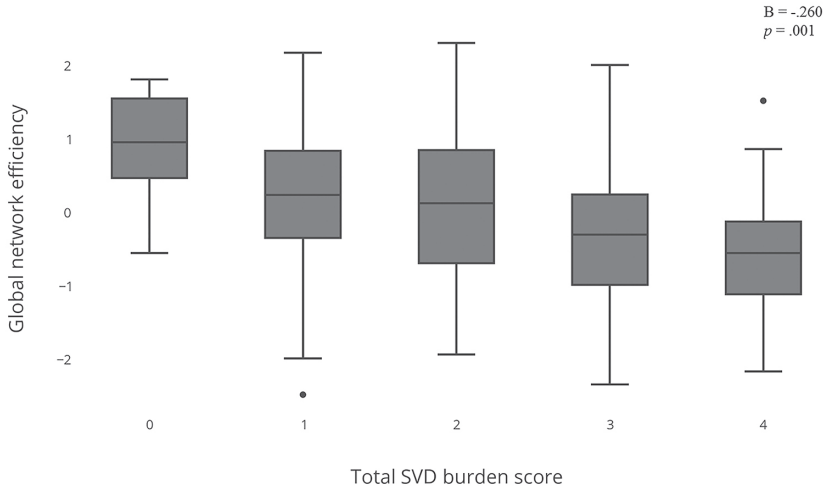

Figure 2. Relationship between total SVD score and global network efficiency. Boxplots showing the relationship between total small vessel disease burden score and global network efficiency (z-scores) in patients with vascular cognitive impairment.

A sensitivity analysis in patients without a diagnosis of AD showed similar results (B = -.361 [-.523 – -.199], *p* = <.001). Exclusion of WMH from the total SVD score showed that the association with global efficiency was not primarily driven by WMH (B = -.247 [-.445 – -.050], *p* = .014). Because 96% of the sample obtained a point for the presence of basal ganglia PVS, we re-calculated the total SVD score using a stricter cut-off value (i.e., >20 PVS, 45% of the sample). The adapted total SVD score, however, did not change the association with global network efficiency (B = -.208 [-.328 – -.088], *p* = .001).

There was no relationship between number of network connections and WMH severity (B = .048 [-.176 – .273], *p* = .671), indicating that WMH severity did not significantly affect the tractography results.

Relationship between total SVD score, global network efficiency and cognition

The analysis between total SVD score and cognition showed that the total SVD score tended to be associated with performance on both information processing speed (B = -.123 [-.273 – .026], trend *p* = .105) and attention and executive functioning (B = -.140 [-.289 – .008], trend *p* = .064), albeit not significantly (see Figure 3). After correction for age, sex, education and vascular risk factors the effect remained non-significant (information processing speed B = -.115 [-.254 – .025], p = .106; attention and executive functioning: B = -.119 [-.273 – .035], *p* = .129).

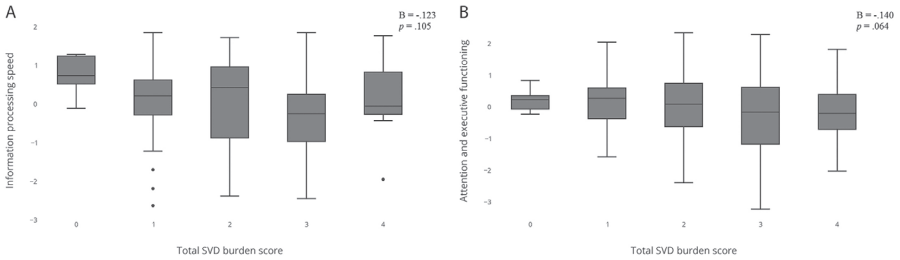

Figure 3. Relationship between total SVD score and cognition. Boxplots showing the relationship between total small vessel disease burden score and information processing speed (A) and attention and executive functioning (B). Information processing speed and attention and executive functioning are shown as z-scores.

As can be seen in Figure 4, global efficiency was associated with both information processing speed (B = .265 [.115 – .414], *p* = .001) and attention and executive functioning (B = .171 [.019 – .324], *p* = .028). After correction for age, sex, education, vascular risk factors and normalized total brain volume, this effect remained significant for information processing speed (B = .223 [.087 – .359], *p* = .001) and attention and executive functioning (B = .175 [.021 – .330], *p* = .027). Lastly, correcting for the degree of the structural networks did not change the results (information processing speed: B =.320 [.082 – .588], *p* = .009; attention and executive functioning: B =.298 [.056 – .539], *p* = .016).

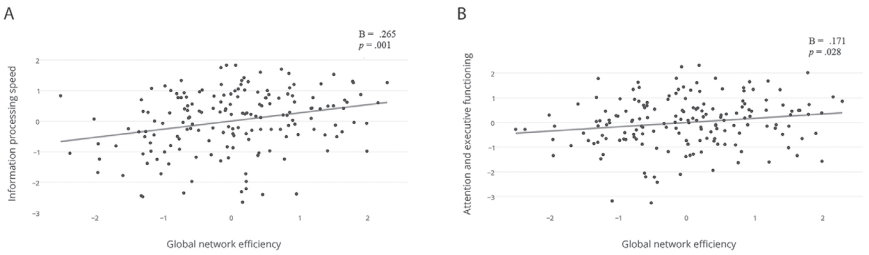

Figure 4. Relationship between global network efficiency and cognition. Scatterplot showing the relationship between global network efficiency and information processing speed (A) and attention and executive functioning (B). Both global network efficiency and cognitive performance are shown as *z*-scores.

Mediation analysis

The association between SVD burden and cognition was similar as reported in a previous study.[10] Albeit, not significant in our study. This could be due to a lower number of subjects. Nevertheless, a valid indirect mediation effect can still be established in the absence of a significant total effect as was shown in previous studies.[34-36] In the current study, mediation analysis showed that global network efficiency mediated the relationship between SVD burden and information processing speed (indirect effect B = -.059 [-.126 – -.017], p = .027), but not the relationship between SVD burden and attention and executive functioning (indirect effect B = -.035 [-.089 – -.005], p = .12).

DISCUSSION

The present study showed a dose-response relationship between the total SVD burden on MRI and decreased global network efficiency in memory clinic patients with vascular brain injury. Furthermore, global network efficiency mediated the association between SVD burden and information processing speed. These findings indicate that the cumulative effect of different manifestations of SVD partly affect cognition by disrupting structural brain connectivity.

Our results complement earlier studies that assessed the relationship between SVD, structural network measures and cognition.[4,5,10] Lawrence et al.[4] and Tuladhar et al.[5] found a mediating role for global network measures in the relationship between individual SVD markers and cognition. Our results indicate

that this mechanistic pathway might be better studied by considering the total burden of SVD than by individual markers. The greater the SVD burden, the lower the efficiency of the brain network to integrate information between remotely connected brain regions. The functional consequences of these network impairments seem to primarily involve information processing speed and executive functioning. [4,5] However, the mediation effect in our study was only significant for processing speed. While it is common to only perform mediation analysis in case of a significant total effect (as described by Baron and Kenny[37]), which in our case would be a significant association between total SVD burden and cognition, recent studies have demonstrated that a valid indirect mediation effect can be established in the absence of a significant total effect.[34-36]

SVD is a heterogeneous disease that manifests itself in different ways. We expected that a total SVD burden score could be better capable of capturing this heterogeneity than individual SVD markers. In the present study, we indeed found that the relationship between total SVD burden and structural brain connectivity was not driven by one of the common individual SVD markers, such as WMH, supporting the cumulative effect of SVD markers on the structural brain network. Staals et al. have shown that SVD markers also have a cumulative effect on cognition.[10] However, the strength of the association between total SVD burden score and cognition in our sample and in the study of Staals et al. were modest, and in our case not significant, which can be explained by the smaller sample size.[10]

Measures of global network connectivity quantify more than what is visible on conventional MRI. For example, diffusion MRI can also detect subtle changes in the so-called normal appearing white matter (NAWM). Diffusion abnormalities in the NAWM, such as decreased FA, are very common in patients with SVD and have been associated with SVD-related cognitive impairment.[38-41] However, whether the diffusion abnormalities in the NAWM indeed reflect SVD-related pathology is not known. Alternatively, it may reflect white matter damage caused by non-vascular pathologies, such as neurodegeneration and age.[7] In our view, diffusion measures and structural network measures should thus not be seen as a specific marker for SVD, but as a sensitive marker that integrates impairments in brain connectivity caused by multiple factors that together explain part of the cognitive performance in patients with SVD.

This study is the first to assess the association between total SVD burden, global network efficiency and cognitive performance in a relatively large sample of patients with different degrees of vascular brain injury. High quality, standardized structural MRI data were used in combination with detailed cognitive testing. One limitation of the DTI data is that only one b-zero image was acquired, which might have confounded the DTI estimates. Also, regions in which WMH is present, have relatively low FA values.[42,43] This may have affected the tractography results. However, we found no association between WMH severity and number of network connections. A possible limitation to this study could be the selection of our patients. Since all patients were recruited from the memory clinic and no selection was made based on absence or presence of co-existing neurodegenerative disorders, patients with mixed diagnoses and mixed pathologies were included in this study sample. As vascular brain injury commonly co-occurs with other pathologies, this does reflect clinical practice. Moreover, a sensitivity analysis in which all patients with AD were excluded, showed that the cumulative effect of SVD markers on global network efficiency was even stronger in this subset of patients. Our sample was selected based on the presence of SVD, which explains why almost all patients had some degree of basal ganglia PVS (96%). However, recalculating the total SVD score for all patients with a higher cut-off for PVS did not change the results. The construction of the total SVD score might be another limitation of this study. The score takes neither location nor number of individual SVD marker into account. Also, the same weight is assigned to each marker. Future studies should evaluate whether the total SVD score can be improved by including such information.

CONCLUSIONS

Our findings support the hypothesis that global network efficiency is sensitive to the cumulative effect of multiple manifestations of SVD on brain connectivity and may therefore serve as a useful marker for functionally relevant disease progression in clinical trials.

REFERENCES

1. Gorelick PB, Scuteri A, Black SE, DeCarli C, Greenberg SM, Iadecola C, et al. Vascular contributions to cognitive impairment and dementia: a statement for healthcare professionals from the American heart association/American stroke association. Stroke. 2011;42:2672-2713.
2. Reijmer YD, Leemans A, Caeyenberghs K, Heringa SM, Koek HL, Biessels GJ, Utrecht Vascular cognitive impairment study group. Disruption of cerebral networks and cognitive impairment in Alzheimer disease. Neurology. 2013;80:1370-1377.
3. Reijmer YD, Fotiadis P, Martinez-Ramirez S, Salat DH, Schultz A, Shoamanesh A, et al. Structural network alterations and neurological dysfunction in cerebral amyloid angiopathy. Brain. 2015;138:179-188.
4. Lawrence AJ, Chung AW, Morris RG, Markus HS, Barrick TR. Structural network efficiency is associated with cognitive impairment in small-vessel disease. Neurology. 2014;83:304-311.
5. Tuladhar AM, van Dijk E, Zwiers MP, van Norden AGW, de Laat K, Shumskaya E, et al. Structural network connectivity and cognition in cerebral small vessel disease. Human Brain Mapping. 2016;37:300-310.
6. Patel B, Markus HS. Magnetic resonance imaging in cerebral small vessel disease and its use as a surrogate disease marker. Int J Stroke. 2011;6:47-59.
7. Sun X, Salat D, Upchurch K, Deason R, Kowall N, Budson A, et al. Destruction of white matter integrity in patients with mild cognitive impairment and Alzheimer disease. Journal of Investigative medicine 2014;62:927-933.
8. Huijts M, Duits A, Van Oostenbrugge RJ, Kroon AA, de Leeuw PW, Staals J. Accumulation of MRI markers of cerebral small vessel disease is associated with decreased cognitive function. A study in first-ever lacunar stroke and hypertensive patients. Front. Aging Neursci. 2013;5:72.
9. Staals J, Makin S, Doubal F, Dennis M, Wardlaw JM. Stroke subtype, vascular risk factors and total MRI brain small-vessel disease burden. Neurology. 2014;83:1228-1234.
10. Staals J, Booth T, Morris Z, Bastin ME, Gow AJ, Corley J, et al. Total MRI load of cerebral small vessel disease and cognitive ability in older people. Neurobiology of Aging. 2015;36:2806-2811.
11. Boomsma JMF, Exalto LG, Barkhof F, van den Berg E, de Bresser J, Heinen R, et al. Vascular Cognitive Impairment in a Memory Clinic Population: Rationale and Design of the "Utrecht-Amsterdam Clinical Features and Prognosis in Vascular Cognitive Impairment" (TRACE-VCI) Study. JMIR Res Protoc. 2017;6:e60
12. Wardlaw JM, Smith EE, Biessels GJ, Cordonnier C, Fazekas F, Frayne R, et al. Neuroimaging standards for research into small vessel disease and its contribution to ageing and neurodegeneration. Lancet Neurol. 2013;12:822-838.
13. Fazekas F, Chawluk JB, Alavi A, Hurtig HI, Zimmerman RA. MR signal abnormalities at 1.5 T in Alzheimer's dementia and normal aging**.** AJR Am J Roentgenol. 1987:149**:**351-356.
14. Doubal FN, MacLullich AM, Ferguson KJ, Dennis MS, Wardlaw JM. Enlarged perivascular spaces on MRI are a feature of cerebral small vessel disease. Stroke. 2010;41:450-454.

15. Fischl B, Salat DH, Busa E, Albert M, Dieterich M, Haselgrove C, et al. Whole brain segmentation: automated labeling of neuroanatomical structures in the human brain. Neuron. 2002;33:341-355.
16. Voevodskaya O, Simmons A, Nordenskjöld R, Kullberg J, Ahlström H, Lind L, et al. The effects of intracranial volume adjustment approaches on multiple regional MRI volumes in healthy aging and Alzheimer's disease. Frontiers in Aging Neuroscience 2014;6:
17. Leemans A, Jeurissen B, Sijbers J, Jones DK (2009): ExploreDTI: a graphical toolbox for processing, analyzing and visualizing diffusion MR data. 17th annual meeting of Intl Soc Mag Reson Med:3537.
18. Leemans A, Jones DK. The B-matrix must be rotated when correcting for subject motion in DTI data. Magn Reson Med. 2009;61:1336-1349.
19. Veraart J, Sijbers J, Sunaert S, Leemans A, Jeurissen B. Weighted linear least squares estimation of diffusion MRI parameters: strengths, limitations, and pitfalls. Neuroimage. 2013:81:335-346.
20. Tax CM, Otte WM, Viergever MA, Dijkhuizen RM, Leemans A. REKINDLE: robust extraction of kurtosis INDices with linear estimation. Magn Reson Med. 2015:73:794-808.
21. Jeurissen B, Leemans A, Jones DK, Tournier JD, Sijbers J. Probabilistic fiber tracking using the residual bootstrap with constrained spherical deconvolution. Human Brain Mapping. 2011;32:461-479.
22. Tax CM, Jeurissen B, Vox SB, Viergever MA, Leemans A. Recursive calibration of the fiber response function for spherical deconvolution of diffusion MRI data. Neuroimage. 2014;86:67-80.
23. Tournier JD, Calamante F, Connelly A. Robust determination of the fibre orientation distribution in diffusion MRI: non-negativity constrained super-resolved spherical deconvolution. Neuroimage. 2007;35:1459-1472.
24. Jeurissen B, Leemans A, Tournier JD, Jones DK, Sijbers J. Investigating the prevalence of complex fiber configurations in white matter tissue with diffusion magnetic resonance imaging. Human Brain Mapping. 2013;34:2747-2766.
25. Tzourio-Mazoyer N, Landeau B, Papathanassiou D, Crivello F, Etard O, Delcroix N, et al. Automated anatomic labelling of activations in SPM using a macroscopic anatomical parcellation of the MNI MRI single-subject brain. Neuroimage. 2002;15:273-289.
26. Rubinov M, Sporns O. Complex network measures of brain connectivity: Uses and interpretations. NeuroImage. 2010;52:1059-1069.
27. Prins ND, van Dijk EJ, den Heijer T, Vermeer SE, Jolles J, Koudstaal PJ, et al. Cerebral small-vessel disease and decline in information processing speed, executive function and memory. Brain. 2005;128:2034-2041.
28. Corrigan JD, Hinkeldy NS. Relationships between parts A and B of the Trail Making Test. J Clin Psychol. 1987;43:402-409.
29. Stroop JR. Studies of interference in serial verbal reactions. Journal of Experimental Psychology. 1935;18:643-662.
30. Moses JA, Jr., Pritchard DA, Adams RL. Neuropsychological information in the Wechsler Adult Intelligence Scale-Revised. Arch Clin Neuropsychol. 1997;12:97-109.

31. Deelman BG, Liebrand WB, Koning-Haanstra M, van den Berg W. Measurements of aphasic disorders: a brief description of the SAN-battery. Gerontologie. 1980;11:17-21.
32. Hayes AF. Introduction to mediation, moderation, and conditional process analysis: A regression based approach. New York, NY: The Guilford Press; 2013.
33. Heinen R, Bouvy WH, Mendrik AM, Viergever MA, Biessels GJ, de Bresser J. Robustness of Automated Methods for Brain Volume Measurements across Different MRI Field Strengths. PLoS ONE 2016;10: e0165719.
34. Shrout PE, Bolger N. Mediation in experimental and nonexperimental studies: New procedures and recommendations. Psychological Methods. 2002;7:422-445.
35. Hayes AF. Beyond Baron and Kenny: Statistical mediation analysis in the new millennium. Communication Monographs. 2009;76:408-420
36. Zhao X, Lynch JG jr, Chen Q. Reconsidering Baron and Kenny: Myths and truths about mediation analysis. Journal of Consumer Research. 2010;37:197–206.
37. Baron RM, Kenny DA. Moderator-Mediator Variables Distinction in Social Psychological Research: Conceptual, Strategic, and Statistical Considerations. Journal of Personality and Social Psychology. 1986;51:1173–82
38. O'Sullivan M, Summers PE, Jones DK, Jarosz JM, Williams SCR, Markus HS. Normal-appearing white matter in ischaemic leukoaraiosis: A diffusion tensor MRI study. Neurology. 2001;57:2307-2310.
39. O'Sullivan M, Morris RG, Huckstep B, Jones DK, Williams SCR, Markus HS. Diffusion Tensor MRI correlates with executive functioning in patients with ischaemic leukoaroaiosis. J Neurol Neurosurg Psychiatry. 2004;75:441-447
40. Van Norden AGW, de Laat KF, van Dijk EJ, IWM van Uden, van Oudheusden LJB, Gons RAR, et al. Diffusion tensor imaging and cognition in cerebral small vessel disease: The RUN DMC study. Biochim. Biophys. Acta. 2012;1822:401–407.
41. Tuladhar AM, van Norden AGW, de Laat KF, Zwiers MP, van Dijk EJ, Norris DG, et al. White matter integrity in small vessel disease is related to cognition. NeuroImage Clinical 2015;7:518-524.
42. Bastin ME, Clayden JD, Pattie A, Gerrish IF, Wardlaw JM, Deary IJ. Diffusion tensor and magnetization transfer MRI measurements of periventricular white matter hyperintensities in old age. Neurobiology of aging 2009;30:125-136.
43. Maniega SM, Valdes Hernandez MC, Clayden JD, Royle NA, Murray C, Morris Z, et al. White matter hyperintensities and normal-appearing white matter integrity in the aging brain. Neurobiology of Aging. 2015;36:909-918,
44. Verhage F.: Intelligentie en leeftijd: onderzoek bij Nederlanders van twaalf tot zevenenzeventig jaar. 1964.

6

CHAPTER

Brain network disruption and cognitive decline: relevance of critical white matter connections

Naomi Vlegels, Bruno M. de Brito Robalo, Huiberdina L. Koek, Yael D. Reijmer, Geert Jan Biessels, on behalf of the Utrecht Vascular Cognitive Impairment study group.

ABSTRACT

Background. Disrupted white matter connections, in particular critical connections, are believed to be a cause of cognitive dysfunction in multiple dementia etiologies. Both neurodegenerative and vascular etiologies of dementia have been suggested to specifically affect these critical connections. We test the hypothesis that disrupted critical white matter connections form a final common pathway to cognitive decline in memory clinic patients with mixed etiologies.

Methods. We selected 186 memory clinic patients with vascular and/or neurodegenerative etiologies. For all patients, white matter networks were reconstructed from diffusion-weighted MRI. Critical white matter connections were defined as the 10% connections with the highest edge centrality, all other connections were defined as non-critical connections. Cognitive decline was defined as an increase on the clinical dementia rating scale over 2 years' time. White matter hyperintensity (WMH) volume was used as a measure of vascular disease, medial temporal lobe (MTL) volume as a measure of neurodegeneration.

Results. Disruption of critical connections was associated with a higher odds ratio of cognitive decline (OR = 1.54 (1.06 – 2.23), p = .023). Notably, such an association was also found for disruption of non-critical connections (OR =1.86 (1.24 – 2.77), p =.002). Furthermore, WMH volume as well as MTL volume were associated with disruptions to both critical (p < .001, p = .027, respectively) and non-critical connections (p < .001, p = .003).

Conclusion. Disruption of white matter connections in memory clinic patients predicts cognitive decline. However, this is not specific for critical connections. Moreover, neither vascular injury nor neurodegeneration appear to specifically affect critical connections.

INTRODUCTION

Disruption of white matter connections, particularly those that that are critical for overall network efficiency, is believed to be a cause of cognitive dysfunction in multiple dementia etiologies.[1–6] Two of the leading causes of dementia, neurodegeneration (e.g., Alzheimer's disease) and cerebrovascular disease, which frequently co-occur in elderly,[7] have been suggested to specifically affect these critical white matter connections.[5,6]

Network connections are considered to be critical if they are highly interconnected. Critical connections function as the "highways of the brain and play a key role in network integration. Disruption of critical connections results in disintegration of the network and is therefore likely to disproportionally impact global network performance[8,9] and lead to clinical symptoms. While it has been well established in cross-sectional studies that network disruption is related to poor cognitive functioning in patients with for example Alzheimer's disease (AD) or small vessel disease (SVD),[3,4,10] emerging literature suggests that this relationship may be primarily driven by disruption of critical network connections.[2,11] However, the specific role of critical connections in cognitive decline over time is less studied. One earlier longitudinal study, performed in patients with small vessel disease (SVD) found no specific role for critical connections.[12]

In addition it has been suggested that critical connections of the brain network might be more vulnerable to disease effects because of their higher biological costs.[5,6,13] Yet it is not completely clear whether critical network connections are indeed disproportionally affected by cerebrovascular disease and/or neurodegeneration.

In this study, we assessed if disrupted critical white matter connections form a final common pathway to cognitive decline in memory clinic patients with mixed etiologies.

METHODS

Study population

Patients were part of a prospective study and were recruited from the memory clinic of the University Medical Center Utrecht (UMC Utrecht) between November 2011 and April 2017. Patients were eligible to participate if they were referred to the memory clinic for the evaluation of cognitive problems, had a clinical dementia rating (CDR) scale score ≤ 1,[14] and a Mini Mental State Exam (MMSE) of ≥ 20.[15] Patients with evidence for a primary etiology other than neurodegenerative disease or SVD (e.g., without cognitive problems due to alcohol abuse, epilepsy, brain tumor) were not eligible for this study. Patients underwent a one-day memory clinic evaluation consisting of a physical examination, an interview, brain MRI, neuropsychological assessment and basic laboratory testing. Baseline CDR score and T1-weighted and Diffusion Tensor Imaging (DTI) should be available for inclusion. From 228 eligible patients 29 were excluded for incomplete data, leaving 199 patients. Following quality assessment of the T1-weighted and DTI scans, 186 patients were included in the cross-sectional analysis of the present study. For 140 patients (75%), a second CDR score at one- or two-year follow-up was available. These 140 patients were included in our longitudinal analysis. Patients were lost to follow-up for the following reasons, refusal to participate (n=26), CDR not administered at follow-up (n = 10), death (n = 4), hospitalization (n = 1), and unknown (n = 5). The study was approved by the institutional review board of the UMC Utrecht. All procedures were in accordance with the ethical standards of the responsible committee on human experimentation (institutional and national) and with the Helsinki Declaration of 1975, as revised in 2013. All patients provided informed consent prior to any research procedures.

Clinical diagnosis

Clinical diagnoses were established at multidisciplinary consensus meetings after the one-day memory clinic evaluation. Patients were divided in three categories: no objective cognitive impairment (NOCI), mild cognitive impairment (MCI) and dementia. NOCI was defined as having cognitive complaints, but without objective cognitive impairment on neuropsychological testing (also referred to as subjective cognitive impairment).[16] MCI was defined as complaints or deterioration from prior

functioning and objective evidence of impairment in at least one cognitive domain. Daily living activities were normal or mildly impaired.[17] Dementia was diagnosed when deficits were present in at least two cognitive domains at neuropsychological testing and when there was interference in daily living. Further etiological classifications of dementia were made based on internationally established criteria (without knowledge of CSF biomarkers) in vascular, neurodegenerative or unknown origin.[18–20]

Cognitive dysfunction and decline

The CDR scale was used as a global measure of cognitive dysfunction.[14] The CDR scale assesses functional and cognitive abilities and ranges from 0-3, indicating: no cognitive dysfunction (CDR = 0), mild cognitive dysfunction (CDR = 0.5), severe cognitive dysfunction (CDR = 1), moderate dementia (CDR = 2) and severe dementia (CDR = 3). Cognitive decline was defined as ≥ 0.5 increase on the CDR or institutionalization over two-years' time. Patients with follow-up CDR data were divided into three groups: stable cognition (no decline on the CDR score), moderate decline (increase between 0.5 and 1) and rapid decline (increase of >1). We used this relatively coarse scale because we were interested in clinically relevant cognitive dysfunction and decline.

MRI data acquisition

All patients underwent a brain MRI scan using a Philips 3-tesla scanner (Achieva, Philips, Best, the Netherlands). The standardized MRI protocol included the following transversal 2D sequences (48 slices, voxel size: 0.96 x 0.96 x 3.00 mm): T2-weighted, T2*-weighted, and fluid-attenuated inversion recovery sequence (FLAIR). The MRI protocol also included a 3D T1-weighted sequence (192 slices, voxel size: 1.00 x 1.00 x 1.00 mm, TR/TE: 7.9/4.5 ms), and a diffusion-weighted sequence (48 slices, voxel size: 1.72 x 1.72 x 2.50 mm, TR/TE: 6600/73 ms, 45 gradient directions with a b-value of 1200 s/mm^2 and one with a b value of 0 s/mm^2).

Total brain, white matter hyperintensity, and medial temporal lobe volume

A semi-automated processing pipeline was used to obtain brain volume measurements as previously described.[21] In short, lesion filling was performed on 3D-T1 images, using the SLF toolbox (http://atc.udg.edu/nic/slfToolbox/index.html) for Statistical Parametric Mapping (SPM) version 12 (Institute of Neurology, London, United Kingdom) with default settings. Lesion filled 3D T1 images were automatically segmented into grey matter, white matter and cerebrospinal fluid (CSF) using the Computational Anatomical Toolbox (CAT) 12 toolbox (version R1073, C. Gaser, Structural Brain Mapping Group, Jena University Hospital, Jena, Germany) for SPM version 12. Total brain volume was defined as the sum of grey matter and white matter volumes. Total intracranial volume was determined by the sum of total brain volume and CSF. As a marker of vascular disease we calculated white matter hyperintensity (WMH) volumes.[22,23] WMH volumes were segmented by the lesion prediction algorithm as implemented in the Lesion Segmentation Toolbox (v 2.0.9) for SPM using FLAIR images. As a marker for neurodegeneration, we calculated medial temporal lobe (MTL) volume.[24] MTL volume was calculated by registering the Automated Anatomical Labeling (AAL) template to the 3D-T1 weighted images with affine registration methods in CAT12 [25]. The AAL template parcellates the segmented grey matter into 90 cortical and subcortical regions. MTL volume was calculated for each patient by summing the grey matter volumes of the hippocampus, parahippocampal gyrus and the amygdala region. To account for head size variability, total brain volume, MTL volume and WMH volume were all calculated as a percentage of the total intracranial volume.

DTI processing and network reconstruction

Diffusion weighted images were processed with ExploreDTI (version 4.8.6).[26] Pre-processing included correction for subject motion, eddy currents and EPI distortion. Subject motion, including rotation of the B-matrix,[27,28] was corrected by realigning the diffusion-weighted volumes (b = 1200 s/mm^2) with the b0 image. For the correction of eddy currents and EPI distortion, the diffusion-weighted image was non-rigidly registered to the 3D-T1 weighted image. Pre-processing was followed by robust tensor estimation using the Robust Extraction of Kurtosis INDices with Linear Estimation (REKINDLE) approach.[29] For each patient, whole-

brain tractography was performed using constrained spherical deconvolution (CSD)-based tractography, which allows for the reconstruction of tracts in crossing fiber regions.[30] Fiber tracts were reconstructed by setting seed points uniformly throughout the white matter of the brain at 2 mm isotropic resolution. Fiber tracts were terminated when they deflected in an angle of > 45° or if they entered a voxel with a fiber orientation distribution threshold of < 0.1.

All 3D-T1 weighted images were parcellated into 90 regions according to the AAL atlas as described in the paragraph 2.4. In order to have the fiber tractography and the 90 brain regions in the same space, the diffusion-weighted images were registered to the T1-weighted images. Each AAL region represents a node in the brain network. Two nodes were considered to be connected if at least one streamline had endpoints located in two regions, resulting in a 90x90 binary connectivity matrix. The binary connectivity matrix was multiplied by the mean diffusivity (MD) resulting in an MD-weighted connectivity matrix. We chose to weight the edges by MD as this measure has frequently been shown to be altered in AD and SVD.[31,32] An FA threshold of > 0.2 was used on all connectivity matrices to minimize errors due to partial volume effects.

Critical network connections

Connections within the brain network that have an important topological position in the network are considered to be critical for global network integration.[33] Earlier literature mentions two different definitions for critical network connections: 1) connections with high edge centrality (i.e., connections that participate in a high number of communication paths)[2] and 2) connections that form a direct link between hub nodes.[34] In our primary analyses critical network connections were defined as connections with high edge centrality, since that definition is mathematically most directly related to global network efficiency. In a sensitivity analysis, critical network connections were defined as connections between hub nodes. To define the subset of connections with high edge-betweenness centrality, we first calculated the average brain network of the study sample by including those connections that occurred in 2/3 of the participants.[35] Centrality of each edge within the average network was quantified by the edge betweenness centrality (for the exact mathematical definition see[36]). The 10% connections with highest edge betweenness centrality were considered to be central network connections.

The subset of central network connections is visualized in Figure 1. The average MD-values of the critical connections were calculated for each patient. Secondarily, in a sensitivity analysis we defined critical connections as connections between hub nodes, i.e., hub-hub connections. Hub connections were selected as follows: first, betweennees centrality was calculated for each patient separately and then averaged, secondly, the 10 nodes with the highest average betweenness centrality were selected as hub nodes, as described previously.[34] All connections running between hub nodes were then defined as 'hub-hub connections'.[34] Lastly, the average MD-values of the hub-hub connections were calculated for each patient. Non-critical network connections were defined as all connections that were neither included as central connections nor hub-hub connections. Non-critical network connections were also weighted by the average MD-values for each patient.

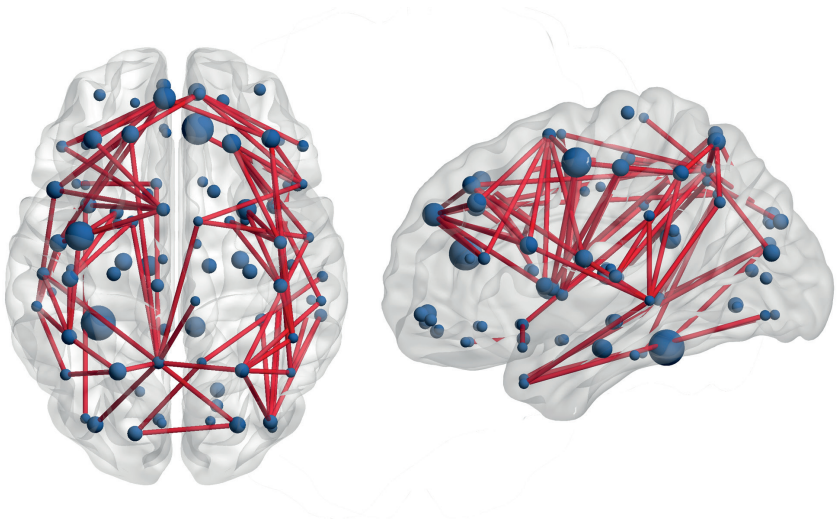

Figure 1. Subset of critical connections. Figure shows the subset of critical connections (in red) based on the highest 10% edge betweenness centrality from an axial view and a sagittal view. The larger nodes indicate hub nodes which were defined based on the binary betweenness centrality.

Statistical analyses

All analyses were performed using SPSS version 25 (IBM Corp. Released 2017. IBM SPSS Statistics for Windows, Version 25.0. Armonk, NY: IBM Corp.). All associations were corrected for age. Because sex was not a significant predictor in any of the models it was not included in the final analyses. Effect estimates and 95%

confidence intervals were calculated and the significance level was established at ≤ α = 0.05. WMH volume, MTL volume and MD of the white matter connections were transformed into z-scores to ease interpretation of the results. The association between the MD of (non)-critical network connections and cognitive dysfunction was evaluated with a logistic regression analysis. The association between MD of (non)-critical network connections and cognitive decline was evaluated with an ordinal regression analysis. The association between WMH volume/MTL volume and the MD of (non-)critical network connections was tested with linear regression analyses.

RESULTS

Table 1 shows the baseline characteristics of 186 patients included in the study, of whom 78 (41.9%) were diagnosed with dementia (subtypes in table 1). Of the 186 patients, 5 showed no cognitive dysfunction at baseline (CDR=0), 137 had mild cognitive dysfunction (CDR=0.5), and 44 had severe cognitive dysfunction (CDR=1). Because only 5 patients had a CDR of 0 at baseline, we merged the no cognitive dysfunction (CDR = 0) and mild cognitive dysfunction groups (CDR = 0.5) in further baseline analyses. Of those with longitudinal cognitive data (n = 140), 81 patients (58%) remained cognitively stable (no change in CDR score), 44 patients (31%) showed moderate cognitive decline (increase of 0.5 to 1 on CDR score) and 15 patients (11%) showed rapid cognitive decline (increase > 1 on CDR score) over a mean follow-up of 22 ± 7 months.

Associations between impairments of (non)-critical network connections and cognition

The disruption of critical network connections, reflected by a higher MD, was associated with a higher odds ratio of cognitive dysfunction at baseline (OR(CI95) per SD increase in MD = 1.51 (1.03 – 2.22), p = .036) and with a higher odds ratio of cognitive decline over time (OR = 1.54 (1.06 – 2.23), p = .023). Notably, a similar association was found between the MD of non-critical network connections and cognitive dysfunction and cognitive decline (cognitive dysfunction at baseline: OR = 1.76 (1.16 – 2.67), p = .008; cognitive decline: OR =1.86 (1.24 – 2.77), p =.002), indicating that the association between impairments of network connections and cognitive decline was not specific to critical connections Figure 2 shows a visual representation of the MD levels of critical and non-critical connections over the different cognitive decline groups.

Table 1. Sample characteristics

	Study sample (N=186)
Demographic characteristics	
Female sex	81 (43.5)
Age, years	74.9 ± 7.99
MMSE	26 [4]
CDR scale	
0	5 (2.7)
0.5	137 (73.7)
1	44 (23.7)
Diagnosis[a]	
Dementia	78 (41.9)
Alzheimer's disease	72 (38.7)
Vascular dementia	2 (1.1)
Frontotemporal dementia	1 (0.5)
Semantic dementia	1 (0.5)
Unknown	3 (1.6)
MCI	92 (49.5)
No objective cognitive impairment	15 (8.1)
Imaging markers	
Brain volume, % TIV[b]	67.9 [5.25]
WMH volume, % TIV[b]	1.24 [2.01]
Lacunar infarct[a]	60 (32.3)
Cortical infarct[c]	27 (14.5)
Microbleeds[d]	46 (24.7)

Data are presented as n (%), mean ± SD, median [interquartile range].
Abbreviations; SD = standard deviation; MMSE = Mini Mental State Exam; CDR = Clinical dementia rating; MCI = Mild cognitive impairment; TIV = Total intracranial volume; WMH = white matter hyperintensity
[a] = 1 missing value. [b] = 5 missing values. [c] = 2 missing values. [d] = 9 missing values

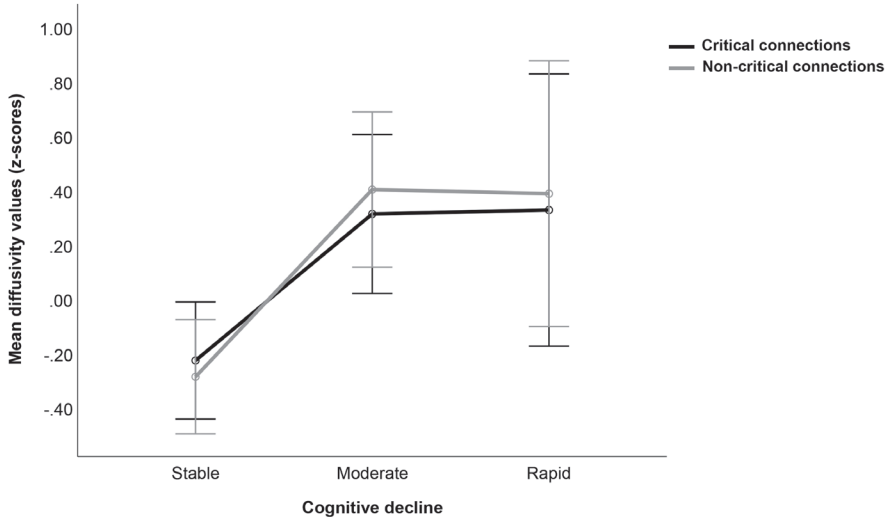

Figure 2. Disruption of (non)-critical connections and cognitive decline. Lines indicate the mean diffusivity values in z-scores for both critical and non-critical connections per patient group (i.e., those who showed stable cognition, moderate cognitive decline, and rapid cognitive decline over 2 years). Error bars represent the standard error

Associations between WMH/MTL volume and disruption of (non)-critical connections

As can be seen in Figure 3, greater WMH volume was associated with disrupted white matter connectivity, reflected by a higher MD of both critical and non-critical network connections (critical: standardized regression coefficient B = .572 (.450 – .693), $p < .001$; non-critical: B = .572 (.459 – .685), $p < .001$). Smaller MTL volume was also associated with higher MD of both critical and non-critical network connections (critical: B = -.160 (-.303 – -.018), $p = .027$; non-critical: (B = -.205 (-.338 – -.071), $p = .003$), see Figure 4. In multivariate models which included both WMH and MTL volume, WMH volume remained a significant contributor to higher MD in critical connections (B = .634 (.517 – .751), $p < .001$), while the contribution of MTL volume attenuated (B = -.116 (-.234 – .002), $p = .054$). Whereas both WMH volume (B = .645 (.535 – .755), $p < .001$) and MTL volume (B = -.177 (-.287 – -.066), $p = .002$) remained significant contributors to the MD of non-critical network connections.

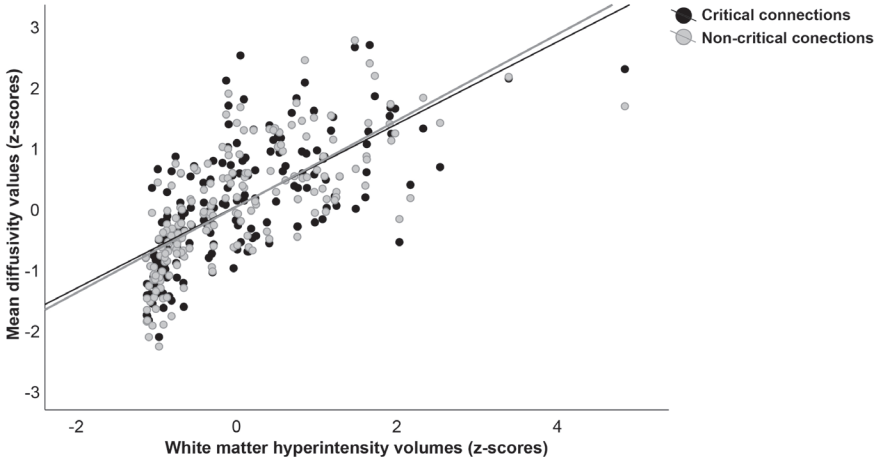

Figure 3. Association between white matter hyperintensity volume and mean diffusivity of (non)-critical connections. Figure shows the association between normalized white matter hyperintensity volumes (z-scores) and mean diffusivity values (z-scores) of critical connections and of non-critical network connections.

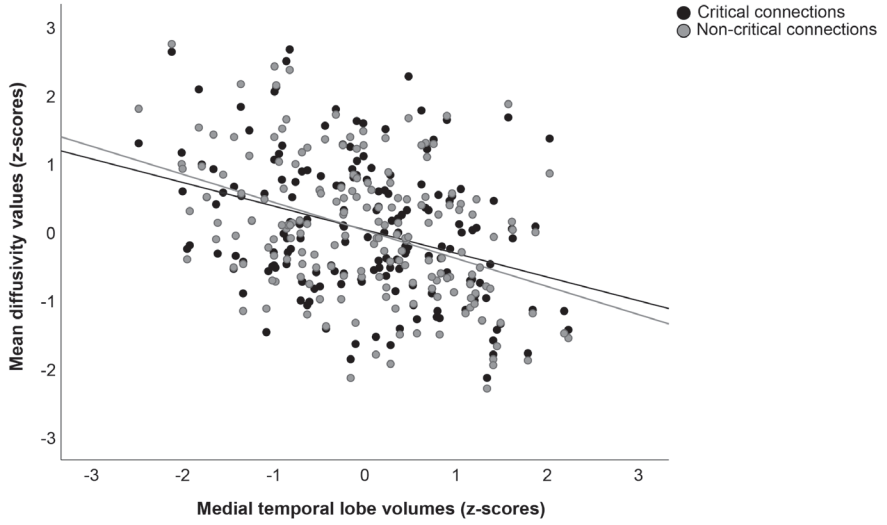

Figure 4. Association between medial temporal lobe volume and mean diffusivity of (non)-critical connections. Figure shows the association between the normalized medial temporal lobe volumes (z-scores) and mean diffusivity values (z-scores) for critical connections and non-critical network connections.

Sensitivity analysis: critical connections defined as hub-hub connections

We performed a sensitivity analysis in which critical network connections were defined as hub-hub connections. The sensitivity analysis yielded similar results to the main analysis and are summarized in Table 2.

Table 2. Sensitivity analysis: critical connections defined as hub-hub connections

	MD of hub-hub connections	
	OR (CI95)	***p***
Cognitive dysfunction at BL	1.55 (1.11 – 2.28)	.025
Cognitive decline	1.56 (1.08 – 2.26)	.018
	B (CI95)	***p***
WMH volume	.561 (.440 – .681)	<.0001
MTL volume	-.208 (-.346 – .070)	.003

Abbreviations: MD = mean diffusivity; OR = odds ratio; CI95 = 95% confidence interval; BL = baseline; WMH = white matter hyperintensity; MTL = medial temporal lobe. All associations were corrected for age. Cognitive dysfunction was defined as the Clinical Dementia Rating (CDR) score at baseline. Cognitive decline was defined as the change in CDR over two years' time.

DISCUSSION

The main finding of this study is that the disruption of white matter connections in memory clinic patients with mixed etiologies predicts cognitive decline over two years' time. However, we found that this association is not specific for critical connections as non-critical connections showed similar connections to cognitive decline. Moreover, neither vascular injury nor neurodegeneration appear to preferentially affect critical connections over non-critical connections.

Critical brain network connections are hypothesized to be important for higher-order cognitive functioning, because of their contribution to global network efficiency.[10] Indeed, damage to these white matter connections has been related to cognitive dysfunction in patients with SVD and early onset AD.[11,37] Our findings add two important aspects to this hypothesis, namely that disruption of critical connections is not only related to cognitive dysfunction, but also to future cognitive decline; and secondly, that the same is true for disruption of non-critical network connections. Hence, global impairments in network connectivity were associated with cognitive impairment and decline in this memory-clinic cohort.

The equal involvement of critical and non-critical white matter connections in cognitive outcome could be a consequence of disease progression. It is possible that critical network connections are among the first connections to get affected in the pre-clinical phase of neurodegenerative disease[38] and that white matter abnormalities propagate to non-critical connections as the disease progresses. As a result, diffusion abnormalities in critical connections may have reached a ceiling effect at the clinical stage of the disease, making them less sensitive to variation in cognitive outcome. This is in line with previous cross-sectional studies showing a clear preferential role of abnormal critical network connections over non-critical connections for the development of cognitive dysfunction in cognitively healthy elderly,[39] whereas this distinction is less pronounced in symptomatic memory-clinic patients.[2,40] Although we did not have enough cognitively healthy subjects to test this hypothesis, exploration of the data showed a steeper increase from CDR 0 to 0.5 for critical versus non-critical connections, suggesting that critical connections are the first to be affected (Supplementary figure 1).

A second hypothesis regarding the clinical relevance of critical network connections is that these connections are more vulnerable to disease processes because they require more energy to be maintained.[5,13,33] We found no evidence for a specific effect of vascular disease and neurodegeneration on critical network connections. Previous studies examining these associations in patients with AD and SVD have been inconclusive. Greater disruptions in critical connections were found in case-control studies,[11,37] while equal to or greater disruptions in non-critical connections were mostly found for analyses within patient groups.[12,40,41] These conflicting findings may again be a consequence of a ceiling effect in diffusion abnormalities in critical connections, making the diffusion abnormalities sensitive to the presence of vascular disease and/or neurodegeneration, but not to the severity of the disease. The idea that white matter abnormalities in vascular and neurodegenerative disease start in one region of the brain and subsequently spread over the brain network as the disease progresses has gained attention in recent years, with an increasing number of studies examining the exact mechanisms of a network spread.[42–44] White matter abnormalities, such as axonal injury or demyelination, are thought to spread through mechanisms of Wallerian degeneration. Furthermore, amyloid and pathological tau may propagate along white matter connections.[45] Studies looking into spreading of white matter brain

network impairments could further increase our understanding of the dynamic and possibly non-linear relationship between brain network injury and cognitive functioning.

Strengths of our study are the high-quality DTI data, the relatively large sample size, and longitudinal data on cognitive status. This allowed us to assess structural connectivity measures in association to cognitive decline. Another strength is that we used two common definitions for critical network connections (i.e., central and hub-hub connections). The associations were consistent for both definitions and for the cross-sectional as well as the longitudinal analyses, which reduces the chance that our findings are false positives.

A limitation to this study is that neurodegeneration was defined as a broad construct and was measured by a marker of brain injury (i.e., MTL volume) that does not reflect a specific etiology such as AD. However, WMH volume and MTL volume are both widely used an validated biomarkers of cerebrovascular disease and neurodegeneration respectively in memory clinic patients.[22,24] A second limitation is that we lacked pre-symptomatic subjects. Therefore, we were unable to examine white matter abnormalities across the different disease stages and, in particular, if critical connections were among the first to be affected. Lastly, the study sample consisted of a heterogeneous group with both vascular and neurodegenerative disease, meaning that we cannot interpret our findings in light of a specific disease process or mechanism. However, the heterogeneity of our sample does reflect clinical reality in which these two disease processes frequently co-occur and highlights the importance of network disturbances in cognitive decline across these two conditions.

In conclusion, disruption of white matter connections in memory clinic patients predicts cognitive decline. However, this is not specific for critical connections. Moreover, neither vascular injury nor neurodegeneration appear to specifically affect critical connections. The potential significance of certain network connections to the development of dementia should be further explored by longitudinal studies starting in the pre-symptomatic stage.

REFERENCES

1. Reijmer YD, Leemans A, Brundel M, et al. Disruption of the cerebral white matter network is related to slowing of information processing speed in patients with type 2 diabetes. *Diabetes* 2013; 62: 2112–2115.
2. Reijmer YD, Fotiadis P, Piantoni G, et al. Small vessel disease and cognitive impairment: The relevance of central network connections. *Hum Brain Mapp* 2016; 37: 2446–2454.
3. Tuladhar AM, van Dijk E, Zwiers MP, et al. Structural network connectivity and cognition in cerebral small vessel disease. *Hum Brain Mapp* 2016; 37: 300–310.
4. Heinen R, Vlegels N, de Bresser J, et al. The cumulative effect of small vessel disease lesions is reflected in structural brain networks of memory clinic patients. *NeuroImage Clin* 2018; 19: 963–969.
5. Griffa A, Van den Heuvel MP. Rich-club neurocircuitry: function, evolution, and vulnerability. *Dialogues Clin Neurosci* 2018; 20: 121–132.
6. de Haan W, Mott K, van Straaten ECW, et al. Activity Dependent Degeneration Explains Hub Vulnerability in Alzheimer's Disease. *PLoS Comput Biol*; 8. Epub ahead of print 2012. DOI: 10.1371/journal.pcbi.1002582.
7. Kapasi A, DeCarli C, Schneider JA. Impact of multiple pathologies on the threshold for clinically overt dementia. *Acta Neuropathol* 2017; 134: 171–186.
8. Albert R, Jeong H, Barabasi A-L. Error and attack tolerance of complex networks. *Nature* 2000; 406: 378–382.
9. Irimia A, Van Horn JD. Systematic network lesioning reveals the core white matter scaffold of the human brain. *Front Hum Neurosci* 2014; 8: 1–14.
10. Reijmer YD, Leemans A, Caeyenberghs K, et al. Disruption of cerebral networks and cognitive impairment in Alzheimer disease. *Neurology* 2013; 80: 1370–1377.
11. Tuladhar AM, Lawrence A, Norris DG, et al. Disruption of rich club organisation in cerebral small vessel disease. *Hum Brain Mapp* 2017; 38: 1751–1766.
12. van Leijsen EMC, van Uden IWM, Bergkamp MI, et al. Longitudinal changes in rich club organization and cognition in cerebral small vessel disease. *NeuroImage Clin* 2019; 24: 102048.
13. Crossley NA, Mechelli A, Scott J, et al. The hubs of the human connectome are generally implicated in the anatomy of brain disorders. *Brain* 2014; 137: 2382–2395.
14. Morris JC. The Clinical Dementia Rating (CDR): Current version and scoring rules. *Neurology* 1993; 43: 2412–2414.
15. Folstein MF, Folstein SE, McHugh PR. Mini-mental state. A grading the cognitive state of patiens for the clinician. *J Psychiatr Res* 1975; 12: 189–198.
16. Jessen F, Amariglio RE, Van Boxtel M, et al. A conceptual framework for research on subjective cognitive decline in preclinical Alzheimer's disease. *Alzheimer's Dement* 2014; 10: 844–852.
17. Winblad B, Palmer K, Kivipelto M, et al. Mild cognitive impairment - Beyond controversies, towards a consensus: Report of the International Working Group on Mild Cognitive Impairment. *J Intern Med* 2004; 256: 240–246.
18. Román GC, Tatemichi TK, Erkinjuntti T, et al. Vascular dementia: Diagnostic criteria for

research studies: Report of the ninds-airen international workshop*. *Neurology* 1993; 43: 250–260.

19. Rascovsky K, Hodges JR, Knopman D, et al. Sensitivity of revised diagnostic criteria for the behavioural variant of frontotemporal dementia. *Brain* 2011; 134: 2456–2477.
20. McKhann G, Drachman D, Folstein M, et al. Clinical diagnosis of Alzheimer's disease: Clinical diagnosis Report of the NINCDS-ADRDA Work Group* under the auspices of Department of Health and Human Services Task Force on Alzheimer's Disease. *Neurology* 1984; 34: 939–944.
21. Groeneveld O, Reijmer Y, Heinen R, et al. Brain imaging correlates of mild cognitive impairment and early dementia in patients with type 2 diabetes mellitus. *Nutr Metab Cardiovasc Dis* 2018; 28: 1253–1260.
22. Wardlaw JM, Smith EE, Biessels GJ, et al. Neuroimaging standards for research into small vessel disease and its contribution to ageing and neurodegeneration. *Lancet Neurol* 2013; 12: 822–838.
23. Wardlaw JM, Valdés Hernández MC, Muñoz-Maniega S. What are white matter hyperintensities made of? Relevance to vascular cognitive impairment. *J Am Heart Assoc* 2015; 4: 001140.
24. ten Kate M, Barkhof F, Boccardi M, et al. Clinical validity of medial temporal atrophy as a biomarker for Alzheimer's disease in the context of a structured 5-phase development framework. *Neurobiol Aging* 2017; 52: 167–182.
25. Tzourio-Mazoyer N, Landeau B, Papathanassiou D, et al. Automated anatomical labeling of activations in SPM using a macroscopic anatomical parcellation of the MNI MRI single-subject brain. *Neuroimage* 2002; 15: 273–289.
26. Leemans A, Jeurissen B, Sijbers J, et al. ExploreDTI: a graphical toolbox for processing, analyzing, and visualizing diffusion MR data. In: *17th Annual Meeting of Intl Soc Mag Reson Med*. Hawaii, USA, 2009, p. 3537.
27. Leemans A, Jones DK. The B-matrix must be rotated when correcting for subject motion in DTI data. *Magn Reson Med* 2009; 61: 1336–1349.
28. Veraart J, Sijbers J, Sunaert S, et al. Weighted linear least squares estimation of diffusion MRI parameters: Strengths, limitations, and pitfalls. *Neuroimage* 2013; 81: 335–346.
29. Tax CMW, Otte WM, Viergever MA, et al. REKINDLE: Robust Extraction of Kurtosis INDices with Linear Estimation. *Magn Reson Med* 2015; 73: 794–808.
30. Jeurissen B, Leemans A, Jones DK, et al. Probabilistic fiber tracking using the residual bootstrap with constrained spherical deconvolution. *Hum Brain Mapp* 2011; 32: 461–479.
31. Acosta-Cabronero J, Alley S, Williams GB, et al. Diffusion Tensor Metrics as Biomarkers in Alzheimer's Disease. *PLoS One*; 7. Epub ahead of print 2012. DOI: 10.1371/journal.pone.0049072.
32. Banerjee G, Wilson D, Jäger HR, et al. Novel imaging techniques in cerebral small vessel diseases and vascular cognitive impairment. *Biochim Biophys Acta - Mol Basis Dis* 2016; 1862: 926–938.
33. Van Den Heuvel MP, Sporns O, Collin G, et al. Abnormal rich club organization and functional brain dynamics in schizophrenia. *JAMA Psychiatry* 2013; 70: 783–792.

34. van den Heuvel MP, Sporns O. Rich-Club Organization of the Human Connectome. *J Neurosci* 2011; 31: 15775–15786.
35. de Reus MA, van den Heuvel MP. Estimating false positives and negatives in brain networks. *Neuroimage* 2013; 70: 402–409.
36. Bullmore E, Sporns O. Complex brain networks: Graph theoretical analysis of structural and functional systems. *Nat Rev Neurosci* 2009; 10: 186–198.
37. Daianu M, Mezher A, Mendez MF, et al. Disrupted rich club network in behavioral variant frontotemporal dementia and early-onset Alzheimer's disease. *Hum Brain Mapp* 2016; 37: 868–883.
38. Dean III DC, Hurley SA, Kecskemeti SR, et al. Association of Amyloid Pathology with Myelin Alteration in Preclinical Alzheimer Disease. *JAMA Neurol* 2017; 74: 41–49.
39. Baggio HC, Segura B, Junque C, et al. Rich club organization and cognitive performance in healthy older participants. *J Cogn Neurosci* 2015; 27: 1801–1810.
40. Daianu M, Jahanshad N, Nir TM, et al. Rich club analysis in the Alzheimer's disease connectome reveals a relatively undisturbed structural core network. *Hum Brain Mapp* 2015; 36: 3087–3103.
41. Sun Y, Bi Q, Wang X, et al. Prediction of Conversion From Amnestic Mild Cognitive Impairment to Alzheimer ' s Disease Based on the Brain Structural Connectome. *Front Neurol* 2019; 9: 1–15.
42. Oxtoby NP, Garbarino S, Firth NC, et al. Data-Driven Sequence of Changes to Anatomical Brain Connectivity in Sporadic Alzheimer's Disease. *Front Neurol* 2017; 8: 1–11.
43. 43. Iturria-Medina Y, Carbonell FM, Sotero RC, et al. Multifactorial causal model of brain (dis)organization and therapeutic intervention: Application to Alzheimer's disease. *Neuroimage* 2017; 152: 60–77.
44. Avena-Koenigsberger A, Misic B, Sporns O. Communication dynamics in complex brain networks. *Nat Rev Neurosci* 2017; 19: 17–33.
45. Raj A, Iturria-Medina Y. Network spread models of neurodegenerative diseases. *Front Neurol* 2019; 9: 1159.

SUPPLEMENTARY MATERIAL

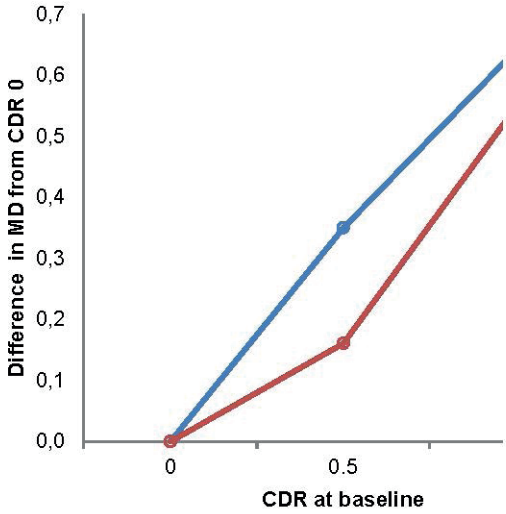

Supplementary figure 1. Lines show the increase in MD, indicating disrupted connectivity, from CDR 0 to CDR 0.5 and CDR 1 for critical and non-critical connections. Exploration of the data shows a steeper increase from CDR 0 to 0.5 for critical versus non-critical connections, suggesting that critical connections are the first to be affected. Of note, only 5 patients had a CDR score of 0 at baseline, therefore no statistics were performed on these data.

7

CHAPTER

Neither Alzheimer's Disease nor vascular pathologies differentially affect critical and non-critical white matter connections

Naomi Vlegels, Bruno M. de Brito Robalo, Alberto de Luca, Wiesje M. van der Flier, Dominantly Inherited Alzheimer Network (DIAN), Randall Bateman, Tammie L. S. Benzinger, Carlos Cruchaga, Dave M. Cash, Hiroshi Mori, Igor Yakushev, Marco Duering, Sofia Finsterwalder, Benno Gesierich, Anna Kopczak, Yael D. Reijmer, Geert Jan Biessels

Submitted

ABSTRACT

Introduction. Both Alzheimer's disease (AD) and small vessel disease (SVD) have been suggested to disrupt so-called critical white matter (WM) connections of the brain more than non-critical connections. Here, we systematically evaluated the question if SVD or AD, in pure and mixed forms, indeed more strongly affect critical than non-critical connections.

Methods. We included patients with CADASIL (n=59), Mixed pathology (n=57) and autosomal dominant AD (ADAD; n=50). All patients underwent 3 Tesla MRI brain scans. WM networks were reconstructed from diffusion-weighted MRI. Critical connections (10% highest edge centrality) and non-critical connections were weighted by mean diffusivity (MD). We used WM hyperintensity (WMH) volume as SVD burden marker (CADASIL and Mixed), and CSF amyloid beta^{42} (Aβ), p-tau levels, and estimated years of onset (EYO; for ADAD) as AD burden markers (ADAD and Mixed). Associations between these disease burden markers and critical and non-critical connections were tested with linear regression analyses.

Results. WMH volume was 6.3 (SD 6.7)% of intracranial volume in CADASIL, 1.8 (1.9)% in mixed, and 0.17 (0.14)% in ADAD. In CADASIL and Mixed, WMH volume was equally related to MD of critical and non-critical connections (CADASIL Standardized Beta (B)=0.70; B=0.70, Mixed B=0.71; B=0.79, all p<0.001), reflected in very similar effect sizes. In ADAD and Mixed, Aβ-positivity was not significantly associated with MD of either critical or non-critical connections (ADAD Estimated Marginal Means (EMM)=-0.38; EMM=-0.47, Mixed EMM=-0.25; EMM = -0.31, all p>0.05). In ADAD, Aβ^{42} levels and EYO were similarly related to both connection types (Aβ^{42} B=-0.25; B=-0.31, EYO B=0.59; B=0.64, all p<0.001). In ADAD and Mixed, effect sizes for associations of tau with critical and non-critical connections were also similar (ADAD: B=0.33, p=0.003, B=0.21, p = 0.09; Mixed B=0.07; B=-0.07, both p>0.05). Sensitivity analyses with different definitions of connectivity also showed no differential effects for critical and non-critical connections.

Conclusion. The burden of SVD, more so than AD, was significantly related to the integrity of white matter connections, but we found no support for earlier hypotheses that critical connections are more vulnerable to these disease effects than non-critical connections.

INTRODUCTION

Alzheimer's disease (AD) and small vessel disease (SVD) are the two most common causes of cognitive impairment and dementia.[1] In both of these diseases white matter (WM) connections have been found to be disrupted, which likely contributes to cognitive dysfunction.[2–4] WM connections with a critical role in the cerebral network have attracted particular attention in both SVD and AD research, as damage to these connections may have a bigger impact on cognition than other connections.[5,6] Connections are considered to be critical if they connect a high number of regions. These critical WM connections thus function as the "highways" of the brain and play a key role in network integration. The prominent role of critical connections also comes with higher energy demands and thus with higher biological costs.[6,7] These higher biological costs have been hypothesized to make critical connections more vulnerable to disease processes, such as SVD and AD.[6,7] However, to date, it is not clear whether critical and non-critical connections are indeed differentially affected by SVD and AD pathology, while such insights could help to better understand disease mechanisms. Some earlier studies report a vulnerability of critical connections, independent of non-critical connections.[8,9] Other studies have reported an equal or greater vulnerability of non-critical WM connections for SVD and AD pathology.[10–12] The variability in findings of previous studies might be explained by the lack of systematic comparison of critical and non-critical connections. Moreover, previous studies may not have sufficiently disentangled effects of SVD and AD, not considering mixed pathologies.

In this study we systematically tested the hypothesis that critical connections are more strongly affected by disease burden than non-critical connections in both SVD and AD, in patients with pure (i.e., monogenic) and mixed forms of these diseases.

METHODS

Study design

To systematically explore the impact of SVD and AD burden along the spectrum of these diseases, we included three samples: 1) patients with an autosomal dominant variant of SVD, 2) a memory clinic population with mixed pathology (probably AD and SVD) and 3) patients with an autosomal dominant variant of AD. In each of these samples, we related the impact of widely accepted markers of disease burden (both SVD and AD) to the connections of the structural brain network.

Study population

Autosomal dominant SVD

As an autosomal dominant SVD sample, we included 59 patients with Cerebral Autosomal Dominant Arteriopathy with Subcortical Infarcts and Leukoencephalopathy (CADASIL), recruited from a single-centre study (VASCAMY) at the Institute of Stroke and Dementia Research, LMU Munich.[13,14] The CADASIL diagnosis was confirmed by molecular genetic testing or skin biopsy.[15,16] All patients provided written informed consent.

Mixed pathology

We included 57 subjects from the Parelsnoer study recruited at the memory clinic of the University Medical Centre Utrecht.[17] At baseline, all subjects had a clinical dementia rating (CDR) scale score ≤ 1, and a Mini Mental State Exam (MMSE) of ≥ 20. Subjects did not have another clinically apparent primary aetiology than neurodegenerative disease or SVD. For this study, we included all subjects from the cohort with T1-weighted and diffusion-weighted scans and available data on their amyloid status. All patients provided written informed consent.

Autosomal dominant AD

As an autosomal dominant AD (ADAD) sample, we included 50 subjects from the observational study of the Dominantly Inherited Alzheimer Network (DIAN; data freeze 14 downloaded in December 2021).[18,19] DIAN enrols individuals with a

known Autosomal Dominant Alzheimer's disease (ADAD) mutation (APP, PSEN1 or PSEN2) and their non-carrier siblings. In this study, we included pre-symptomatic and symptomatic mutation carriers. Subjects were eligible for this study if they had an available T1-weighted and diffusion-weighted MRI scan. Subjects had no other known neurological or psychiatric disease. All patients provided written informed consent.

MRI data acquisition

MRI data for all samples were acquired on 3 Tesla systems and included 3D-T1 weighted, diffusion-weighted MRI, and T2-weighted fluid-attenuated inversion recovery (FLAIR) scans. Each study used a standardized protocol but acquisition parameters differed across studies. MRI protocols have been published for the CADASIL[20] and Mixed sample.[3] For the ADAD sample, acquisition parameters of the T1 and FLAIR have been previously published.[21] Acquisition parameters and scanner types of all study samples can be found in Supp. Table 1.

Small vessel disease markers

We used WMH volume as primary marker of SVD burden because it is a robust, continuous marker of the disease with a large range in both genetic and sporadic forms. In ADAD, we did not perform analyses on WMH burden in relation to connection strength, because in the age-group studied WMH volume is low[22], as can also be seen in Table 1.

We determined normalized WMH volume for the CADASIL and Mixed sample by dividing WMH volume by total brain volume. For CADASIL, WMH volume was calculated by a semi-automated procedure which has been previously described.[14] In short, 3D FLAIR images were first segmented into tissue probability maps. CSF and WMH were then separated by histogram segmentation based on the Otsu method[23] and lastly, WMH segmentations were manually edited and cleaned from misclassified artefacts. For the Mixed sample, WMH volume was calculated by a semi-automated procedure.[24] WMH were segmented using FLAIR images by the lesion prediction algorithm (http://nbn-resolving.de/urn:nbn:de:bvb:19-203731) as implemented in the Lesion Segmentation Toolbox (v 2.0.9; (www.statistical-modelling.de/lst.htm) for SPM12. All automated segmentations were checked

visually and manually corrected if needed. Manual segmentations of infarcts were used to correct WMH segmentations.

Alzheimer's Disease markers

We used CSF Aβ[42] and p-tau levels as biomarkers of AD in the Mixed and ADAD sample. These markers were not available for CADASIL.

Concentrations of CSF Aβ42 in ADAD were measured by plate-based enzyme-link immunosorbant assay (ELISA) methods (INNOTEST™ Aβ1-42, Innogenetics, Ghent, Belgium). Hyperphosphorylated tau (P-tau) was analysed by multiplexed Luminex-based immunoassay (INNO-BIA AlzBio3, Fujirebio). For more details see Fagan et al. 2014.[25] To establish Aβ-status, we used a cut-off of <600 pg/ml.[26] Additionally, estimated years from symptom onset (EYO) was assessed in the ADAD sample. EYO was determined based on the age of onset of the parent from whom the patient inherited the mutation.[19]

For the Mixed sample, CSF Aβ42 and p-tau were available in a subgroup (n = 38). Concentrations of CSF Aβ42 and p-tau were analysed using ELISA methods (Innotest beta-amyloid (1-42) and Innotest hTAU-Ag; Innogenetics, Ghent, Belgium).[27] To establish Aβ-status, we used a cut-off of <640 pg/ml for the subgroup with available CSF data.[28] For the rest of the sample (n=22), [18F] Florbetaben PET data was available(part of the ABIDE study[27]) and Aβ-status was determined through visual read.[27] Three subjects had both PET and CSF data available, for all three Aβ-status was concordant between the two methods.

Diffusion processing and network reconstruction

After visual inspection to exclude major artefacts, raw diffusion images were pre-processed using ExploreDTI[29] (v 4.8.6) and MRtrix v3.0 package.[30] Pre-processing included: 1) Correction of signal drift[31] (ExploreDTI) 2) Denoising the data ('dwidenoise; MRtrix) 3) Removal of Gibbs ringing artefacts[32] ('mrdegibbs'; MRtrix) and lastly 4) Correction for subject motion, eddy currents and susceptibility artefacts based on registration to the T1-weighted images in ExploreDTI, including rotation of the B-matrix.[33,34] Pre-processing was followed by computing the diffusion tensors with robust estimators[35] from which we determined FA and MD. Subsequently we performed whole-brain tractography using constrained

spherical deconvolution (CSD).[36] CSD allows for the reconstruction of more complex pathways than DTI, i.e., multiple fiber directions in one voxel, as found in regions of crossing fibers.[36] Fiber tracts were reconstructed by starting seed points uniformly throughout the data at 2 mm isotropic resolution. Streamlines were terminated when they entered a voxel with a fiber orientation distribution threshold of <0.1, or when they deflected with an angle > 45°. The Automated Anatomic Labeling[37] (AAL) template was non-linearly registered to each subjects 3D-T1 image (in native space) using the Computational Anatomical Toolbox (CAT) 12 toolbox (version R1073, C. Gaser, Structural Brain Mapping Group, Jena University Hospital, Jena, Germany) for SPM version 12. The AAL template consists of 90 cortical and subcortical brain regions. Each AAL region represents a node in the brain network. Two nodes are considered to be connected if at least five streamlines had endpoints located in two regions, resulting in a 90x90 binary connectivity matrix. This binary connectivity matrix was multiplied by the mean diffusivity (MD) in the primary analyses and multiplied by the fractional anisotropy (FA) in a subsequent sensitivity analysis, resulting in an MD-weighted and FA-weighted connectivity matrix. These steps are further explained in the following sections.

Critical network connections

Connections within the brain network with an important topological position in the network are considered to be critical for global network functioning.[38] Earlier literature mentions two different definitions for critical network connections: 1) connections with high edge centrality (i.e., connections that participate in a high number of communication paths)[5] and 2) connections that form a direct link between hub nodes.[39] In the primary analysis, critical connections were defined as connections with high edge centrality. In these analyses, critical connections and non-critical connections were defined separately for each study sample. To define the connections with highest edge centrality, we first calculated the average brain network of each study sample based on the binary connectivity matrix by including those connections that occurred in at least 2/3 of the participants.[40] Centrality of each edge within the average network was quantified by the edge betweenness centrality (for the exact mathematical definition see Bullmore & Sporns, 2009[41]). The 10% connections with the highest edge betweenness centrality were considered to be central network connections.[5]

In sensitivity analyses, we defined critical connections as rich club connections, i.e., connections between hub nodes. These connections were selected as follows: first betweenness centrality was calculated for each patient separately and then averaged, secondly the 10 nodes with the highest average betweenness centrality were selected as hub nodes. All connections running between hub nodes were then defined as rich club connections.[39] All connections running to a hub node, were defined as feeder connections and all other connections were defined as peripheral connections.[39]

Non-critical connections were defined as connections that were neither included as central connections nor rich club connections.[40]

All these subtypes were weighted by MD-values in the primary analyses and FA-values in sensitivity analyses.

Statistical analysis

All statistical analyses were performed in R (version 3.5.1).[42] Associations between SVD burden markers and AD biomarkers (independent variables) and connection measures (dependent variables) were assessed with robust linear regression analyses with M-estimation (implemented in the R-package MASS)[43] within each sample. The only exception was for Aβ-positivity, a dichotomous measure, which was related to connection strength with a one-way ANOVA. Variables were log transformed in case of non-normal distribution (Shapiro-Wilk test). Given that age is a strong indicator of disease burden in both CADASIL and ADAD, all primary regression analyses were not adjusted for age. In the Mixed sample we performed a sensitivity analysis in which we did adjust for age.

Our objective was to detect differential relationships of critical and non-critical connections with disease burden. This was operationalized by comparing effect sizes and regression plots of the observed associations between these connections. Because all analyses assessed both critical and non-critical connections as an outcome, we used a Bonferroni correction of factor 2 (i.e., $p<0.025$).

RESULTS

Characteristics of the three samples are summarized in Table 1. As expected, patients with monogenic SVD and AD were considerably younger than patients from the mixed pathology sample. WHM volume was highest in CADASIL, intermediate in the Mixed sample, and low in ADAD. AD biomarkers had a large range in both ADAD and Mixed, which was expected given that ADAD consists of both symptomatic and pre-symptomatic patients and the Mixed sample consists of patients with mixed pathology.

SVD burden equally relates to critical and non-critical connections

In CADASIL, WMH volume was strongly associated with MD strength of critical and non-critical connections (critical: standardized beta (B) (95% confidence interval (CI)) = 0.70 (0.53 – 0.88), $p < 0.001$; non-critical: B(CI) = 0.70 (0.53 – 0.88), $p < 0.001$). In the Mixed sample, WMH volume was similarly associated to MD strength of critical and to non-critical connections (critical: B(CI) = 0.71 (0.54 – 0.88), $p < 0.001$; non-critical: B(CI) = 0.79 (0.64 –0.93), $p < 0.001$) (Fig. 1, Supp. table 2a).

Sensitivity analyses using FA-weighted instead of MD-weighted connections, using rich club connections to define the core network, yielded comparable findings, without differential effects between the connection types (Supp. table 2a).

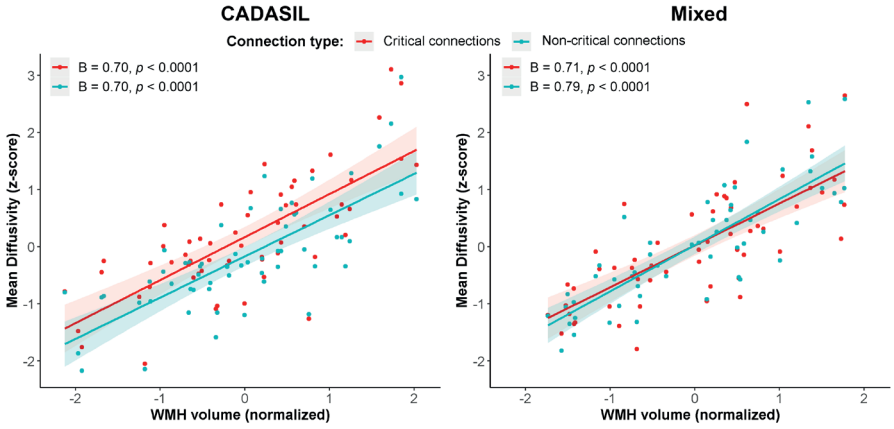

Figure 1. The association between white matter hyperintensitiy volume and mean diffusivity (MD) of critical and non-critical connections in CADASIL (left) and Mixed (right) samples. In both plots the corresponding standardized beta coefficient and p-value is shown for critical (red) and non-critical (blue) connections.

Table 1. Sample characteristics

	CADASIL n = 59	Mixed n = 57	ADAD n = 50
Age in years	52.8 ± 9.9	73.8 ± 7.5	38.5 ± 11.7
EYO, in years	-	-	-7.9 (23.6) [-36 – 11.8]
Female, n(%)	41 (69)	20 (35)	34 (68)
MMSE	30 (1) [22 – 30]	27 (3) [19 – 30][a]	29 (2) [10 – 30]
CDR, n(%)		[a]	
0	50 (84.7)	1 (1.8)	34 (68)
0.5	8 (13.5)	40 (70.2)	8 (16)
1	1 (1.7)	15 (26.3)	5 (10)
2	0 (0)	0 (0)	3 (6)
BPF	79.1 (5.4) [69.9 –87.2]	68.4 (5.9) [62.3 – 74.9][b]	70.9 (5) [58 – 82][a]
WMH volume, % of TBV	6.3 (6.7) [0.09 – 23]	1.8 (1.9) [0.12 – 6.2][a]	0.17 (0.14) [0.08 – 0.5]
CSF $A\beta^{42}$	-	621 (168) [363 – 1641][c]	485 (444) [226 – 1463][d]
CSF t-tau	-	477 (376.5) [140 – 1274][c]	91.4 (82.5) [8 – 272][d]
CSF p-tau	-	62.5 (42.5) [19 – 166][c]	49.7 (55.5) [14 – 131][d]

Data are presented in mean ± standard deviation, n (%) or median (IQR) [min, max].
Abbreviations: EYO = Estimated years from symptom onset; MMSE = Mini Mental State Exam; CDR = Clinical Dementia Rating scale; BPF = Brain Parenchymal Fraction; WMH = White matter hyperintensity; CSF = Cerebral Spinal Fluid; Aβ = Amyloid beta; t-tau = Total tau; p-tau = phosphorylated tau.
[a] = 1 missing; [b] = 2 missing; [c] = 19 missing; [d] = 8 missing

AD burden shows no differential effect on connection types

In both ADAD and Mixed, Aβ markers were not associated with MD strength of either critical and non-critical connections. In amyloid positive ADAD patients compared to amyloid negative ADAD patients, MD was somewhat elevated, albeit not significantly, in critical (estimated marginal means (EM) (Standard Error (SE) = -0.38 (0.27), p = 0.17) as well as in non-critical connections (EM (SE) = -0.47 (0.24), p = 0.06) (Fig. 2b). In Mixed patients, effect sizes of amyloid positivity for the two connection types were also very similar (critical: EM (SE) = -0.25 (0.27), p = 0.35; non-critical: EM (SE) = -0.31 (0.27), p = 0.25) (Fig. 2c; Supp. table 3b). In ADAD we additionally tested the association with CSF $A\beta^{42}$ levels (critical: B (CI) = -0.25 (-0.48 – -0.02), p = 0.04; non-critical: B (CI) = -0.31 (-0.54 – -0.08), p = 0.01) and EYO (critical: B (CI) = 0.59 (0.37 – 0.82), p < 0.001; non-critical: B (CI) = 0.64 (0.42 – 0.86), p < 0.001). While the association between $A\beta^{42}$ and critical connections did not survive the

Bonferroni correction, effect sizes were again found to be equal between critical and non-critical connections, see Fig. 2a & 3 and Supp. tables 2c-d.

CSF p-tau levels in ADAD were significantly associated with critical (B(CI) = 0.33 (0.13 – -0.54), p = 0.003) but not to non-critical connections (B(CI) = 0.21 (-0.03 – 0.45), p = 0.09), although effect sizes were in the same range. In Mixed patients, CSF p-tau levels showed similar effect sizes in critical and non-critical connections (critical: B = 0.07 (-0.27 – 0.41), p = 0.7, non-critical: B=-0.07 (-0.40 – 0.26), p = 0.66) (Fig. 4, Supp. table 2e).

Again, sensitivity analyses with FA-weighted connections and with the rich club definition of connections yielded comparable findings (Supp. tables 2b-e).

In light of the observed high concordance for the analyses of critical and non-critical connections, we also performed post-hoc analyses where we assessed the direct interrelation of the MD strength between critical and non-critical connection in each sample. This showed high inter-correlations between the connection types (all correlation coefficients > 0.84, Supp. Fig.

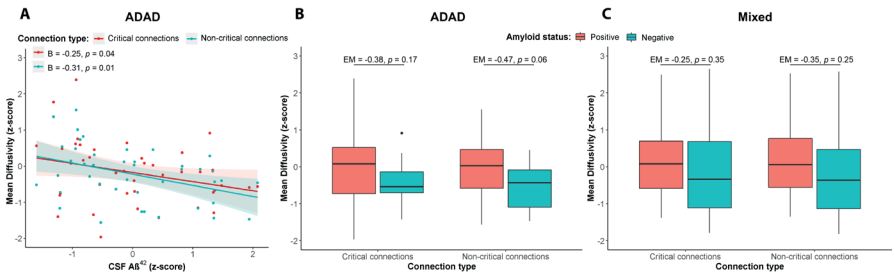

Figure 2. The association between Amyloid-beta (Aβ) and mean diffusivity (MD) of the critical and non-critical connections in ADAD (left and middle) and Mixed (right). The left plot shows the association for CSF Aβ42 levels with the standardized regression coefficient (B) and p-value shown for critical (red) and non-critical (blue) connections. For the middle and right plot Aβ-status is assessed. Estimated marginal means (EM) and p-values are shown for the difference between Aβ-positive and Aβ-negative patients.

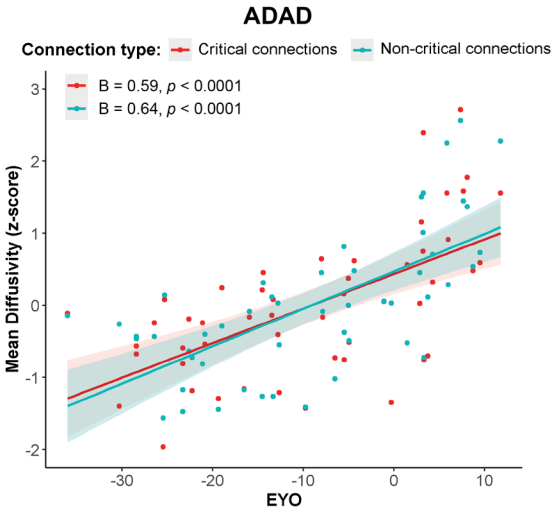

Figure 3. The association between estimated years from symptom onset (EYO) and mean diffusivity (MD) of critical and non-critical connections. In the plot, the standardized regression coefficient (B) and p-value is shown for critical (red) and non-critical (blue) connections.

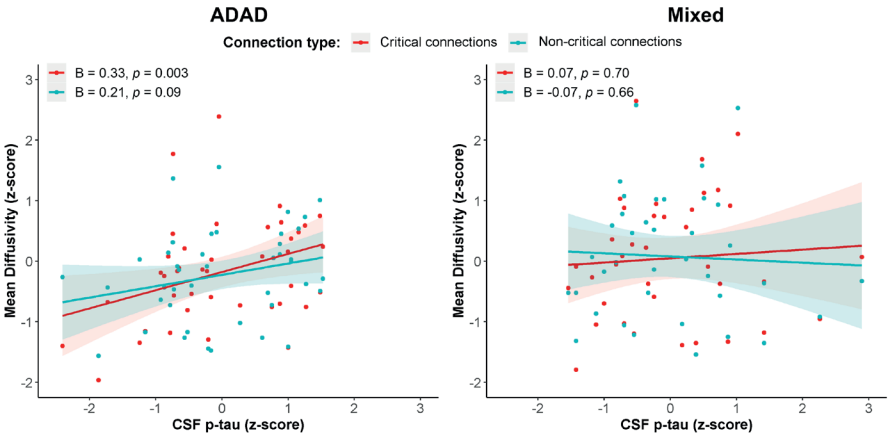

Figure 4. The association between CSF p-tau levels and mean diffusivity (MD) of critical and non-critical connections in ADAD (left) and Mixed (right) samples. In both plots the corresponding standardized beta coefficient and p-value is shown for critical (red) and non-critical (blue) connections.

DISCUSSION

Using a systematic approach, including pure and mixed forms of SVD as well as AD, with biomarker supported assessment of disease burden, we could not confirm the hypothesis that critical connections are more vulnerable to these diseases than non-critical WM connections.

In the different cohorts studied, due to inclusion of people at different stages of disease, we managed to obtain substantial variance in disease burden, which is an advantage for testing our hypothesis. Both in pure and mixed SVD, we found strong correlations between WMH volume, as indicator of SVD burden, and the strength of WM connections. For AD markers, we found only a weak association with strength of WM connections in both the pure and Mixed AD sample. Based on earlier literature, these differential associations for SVD and AD markers were expected (SVD[3,4,8,44,45], AD[22,46,47]). Furthermore, the absolute effect sizes for the relations with AD markers in the ADAD sample seemed slightly stronger than the effect sizes in the Mixed sample. An example of which is the difference in effect sizes between ADAD and Mixed in the relationship with CSF p-tau. These stronger associations in ADAD are in line with previous work in which there was an apparent effect of AD on diffusion measures in ADAD patients, but less so in patients with mixed pathology, where the effects appeared to be masked by the presence of SVD.

In SVD, we observed a strong similarity in the relation between WMH volume and critical and noncritical connections across our analyses. This was seen for both MD- and FA-weighted networks, and also in sensitivity analyses with alternative definitions for critical connections. Few previous studies have specifically assessed possible differential effects of SVD on critical and non-critical connections.[5,8,10,48] By comparing effect sizes for abnormalities in rich club connections in patients with SVD relative to controls, Lee et al., (2018)[48] found that patients with subcortical vascular dementia had significantly less rich club connections than controls, independent of a loss of overall connections. Using a similar analytic approach, Tuladhar and colleagues (2017)[8] examined rich club organization in two cohorts of patients with SVD and found a greater loss of strength of rich club connections than that of non-rich club connections relative to controls. However, there was no formal statistical test comparing the effect sizes for the two connection types. A

follow-up study from the same group[10], using a more direct approach in relating SVD burden to connectivity strength, found no differential effect of disease on critical and non-critical connections. Furthermore, in line with our findings, Reijmer et al. (2016)[5] related WMH, lacunes and microbleeds to critical and non-critical connections in a mixed memory clinic population and also found no differential effects. These earlier findings in combination with the findings of the current systematic study make it improbable that critical and non-critical connections are differentially affected by SVD. One reason for this might be that SVD is a diffuse rather than a focal disease.[49] This is also hinted towards by findings of the present study. While we found that critical and non-critical connections were almost collinear, they showed a relatively low spatial overlap, meaning that they do not represent the same connections in the same brain areas.

For AD, we again found no indication for a differential effect on critical or non-critical connections across our analyses. As noted in the second paragraph, the association between AD biomarkers and strength of WM connections is relatively weak, compared to that of SVD burden.[22] This possibly explains why the effect of AD burden on critical and non-critical connections has -to the best of our knowledge- not been studied to date. There have been few previous studies that assessed a potential differential effect on WM connections by comparing patients with controls and results have been ambiguous.[9,11,12,48] Lee et al. (2018)[48] examined patients with AD dementia and found a significant reduction in the number of rich club connections, independent of overall loss of connections. One study in patients with early onset AD found rich club connections to be more affected than non-rich club connections[9], while an earlier study, from the same group, which assessed patients from the ADNI cohort found no such differential effect.[11] Lastly, in patients with amnestic MCI, no differences were found in the number of rich club nodes or the strength of connections between patients and controls.[12] One explanation for these differential results might be that they were all performed in slightly different groups of patients and different choices in network definitions were made. However, in our study we tested both a pure AD and a mixed pathology sample as well as four different definitions of the structural brain network and we found very similar results across all conditions. It is important to note that we were the first study that took a more direct approach by assessing the effect of disease burden, rather than absence or presence of disease, on the connections, which

may also explain differences with previous studies. Yet, taken together, the results of our systematic evaluation, combined with previous work, make it unlikely that AD has a differential effect on critical or non-critical WM connections.

Our study has several strengths. The main strength of the current study is our systematic approach and especially the inclusion of three samples that cover the pure and mixed forms of SVD and AD. This allowed us to independently validate our findings and gave us the opportunity to study the effect of disease with minimal age-related confounders. Of note, the consistency of the findings persisted despite differences in patient characteristics and scan protocols across samples, supporting validity of the observations.

One limitation of our study is that CADASIL and ADAD are both highly selected samples, which are not generalizable to most sporadic SVD and AD populations. However, both samples gave us the unique opportunity to study SVD and AD with minimal age-related confounders. On the other hand, we also included a mixed pathology sample, which is much more heterogeneous and thus less specific but is closer to what is observed in clinical practice. Furthermore, for the CADASIL sample we had no AD biomarkers available and for the ADAD sample we did not assess SVD burden, but these were not the markers we were interested in for these groups and both SVD and AD biomarkers were available for the mixed pathology sample. Another limitation is that, while we assessed two weightings of the diffusion-based network and two definitions of critical connections, this by no means exhausts all possible options with regards to network definition. However, there is no golden standard and none of the options we assessed changed the interpretation of the result. Interestingly, the connection types showed high inter-correlations, which could suggest that there is a high spatial overlap between these connections. We further investigated this in a representative patient, to see if this was due to a high spatial overlap between the types of connections. This did not appear to be the case; the spatial overlap was around 23%.

Finally, all three samples had a modest sample size so there might be limited power. Nonetheless, all the results that were obtained were highly consistent in terms of direction of effects and effect sizes.

Of note, while critical and non-critical WM connections appear to be equally disrupted by SVD and AD, this does not imply that both connection types are

equally involved in normal or abnormal cognitive functioning. There is extensive literature, with a firm theoretical and experimental basis, that shows how network connections that have a more central role in the network are more critically involved in cognitive functioning.[6,7] In addition, the current observations on structural connectivity should not be equated to functional connectivity, which has a very different physiological and neuroanatomical basis. There is an extensive literature on specific functional subnetwork changes in AD, among others involving the default-mode-network in AD for example.[50]

In conclusion, we have demonstrated that critical and non-critical WM connections are similarly affected by disease burden in SVD as well as in AD. Apparently, critical connections are not more vulnerable to these diseases, refuting early hypotheses.

REFERENCES

1. O'Brien JT, Thomas A. Vascular dementia. *Lancet* 2015; 386: 1698–1706.
2. Reijmer YD, Leemans A, Caeyenberghs K, et al. Disruption of cerebral networks and cognitive impairment in Alzheimer disease. *Neurology* 2013; 80: 1370–1377.
3. Heinen R, Vlegels N, de Bresser J, et al. The cumulative effect of small vessel disease lesions is reflected in structural brain networks of memory clinic patients. *NeuroImage Clin* 2018; 19: 963–969.
4. Tuladhar AM, van Dijk E, Zwiers MP, et al. Structural network connectivity and cognition in cerebral small vessel disease. *Hum Brain Mapp* 2016; 37: 300–310.
5. Reijmer YD, Fotiadis P, Piantoni G, et al. Small vessel disease and cognitive impairment: The relevance of central network connections. *Hum Brain Mapp* 2016; 37: 2446–2454.
6. Griffa A, Van den Heuvel MP. Rich-club neurocircuitry: function, evolution, and vulnerability. *Dialogues Clin Neurosci* 2018; 20: 121–132.
7. de Haan W, Mott K, van Straaten ECW, et al. Activity Dependent Degeneration Explains Hub Vulnerability in Alzheimer's Disease. *PLoS Comput Biol*; 8. Epub ahead of print 2012. DOI: 10.1371/journal.pcbi.1002582.
8. Tuladhar AM, Lawrence A, Norris DG, et al. Disruption of rich club organisation in cerebral small vessel disease. *Hum Brain Mapp* 2017; 38: 1751–1766.
9. Daianu M, Mezher A, Mendez MF, et al. Disrupted rich club network in behavioral variant frontotemporal dementia and early-onset Alzheimer's disease. *Hum Brain Mapp* 2016; 37: 868–883.
10. van Leijsen EMC, van Uden IWM, Bergkamp MI, et al. Longitudinal changes in rich club organization and cognition in cerebral small vessel disease. *NeuroImage Clin* 2019; 24: 102048.
11. Daianu M, Jahanshad N, Nir TM, et al. Rich club analysis in the Alzheimer's disease connectome reveals a relatively undisturbed structural core network. *Hum Brain Mapp* 2015; 36: 3087–3103.
12. Sun Y, Bi Q, Wang X, et al. Prediction of Conversion From Amnestic Mild Cognitive Impairment to Alzheimer ' s Disease Based on the Brain Structural Connectome. *Front Neurol* 2019; 9: 1–15.
13. Duering M, Csanadi E, Gesierich B, et al. Incident lacunes preferentially localize to the edge of white matter hyperintensities: insights into the pathophysiology of cerebral small vessel disease. *Brain* 2013; 136: 2717–2726.
14. Baykara E, Gesierich B, Adam R, et al. A Novel Imaging Marker for Small Vessel Disease Based on Skeletonization of White Matter Tracts and Diffusion Histograms. *Ann Neurol* 2016; 80: 581–592.
15. Joutel A, Corpechot C, Ducros A, et al. NATURE · VOL 383 · 24 OCTOBER 1996 LETTERS TO NATURE 7. Frani;ois. *Earth Planet Sci Lett* 1987; 92: 4141–4163.
16. Peters N, Opherk C, Bergmann T, et al. Spectrum of Mutations in Biopsy-Proven CADASIL. *Arch Neurol* 2005; 62: 1091.
17. Aalten P, Ramakers IHGB, Biessels GJ, et al. The Dutch Parelsnoer Institute - Neurodegenerative diseases; methods, design and baseline results. *BMC Neurol* 2014; 14: 1–8.

18. Moulder KL, Snider BJ, Mills SL, et al. Dominantly inherited alzheimer network: Facilitating research and clinical trials. *Alzheimer's Res Ther* 2013; 5: 1–7.
19. Bateman RJ, Xiong C, Benzinger TLS, et al. Clinical and biomarker changes in dominantly inherited Alzheimer's disease. *N Engl J Med* 2012; 367: 795–804.
20. Duering M, Finsterwalder S, Baykara E, et al. Free water determines diffusion alterations and clinical status in cerebral small vessel disease. *Alzheimer's Dement* 2018; 14: 764–774.
21. Caballero MÁA, Suárez-Calvet M, Duering M, et al. White matter diffusion alterations precede symptom onset in autosomal dominant Alzheimer's disease. *Brain* 2018; 141: 3065–3080.
22. Finsterwalder S, Vlegels N, Gesierich B, et al. Small vessel disease more than Alzheimer's disease determines diffusion MRI alterations in memory clinic patients. *Alzheimer's Dement* 2020; 1–11.
23. Otsu N, Smith PL, Reid DB, et al. Otsu_1979_otsu_method. *IEEE Trans Syst Man Cybern* 1979; C: 62–66.
24. Groeneveld O, Reijmer Y, Heinen R, et al. Brain imaging correlates of mild cognitive impairment and early dementia in patients with type 2 diabetes mellitus. *Nutr Metab Cardiovasc Dis* 2018; 28: 1253–1260.
25. Fagan AM, Xiong C, Jasielec MS, et al. Longitudinal change in CSF biomarkers in autosomal-dominant Alzheimer's disease. *Sci Transl Med*; 6. Epub ahead of print 2014. DOI: 10.1126/scitranslmed.3007901.
26. Dakterzada F, López-Ortega R, Arias A, et al. Assessment of the Concordance and Diagnostic Accuracy Between Elecsys and Lumipulse Fully Automated Platforms and Innotest. *Front Aging Neurosci* 2021; 13: 1–12.
27. de Wilde A, van Maurik IS, Kunneman M, et al. Alzheimer's biomarkers in daily practice (ABIDE) project: Rationale and design. *Alzheimer's Dement Diagnosis, Assess Dis Monit* 2017; 6: 143–151.
28. Zwan M, van Harten A, Ossenkoppele R, et al. Concordance between cerebrospinal fluid biomarkers and [11C]PIB PET in a memory clinic cohort. *J Alzheimers Dis* 2014; 41: 801–807.
29. Leemans A, Jeurissen B, Sijbers J, et al. ExploreDTI: a graphical toolbox for processing, analyzing, and visualizing diffusion MR data. In: *17th Annual Meeting of Intl Soc Mag Reson Med*. Hawaii, USA, 2009, p. 3537.
30. Tournier JD, Smith R, Raffelt D, et al. MRtrix3: A fast, flexible and open software framework for medical image processing and visualisation. *Neuroimage* 2019; 202: 116137.
31. Vos SB, Tax CMW, Luijten PR, et al. The importance of correcting for signal drift in diffusion MRI. *Magn Reson Med* 2017; 77: 285–299.
32. Kellner E, Dhital B, Kiselev VG, et al. Gibbs-ringing artifact removal based on local subvoxel-shifts. *Magn Reson Med* 2016; 76: 1574–1581.
33. Leemans A, Jones DK. The B-matrix must be rotated when correcting for subject motion in DTI data. *Magn Reson Med* 2009; 61: 1336–1349.
34. Veraart J, Sijbers J, Sunaert S, et al. Weighted linear least squares estimation of diffusion MRI parameters: Strengths, limitations, and pitfalls. *Neuroimage* 2013; 81: 335–346.

35. Tax CMW, Otte WM, Viergever MA, et al. REKINDLE: Robust Extraction of Kurtosis INDices with Linear Estimation. *Magn Reson Med* 2015; 73: 794–808.
36. Jeurissen B, Leemans A, Jones DK, et al. Probabilistic fiber tracking using the residual bootstrap with constrained spherical deconvolution. *Hum Brain Mapp* 2011; 32: 461–479.
37. Tzourio-Mazoyer N, Landeau B, Papathanassiou D, et al. Automated anatomical labeling of activations in SPM using a macroscopic anatomical parcellation of the MNI MRI single-subject brain. *Neuroimage* 2002; 15: 273–289.
38. Van Den Heuvel MP, Sporns O, Collin G, et al. Abnormal rich club organization and functional brain dynamics in schizophrenia. *JAMA Psychiatry* 2013; 70: 783–792.
39. van den Heuvel MP, Sporns O. Rich-Club Organization of the Human Connectome. *J Neurosci* 2011; 31: 15775–15786.
40. de Reus MA, van den Heuvel MP. Estimating false positives and negatives in brain networks. *Neuroimage* 2013; 70: 402–409.
41. Bullmore E, Sporns O. Complex brain networks: Graph theoretical analysis of structural and functional systems. *Nat Rev Neurosci* 2009; 10: 186–198.
42. R Core Team. R: A language and environment for statistical computing. R Foundation for Statistical Computing, https://www.r-project.org/ (2018).
43. Venables WN, Ripley BD. *Modern applied statistics with S*. 2002. Epub ahead of print 2002. DOI: 10.1007/978-1-4757-2719-7_14.
44. Reijmer YD, Fotiadis P, Martinez-Ramirez S, et al. Structural network alterations and neurological dysfunction in cerebral amyloid angiopathy. *Brain* 2015; 138: 179–188.
45. Lawrence AJ, Chung AW, Morris RG, et al. Structural network efficiency is associated with cognitive impairment in small-vessel disease. *Neurology* 2014; 83: 304 LP – 311.
46. Kantarci K, Schwarz CG, Reid RI, et al. White matter integrity determined with diffusion tensor imaging in older adults without dementia: Influence of amyloid load and neurodegeneration. *JAMA Neurol* 2014; 71: 1547–1554.
47. Pietroboni AM, Scarioni M, Carandini T, et al. CSF β-amyloid and white matter damage: a new perspective on Alzheimer's disease. *J Neurol Neurosurg & Psychiatry* 2018; 89: 352 LP – 357.
48. Lee WJ, Han CE, Aganj I, et al. Distinct Patterns of Rich Club Organization in Alzheimer's Disease and Subcortical Vascular Dementia: A White Matter Network Study. *J Alzheimer's Dis* 2018; 63: 977–987.
49. Ter Telgte A, Van Leijsen EMC, Wiegertjes K, et al. From a Focal To a Global Perspective. *Nat Rev Neurol* 2018; 14: 387–398.
50. Seeley WW, Crawford RK, Zhou J, et al. Neurodegenerative Diseases Target Large-Scale Human Brain Networks. *Neuron* 2009; 62: 42–52.

SUPPLEMENTARY MATERIAL

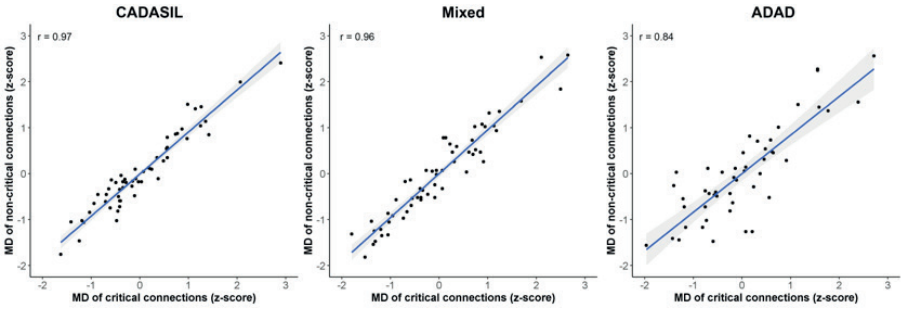

Supplementary Figure 1. Correlation coefficient between critical and non-critical connections

Supplementary table 1. Acquisition parameters

		CADASIL	Mixed	ADAD
Scanner		Siemens Verio	Philips Achieva	Siemens systems
T1	TR [ms]	2500	7.9	2300
	TE [ms]	437	4.5	2.95
	Slice [mm]	1	1	1.2
	In-plane [mm]	1 x 1	1 x 1	1.1 x 1.1
FLAIR	TR [ms]	5000	11000	9000
	TE [ms]	395	125	90
	TI [ms]	1800	2800	2500
	Slice [mm]	1	3	5
	In-plane [mm]	1 x 1	0.96 x 0.96	0.9 x 0.9
Diffusion	TR [ms]	12700	6600	6000
	TE [ms]	81	73	87
	Slice [mm]	2	2.5	2.5
	In-plane [mm]	2 x 2	1.72 x 1.72	2.5 x 2.5
	b-value [s/mm^2]	1000	1200	1000
	directions	30	45	64

ADAD = Autosomal dominant Alzheimer's disease, FLAIR = Fluid attenuated inversion recovery, TE = Echo time, TR = Repetition time.

Supplementary tables 2a to 2e.

The next five tables show the complete results of the robust linear regression models of the CADASIL, Mixed and Autosomal Dominant Alzheimer's Disease (ADAD) sample in relation to white matter hyperintensity volume (2a), Aβ positivity (2b), CSF Aβ42 (2c), CSF p-tau (2d) and estimated years from symptom onset (2e). For each of these disease burden markers we analyzed two different weightings for the connections (1) Mean diffusivity (MD) and 2) Fractional Anisotropy (FA)) and two definitions of importance of connections 1) Critical and non-critical connections and 2) Rich club, feeder and peripheral connections. Results are presented with the standardized beta (St. B) with the 95% confidence interval (CI95) or the estimated marginal means (EMM) with the standard error (St. Error) and the corresponding *p*-value.

Supplementary table 2a. White matter hyperintensity volume

	CADASIL			**Mixed**		
	St. B	CI95	*p*	St. B	CI95	*p*
MD						
Critical	0.70	0.53 – 0.88	< 0.0001	0.71	0.54 – 0.88	< 0.0001
Non–critical	0.70	0.53 – 0.87	< 0.0001	0.79	0.64 – 0.93	< 0.0001
Rich club	0.63	0.43 – 0.83	< 0.0001	0.75	0.58 – 0.92	< 0.0001
Feeder	0.67	0.49 – 0.84	< 0.0001	0.75	0.61 – 0.89	< 0.0001
Peripheral	0.73	0.56 – 0.89	< 0.0001	0.79	0.63 – 0.94	< 0.0001
FA						
Critical	-0.84	-0.98 – -0.70	< 0.0001	-0.66	-0.86 – -0.45	< 0.0001
Non-critical	-0.82	-0.96 – -0.68	< 0.0001	-0.74	-0.93 – -0.54	< 0.0001
Rich club	-0.71	-0.89 – -0.52	< 0.0001	-0.76	-0.94 – -0.59	< 0.0001
Feeder	-0.81	-0.95 – -0.67	< 0.0001	-0.69	-0.89 – -0.5	< 0.0001
Peripheral	-0.84	-0.99 – -0.69	< 0.0001	-0.71	-0.90 – -0.51	< 0.0001

Supplementary table 2b. Aβ positivity

	ADAD			Mixed		
	EMM	St. Error	*p*	EMM	St. Error	*p*
MD						
Critical	-0.38	0.27	0.17	-0.25	0.27	0.35
Non-critical	-0.47	0.24	0.06	-0.31	0.27	0.25
Rich club	-0.37	0.24	0.15	-0.38	0.27	0.16
Feeder	-0.37	0.24	0.14	-0.29	0.27	0.28
Peripheral	-0.50	0.24	0.04	-0.30	0.27	0.27
FA						
Critical	0.63	0.32	0.05	-0.02	0.27	0.94
Non-critical	0.96	0.30	0.003	-0.03	0.27	0.91
Rich club	0.67	0.29	0.03	0.17	0.27	0.54
Feeder	0.91	0.28	0.002	-0.05	0.27	0.86
Peripheral	0.89	0.30	0.006	-0.02	0.27	0.95

Supplementary table 2c. CSF $A\beta^{42}$ levels

	ADAD		
	St. B	CI95	*p*
MD			
Critical	-0.25	-0.48 – -0.02	0.04
Non-critical	-0.31	-0.54 – -0.08	0.01
Rich club	-0.23	-0.47 – 0.001	0.07
Feeder	-0.26	-0.51 – -0.01	0.04
Peripheral	-0.32	-0.55 – -0.1	0.008
FA			
Critical	0.34	0.04 – 0.65	0.03
Non-critical	0.45	0.15 – 0.76	0.006
Rich club	0.36	0.1 – 0.63	0.009
Feeder	0.46	0.2 – 0.73	0.001
Peripheral	0.41	0.11 – 0.72	0.01

Supplementary table 2d. Estimated years from symptom onset

	ADAD		
	St. B	CI95	*p*
MD			
Critical	0.59	0.37 – 0.82	< 0.0001
Non-critical	0.64	0.42 – 0.86	< 0.0001
Rich club	0.47	0.24 – 0.71	0.00024
Feeder	0.63	0.40 – 0.87	< 0.0001
Peripheral	0.64	0.41 – 0.87	< 0.0001
FA			
Critical	-0.07	-0.36 – 0.20	0.58
Non-critical	-0.21	-0.51 – 0.09	0.17
Rich club	-0.16	-0.42 – 0.11	0.25
Feeder	-0.34	-0.62 – -0.06	0.02
Peripheral	-0.12	-0.41 – 0.18	0.43

Supplementary table 2e. CSF p-tau levels

	ADAD			Mixed		
	St. B	CI95	*p*	St. B	CI95	*p*
MD						
Critical	0.33	0.13 – 0.54	0.003	0.07	-0.27 – 0.41	0.7
Non-critical	0.21	-0.03 – 0.45	0.09	-0.07	-0.40 – 0.26	0.66
Rich club	0.16	-0.09 – 0.41	0.2	0.07	-0.28 – 0.43	0.69
Feeder	0.22	-0.02 – 0.46	0.08	-0.03	-0.35 – 0.29	0.85
Peripheral	0.23	-0.01 – 0.46	0.05	-0.06	-0.44 – 0.33	0.77
FA						
Critical	0.11	-0.19 – 0.4	0.49	0.20	-0.13 – 0.52	0.24
Non-critical	-0.11	-0.44 – 0.24	0.53	0.21	-0.16 – 0.58	0.27
Rich club	0.12	-0.15 – 0.40	0.38	0.03	-0.33 – 0.40	0.85
Feeder	-0.04	-0.35 – 0.27	0.81	0.21	-0.12 – 0.55	0.15
Peripheral	-0.13	0.48 – 0.22	0.47	0.23	-0.10 – 0.58	0.19

Supplementary Table 3. DIAN consortium

Last Name	First	Affiliation
Allegri	Ricardo	FLENI Institute of Neurological Research (Fundacion para la Lucha contra las Enfermedades Neurologicas de la Infancia)
Bateman	Randy	Washington University in St. Louis School of Medicine
Bechara	Jacob	Neuroscience Research Australia
Benzinger	Tammie	Washington University in St. Louis School of Medicine
Berman	Sarah	University of Pittsburgh
Bodge	Courtney	Brown University-Butler Hospital
Brandon	Susan	Washington University in St. Louis School of Medicine
Brooks	William (Bill)	Neuroscience Research Australia
Buck	Jill	Indiana University
Buckles	Virginia	Washington University in St. Louis School of Medicine
Chea	Sochenda	Mayo Clinic Jacksonville
Chhatwal	Jasmeer	Brigham and Women's Hospital–Massachusetts General Hospital
Chrem	Patricio	FLENI Institute of Neurological Research (Fundacion para la Lucha contra las Enfermedades Neurologicas de la Infancia)
Chui	Helena	University of Southern California
Cinco	Jake	University College London
Clifford	Jack	Mayo Clinic Jacksonville
Cruchaga	Carlos	Washington University in St. Louis School of Medicine
Donahue	Tamara	Washington University in St. Louis School of Medicine
Douglas	Jane	University College London
Edigo	Noelia	FLENI Institute of Neurological Research (Fundacion para la Lucha contra las Enfermedades Neurologicas de la Infancia)
Erekin-Taner	Nilufer	Mayo Clinic Jacksonville
Fagan	Anne	Washington University in St. Louis School of Medicine
Farlow	Marty	Indiana University
Fitzpatrick	Colleen	Brigham and Women's Hospital-Massachusetts
Flynn	Gigi	Washington University in St. Louis School of Medicine
Fox	Nick	University College London
Franklin	Erin	Washington University in St. Louis School of Medicine
Fujii	Hisako	Osaka City University
Gant	Cortaiga	Washington University in St. Louis School of Medicine
Gardener	Samantha	Edith Cowan University, Perth

Last Name	First	Affiliation
Ghetti	Bernardino	Indiana University
Goate	Alison	Icahn School of Medicine at Mount Sinai
Goldman	Jill	Columbia University
Gordon	Brian	Washington University in St. Louis School of Medicine
Graff-Radford	Neill	Mayo Clinic Jacksonville
Gray	Julia	Washington University in St. Louis School of Medicine
Groves	Alexander	Washington University in St. Louis School of Medicine
Hassenstab	Jason	Washington University in St. Louis School of Medicine
Hoechst- Swisher	Laura	Washington University in St. Louis School of Medicine
Holtzman	David	Washington University in St. Louis School of Medicine
Hornbeck	Russ	Washington University in St. Louis School of Medicine
Houeland DiBari	Siri	German Center for Neurodegenerative Diseases (DZNE) Munich
Ikeuchi	Takeshi	Niigata University
Ikonomovic	Snezana	University of Pittsburgh
Jerome	Gina	Washington University in St. Louis School of Medicine
Jucker	Mathias	German Center for Neurodegnerative Diseases (DZNE) Tubingen
Karch	Celeste	Washington University in St. Louis School of Medicine
Kasuga	Kensaku	Niigata University
Kawarabayashi	Takeshi	Hirosaki University
Klunk	William (Bill)	University of Pittsburgh
Koeppe	Robert	University of Michigan
Kuder-Buletta	Elke	German Center for Neurodegnerative Diseases (DZNE) Tubingen
Laske	Christoph	German Center for Neurodegnerative Diseases (DZNE) Tubingen
Lee	Jae-Hong	Asan Medical Center
Levin	Johannes	German Center for Neurodegnerative Diseases (DZNE) Munich
Martins	Ralph	Edith Cowan University
Mason	Neal Scott	University of Pittsburgh Medical Center
Masters	Colin	University of Melbourne
Maue-Dreyfus	Denise	Washington University in St. Louis School of Medicine
McDade	Eric	Washington University in St. Louis School of Medicine
Mori	Hiroshi	Osaka City University
Morris	John	Washington University in St. Louis School of Medicine

Last Name	First	Affiliation
Nagamatsu	Akem	Tokyo University
Neimeyer	Katie	Columbia University
Noble	James	Columbia University
Norton	Joanne	Washington University in St. Louis School of Medicine
Perrin	Richard	Washington University in St. Louis School of Medicine
Raichle	Marc	Washington University in St. Louis School of Medicine
Renton	Alan	Icahn School of Medicine at Mount Sinai
Ringman	John	University of Southern California
Roh	Jee Hoon	Asan Medical Center
Salloway	Stephen	Brown University-Butler Hospital
Schofield	Peter	Neuroscience Research Australia
Shimada	Hiroyuki	Osaka City University
Sigurdson	Wendy	Washington University in St. Louis School of Medicine
Sohrabi	Hamid	Edith Cowan University
Sparks	Paige	Brigham and Women's Hospital-Massachusetts
Suzuki	Kazushi	Tokyo University
Taddei	Kevin	Edith Cowan University
Wang	Peter	Washington University in St. Louis School of Medicine
Xiong	Chengjie	Washington University in St. Louis School of Medicine
Xu	Xiong	Washington University in St. Louis School of Medicine

CHAPTER 8

General Discussion

GENERAL DISCUSSION

The overarching aim of my thesis was to study the microstructural integrity of the white matter in Alzheimer's disease (AD) and small vessel disease (SVD) to get a better understanding of brain injury and cognitive decline in these conditions. Throughout the chapters of my thesis, these are the key findings that emerged:

1. SVD more than AD determines white matter diffusion MRI alterations in memory clinic patients.
2. SVD and AD could not be disentangled based on their white matter diffusion signature with the techniques we used.
3. For neither disease, critical network connections were not found to be extra vulnerable compared to non-critical connections, the effects of both SVD and AD on the white matter network seem quite diffuse.
4. Diffusion-based measures of white matter integrity appear to be a strong determinant of cognition in SVD and white matter integrity mediates the relationship between SVD burden and cognition.

Diffusion MRI measures as marker of brain injury

Within this general discussion I would like to elaborate on the value of diffusion MRI as an injury marker in both SVD and AD. In order to do so, I will make use of the SVD biomarker framework provided by the HARNESS initiative.[1] Additionally, Textbox 1 provides some background on biomarkers in general and on why diffusion MRI is an injury marker.

The HARNESS initiative provided guidelines for the validation of SVD biomarkers. Cornerstones of validation are to show that markers are: 1) Biologically valid, i.e., establish whether a biomarker measures a specific change related to a disease, discriminates cases versus controls, relates to prognosis, relates to disease progression and if it relates to functional outcomes. I particularly addressed if specific changes related to a disease, among others by trying to identify specific injury diffusion signatures and patterns. 2) Technically valid, i.e., can the biomarker be reliably measured and is it reproducible.

Textbox 1. Biomarkers in SVD and AD: disease process vs injury markers.
The term biomarker refers to "a characteristic that is objectively measured and evaluated as indicator of normal biological processes, pathogenic processes, or pharmacologic responses to a therapeutic intervention."1 This definition is met by a growing number of markers that could be of potential relevance to understand brain changes in SVD and AD. Within my thesis I have mostly assessed two types of markers:

1) Disease process markers – biomarkers that reflect pathologies underlying the disease. Examples are the accumulation of Amyloid Beta and formation of neurofibrillary tangles in AD, for which both imaging and fluid markers have become available. Only recently, disease markers have become available for SVD in the form of small vessel function measures,2,3 but these need further biological and technical validation.

2) Injury markers – biomarkers of brain parenchymal injury as a consequence of different disease processes. Examples are atrophy and white matter hyperintensity volumes. Of note, although white matter hyperintensities and other SVD lesions are in essence injury markers, they have a fair degree of specificity for SVD as the underlying disease process and are therefore also considered as disease process markers in the field.

While these two types of markers reflect different constructs, they are clearly interrelated. Disease processes cause brain injury, which in turn might lead to cognitive impairment. We can visualize this schematically as follows:

1. Biomarkers and surrogate endpoints: Preferred definitions and conceptual framework. Clin Pharmacol Ther 2001: 69: 89-95. 2. Zwanenburg JJM, Van Osch MJP. Targeting cerebral small vessel disease with MRI. Stroke 2017; 48:3175-3182. 3. Van den Brink H, Kopczak A, Arts T, et al. Zooming in on cerebral small vessel function in small vessel diseases with 7T MRI: Rationale and design of the "ZOOM@SVDs" study. Cereb Circ – Cogn Behav 2021; 2: 10013.

3) Feasible, i.e., is the biomarker practical and affordable. I will discuss these factors in light of the findings of this thesis and the broader literature, followed by my view on future perspectives and clinical implications.

Biological validity of diffusion measures as injury markers in SVD

Before addressing the aspects of biological validity that I have specifically explored in my thesis in more detail, I would like to address the ability of diffusion MRI to discriminate cases versus controls, and its relation to disease progression over

time. Diffusion MRI-based measures have been shown to be clearly different between patients and controls and they show a strong association with disease burden.[2–4] However, less research has focused on the discriminative ability of these measures which could be important to evaluate diffusion measures as a diagnostic marker in individual patients. When assessing disease progression over time, it can be quickly noted from the literature that there are relatively few longitudinal diffusion studies, probably because of the challenges that longitudinal diffusion studies come with (which I will get to in the *technical validity* paragraph). Nevertheless, the longitudinal studies that have been performed do suggest that diffusion measures are sensitive to disease progression over time.[5,6]

One problem, which we also showed in **chapter 2** of this thesis, is that current diffusion techniques cannot distinguish between the disease processes underlying SVD and AD. Diffusion measures can inform us on the extent of diffusion of water molecules, as a surrogate for the state of the white matter, but not the underlying causes of increased diffusion. Therefore, diffusion measures should, at least for now, only be used as an injury marker. However, exciting work is being done to improve acquisition and to better characterize diffusion alterations. One example is multi-shell acquisition (i.e., using more than one diffusion weighting) with which more complex parametrization models can be used.[2,7–9] A second acquisition technique is ultra-fast and strong gradient diffusion MRI. This technique is currently being developed and again has the goal to better characterize microstructural changes of the white matter.

All in all, findings from this thesis **(chapters 2, 3, 5-7)** and other literature [2,5,10–12] consistently show that diffusion measures are 1) highly sensitive to SVD-related white matter injury, 2) can detect injury beyond the visible lesions, also in the normal appearing tissue (**chapters 2 and 3;** [3]) and 3) are affected already in early stages of the disease. Interestingly, **chapter 2** not only showed that SVD burden is strongly related to diffusion alterations, but also showed that SVD burden is a stronger determinant for diffusion alterations in memory clinic patients than AD burden.

Capturing spatial patterns of disease

Assessing spatial patterns of injury is in my view important to increase our understanding of disease mechanisms at play and to possibly better identify the

disease. However, in 2017 little was known about 1) whether there were specific patterns of affected tracts, regions or network disturbances and 2) if so, what the pattern of affected white matter in SVD was. In general studies from recent years, including work in this thesis, suggest that SVD has widespread effects on the white matter. On top of this there likely is important regional variation due to local vascular compromise. By analogy, one may compare this to the looks of an old traffic sign that has become globally faint and rusty due to years of exposure to the elements and is additionally riddled with holes by a hail shot. Hence, whether one regards diffusion MRI measures as an indicator of global or local tissue injury in SVD really depends on the way you look at it.

Let's first assess diffusion measures from a *whole-brain perspective*, and take peak width of skeletonized mean diffusivity (PSMD[3]) as an example. PSMD is based on histogram analysis and the assumption that, within patients, the histogram becomes wider because of an increase in the variety of diffusivity values throughout the white matter. The distribution of MD values throughout the skeleton in patients versus controls shows that this assumption appears to be correct.[3] An increase in PSMD is interpreted as a global loss of white matter integrity while it also reflects an increase in regional variation in white matter integrity and shows that not all white matter is equally affected. If we look at it from a *tract-based perspective*, it has been shown that the degree to which white matter tracts are affected by white matter lesions in SVD greatly differs between different tracts.[13] Moreover, different white matter tracts show differences in their loss of white matter integrity[14] and some white matter tracts have been identified as strategic, given that loss of white matter integrity in these tracts relates stronger to cognition than loss of integrity in other tracts.[15] It has also been shown that the extent to which the white matter is disrupted depends on its distance to a lesion. In a study by Reijmer et al. the severity of the disruptions attenuated with increasing distance to the primary lesion.[16] Looking at it from *a network perspective*, like I did within **chapter 7** where we divided the white matter connections into either critical or non-critical connections, we found no differences between the two types of connections. Which suggests that both types of connections are affected towards the same degree. One could argue that since we averaged over many connections, both types of connections consist of equal amounts of variation.

The work in this thesis **(chapters 3, 5, 7)** and the broader literature[17–19] both suggest

that small vessels throughout the white matter are affected in SVD. There is local damage as can be seen from the variation in diffusion values throughout the white matter and from different white matter tracts being differentially affected but, when zooming out, there are no specific subnetworks that are damaged in SVD. Based on the work in my thesis and these considerations, global measures of network topology thus do not appear to be best tool to assess spatial patterns of injury in SVD.

Explaining functional outcome

SVD is a common cause of cognitive impairment and dementia, however when I started my research the relationship between SVD and cognition was poorly understood. In part this is because the SVD lesions as observed on MRI are often only weakly related to cognition. This also meant difficulties in providing patients with an accurate prognosis of their disease. There was thus a need for markers that would better explain functional outcome in SVD.

At the time, there were hints on the sensitivity of diffusion-based measures for both disease markers and cognition.[20,21] The work in this thesis has contributed to the evidence showing that diffusion measures are consistently and strongly associated to cognition **(chapters 5 and 6)**, and thereby outperforming other markers of SVD in both strength of the relationship and explained variance.[3] While less data is available for predicting cognitive decline, the studies that have been performed show promise for diffusion measures as a prognostic marker. In **chapter 6** we observed a relationship with cognitive decline after two years, which is in line with other studies assessing cognitive decline[10,22] and conversion to dementia after five years.[23]

Diffusion measures based on network analysis have been often (and successfully) related to cognitive impairment in SVD with the assumption that these network measures would better capture higher-order cognitive functioning such as processing speed, attention and executive functioning. However, while associations between network-based measures and cognitive impairment are indeed strong, a recent study has shown that complex global network measures have little added value over simpler global white matter diffusion metrics, similar to what we conclude in terms of spatial injury patterns.[24] However, findings of another study

suggest that the incorporation of tract-based information does have added value in predicting cognitive impairment.[25] Given these findings, I would say that while there might be little benefit in performing complex network analysis over the use of global measures of white matter integrity, tract-based information might improve prediction models for cognitive impairment.

Biological validity of diffusion measures as injury markers in AD

Summing-up the findings of my thesis and the findings of other literature, I would say that white matter diffusion measures 1) are affected in early stages of the disease, 2) show generally weak associations with other injury markers and disease markers of AD and 3) an association with cognitive impairment. While this would mean that they meet most 1of the criteria of biological validity to at least some extend, I would also say that for each of the criteria there is a marker that provides a better fit for AD, while also being more specific for AD. With regards to point 2, **chapter 2** of this thesis showed that when compared to SVD, AD contributes little to diffusion alterations. It must be said, however, that this comparison may not be completely fair. In **chapter 2** we assessed the relationship between white matter hyperintensity (WMH) volume and diffusion measures, which are both injury markers, while on the other hand we assessed the association between diffusion measures and Amyloid beta (Aβ) and tau, which are disease markers. Disease markers and injury markers capture different parts of the disease cascade: while one measures disease processes (e.g., the accumulation of Aβ), the other measures the consequential damage of this disease processes. WMH and white matter integrity thus occur more at the same level of the disease cascade and might only therefore expected to be more strongly related. In support of this, the association between diffusion measures and small vessel function measures (i.e., a disease process marker) in **chapter 3**, was also weak. Furthermore, AD is primarily a cortical disease, so even when relating diffusion alterations to other injury markers such as atrophy (**as in chapters 4 and 6)**, the markers have spatial differences and might occur independently from each other. In case of SVD, white matter integrity loss and WMH are probably more tightly related, both on a regional and pathophysiological level.

When looking at the above, diffusion might have value as a marker of AD to study the state of the white matter. Given that these measures are, also in AD, sensitive to white matter changes and affected early.[26,27] But as mentioned before, there are markers providing a better fit for AD. An upcoming injury marker that shows great potential in studying the state of the white matter is neurofilament light chain (NfL), a protein that can be measured either in plasma or CSF samples. Neurofilaments are a component in the cytoskeleton in the neuronal axons and critical for the radial growth and stability of axons.[28,29] Elevations in neurofilament are a general indicator of axonal damage, and it is thus an unspecific marker. Importantly, NfL has been shown to be associated to white matter integrity over the course of AD.[30,31] In my opinion, the availability of NfL makes diffusion measures a less strong candidate to assess disease progression in AD.

Capturing spatial patterns of disease

It is well known that disease markers of AD such as Aβ and tau as well as injury markers such as cortical atrophy follow a certain distribution pattern.[32,33] Furthermore, functional connectivity studies have shown a typical pattern as well,[34,35] probably because these are based on activation of cortical brain areas which are affected by cortical atrophy. However, less research has focused on injury patterns in white matter structure. The few studies that did assess patterns of white matter injury in AD, show that reductions in specific white matter bundles (e.g., cingulum bundle, uncinate fasciculus) are associated with AD. Interestingly, these white matter bundles are related to parts of the network that are functionally disrupted by disease.[36,37] While further research is needed, these findings might suggest that affected white matter tracts in AD form the structural connections between the implicated functional areas.

At the start of my research, brain regions that connect a higher-than-average number of regions with each other, i.e., hubs, were hypothesized to be important for network functioning. The hypothesis stated that hubs would be more vulnerable to disease processes than other parts of the network due to their relatively high metabolic demands. However, we found no evidence for such a vulnerability for white matter hub connections in a systematic study in **chapter 7.** Moreover**,** other studies were also unable to convincingly show such an effect.[38–41] This contrasts with observations on functional hubs, where there are clear hints towards such

a vulnerability.[34,42] This might be because these functional hubs involve cortical areas while we have assessed the connections of the network rather than the brain regions.

Overall, it appears that AD leads to less diffuse white matter damage than SVD, and the different hypotheses and findings do suggest a more specific injury pattern. I would say that an exact pattern is not yet clear but the most convincing data is now pointing towards a pattern that follows the functional architecture of the brain.

Explaining functional outcome

While I have not assessed cognition in AD in much detail within this thesis, other literature finds a relationship between diffusion based measures and cognitive impairment in AD patients.[43,44] A challenge in this is that most studies assessing white matter integrity and cognition in AD have been performed in cohorts that probably suffer from mixed disease.[43,45,46] Given the findings of **chapter 2,** which show us that the presence of even the smallest burden of SVD will lead to an association with diffusion measures, mixed disease makes it difficult to interpret if effects are disease specific. The strong relationship between diffusion measures and cognition in SVD, makes it possible that found associations between diffusion measures and cognitive impairment in mixed disease cohorts reflect SVD-related cognitive impairment rather than AD-related cognitive impairment. A hint towards this is that the relationship with memory is less consistently found than the relationship with processing speed or executive functioning, which are frequently impaired in SVD.[43,44]

While Aβ accumulation alone is generally insufficient to lead to cognitive impairment, pathological tau is a strong predictor of cognitive impairment in AD.[47] Which can probably be understood by both its temporal and spatial characteristics. The temporal characteristics described by the dynamic biomarker model of Jack et al.[48], show that tau is the disease marker closest to symptom onset. Furthermore, pathologic tau starts within the entorhinal cortex close to the hippocampal areas.

Technical validity of diffusion measures in SVD and AD

While the technical validity of diffusion MRI was not specifically assessed in the

work in this thesis, I believe that it should be addressed in this discussion as it plays a role in the impact of my work.

One major challenge of diffusion measures at the moment is that diffusion MRI is susceptible for scanner differences and updates. This creates difficulties for 1) longitudinal studies, among others when scanners are updated in between two scans, 2) the comparison of diffusion measures between different studies or centers and 3) the pooling of data over different centers. This issue is currently mostly being addressed in three ways 1) the development of measures that are more indifferent or robust to scanners, i.e., the earlier mentioned PSMD marker[3] 2) the harmonization of processing procedures as done in the MarkVCID study (which I will discuss later)[49,50] and 3) by focusing on the harmonization of acquisition as well as post-hoc harmonization of data. In a recent paper focusing on post-hoc harmonization by my colleagues they were able to effectively remove acquisition-related differences while preserving SVD-related effects in five different cohorts.[51] Furthermore, in a follow-up study they were able to show that their techniques improve consistency, precision and sensitivity to disease effects.[52] In the coming years, tools should be developed to make such applications more widely available.

One other challenge lies within the processing of diffusion MRI scans. Currently, processing involves many sequential steps with different options. Decisions on how processing is performed are partially arbitrary and differ between studies. To facilitate the use of diffusion measures in multicenter studies guidelines should be set up to ensure a more univocal processing procedure among different centers. Moreover, processing currently requires specialistic knowledge and training. These procedures should be simplified to make usage in clinical trials or even clinical practice feasible. An example of a multicenter study in which a lot of effort was put into standardization of processing and minimization of scanner effects is MarkVCID,[49,50] their results are very promising and show that this is possible.

Clinical implications and future perspectives in SVD and AD

In **chapter 2** we have showed that, at least with the current diffusion MRI techniques, we cannot disentangle injury due to AD and SVD, contrary to our expectations at the start of the study. In my view, the necessity of such a distinction based on the diffusion signal has changed. There is still a need to determine the underlying disease processes of functional decline, even more so in case treatment becomes

available. However, the need for an indirect marker such as diffusion MRI has become less urgent given the now available blood-based biomarkers that can determine AD disease processes more easily.[53] Blood-based biomarkers, while long thought to be unattainable have been described as a breakthrough in the field. Recent results have shown great promise, with blood-based markers of Aβ, tau and NfL being able to inform on disease progression and showing potential for monitoring of treatment effects.[53]

The earlier mentioned blood-based protein NfL might also be of interest in SVD. While further studies towards this marker are needed to establish biological validity, the first results are promising for the use of NfL in SVD. NfL has been shown to discriminate between cases and controls in SVD, and to be associated to all SVD MRI markers and diffusion measures.[54] However, it did not outperform diffusion MRI in SVD in association to cognition. I personally think this easily accessible and low-cost white matter injury marker might be used complementary to diffusion measures of white matter integrity in SVD.

In terms of diagnostics, I would say that to determine presence of either SVD or AD, more straightforward options are available than diffusion measures. In case that it is suspected that a patient has AD, this could be confirmed using CSF, PET or blood samples, if indicated. When SVD presence needs to be determined, one could simply assess a structural MRI scan. For SVD there might be a role for diffusion-based measures to assess disease severity. As already discussed within the *Biological validity of diffusion measures as injury markers in SVD* paragraph, diffusion measures are particularly suitable to assess disease severity and outperform visible lesions of SVD in their relationship to cognitive impairment. In this respect, diffusion measures would in my opinion be able to improve prognosis in SVD. Yet, such implementation into clinical practice requires work in both in terms of biological and technical validity. For the biological validity, normative scores should become available and the prognostic and diagnostic value in individual patients should be established. For the technical validity, processing should ideally be automated but at least simplified and pooling of multi-center data should become easier.

At the start of my PhD, diffusion measures were considered to be potentially useful to track disease progression in AD, given that the then available options (markers of neurodegeneration such as atrophy or cognitive decline) only become abnormal

in relatively late stages of the disease. However, as mentioned already above, there have been important developments around blood-based biomarkers. In addition to what I mentioned before, blood-based markers are minimally invasive, have a high acceptability with patients, low cost and are accessible in diverse clinical settings, including lesser developed countries.[53] In the coming years, work should focus on bringing these markers into clinical trials and even more importantly into clinical practice.

Taken together, I see little potential for diffusion measures in AD in a clinical setting. In case we would want to know if a patient with AD has concurrent SVD, a conventional MRI would suffice to assess the presence of SVD markers. In a research setting, there might be potential for cortical diffusion. Cortical diffusion detects altered quality of the grey matter and is thus measured within the primarily affected area. Studies have shown promise for cortical diffusion to provide early information on neurodegeneration[55,56] and it might in that regard be more sensitive than atrophy measures. However, further work on this topic is needed. For SVD, diffusion measures might have a role in assessing disease severity, however processing needs to be simplified and multi-center data pooling should be made more accessible before these measures can be implemented in clinical practice. In the meantime, assessing severity of SVD might soon be easier with blood-based biomarkers such as NfL.

CONCLUSIONS

In conclusion the work in this thesis shows that for SVD, diffusion measures are strong markers, capable of capturing relevant information about the disease. With additional work, they show great promise for the implementation in clinical trials and possibly clinical practice. For AD, there are currently alternative markers that provide more information on relevant aspects of the disease processes and injury and are more specific to AD than diffusion measures of the white matter. I thus see little potential for these markers in AD in a clinical setting. In a research setting, there might be value in diffusion MRI for AD as it provides information on location.

For the future I am looking forward to how the technical challenges will be resolved and the opportunities that this will provide for the wider use of diffusion measures, also in clinical practice. For AD, but who knows, also for SVD, I'm curious to further developments that the blood-based biomarkers will bring.

REFERENCES

1. Smith EE, Biessels GJ, De Guio F, et al. Harmonizing brain magnetic resonance imaging methods for vascular contributions to neurodegeneration. *Alzheimer's & Dementia: Diagnosis, Assessment & Disease Monitoring* 2019; 11: 191–204.
2. Duering M, Finsterwalder S, Baykara E, et al. Free water determines diffusion alterations and clinical status in cerebral small vessel disease. *Alzheimer's and Dementia* 2018; 14: 764–774.
3. Baykara E, Gesierich B, Adam R, et al. A Novel Imaging Marker for Small Vessel Disease Based on Skeletonization of White Matter Tracts and Diffusion Histograms. *Ann Neurol* 2016; 80: 581–592.
4. Lawrence AJ, Tozer DJ, Stamatakis EA, et al. A comparison of functional and tractography based networks in cerebral small vessel disease. *Neuroimage Clin* 2018; 18: 425–432.
5. Zeestraten EA, Benjamin P, Lambert C, et al. Application of Diffusion Tensor Imaging Parameters to Detect Change in Longitudinal Studies in Cerebral Small Vessel Disease. *PLoS One* 2016; 11: e0147836.
6. Zeestraten EA, Lawrence AJ, Lambert C, et al. Change in multimodal MRI markers predicts dementia risk in cerebral small vessel disease. *Neurology* 2017; 89: 1869 LP – 1876.
7. Zhang H, Schneider T, Wheeler-Kingshott CA, et al. NODDI: Practical in vivo neurite orientation dispersion and density imaging of the human brain. *Neuroimage* 2012; 61: 1000–1016.
8. Jensen JH, Helpern JA, Ramani A, et al. Diffusional kurtosis imaging: The quantification of non-gaussian water diffusion by means of magnetic resonance imaging. *Magn Reson Med* 2005; 53: 1432–1440.
9. Konieczny MJ, Dewenter A, ter Telgte A, et al. Multi-shell Diffusion MRI Models for White Matter Characterization in Cerebral Small Vessel Disease. *Neurology* 2021; 96: e698 LP-e708.
10. Nitkunan A, Barrick TR, Charlton RA, et al. Multimodal MRI in Cerebral Small Vessel Disease. *Stroke* 2008; 39: 1999–2005.
11. Patel B, Markus HS. Magnetic Resonance Imaging in Cerebral Small Vessel Disease and its Use as a Surrogate Disease Marker. *International Journal of Stroke* 2011; 6: 47–59.
12. Tuladhar AM, Van Norden AGW, De Laat KF, et al. White matter integrity in small vessel disease is related to cognition. *Neuroimage Clin* 2015; 7: 518–524.
13. Coenen M, Kuijf HJ, Huenges Wajer IMC, et al. Strategic white matter hyperintensity locations for cognitive impairment: A multicenter lesion-symptom mapping study in 3525 memory clinic patients. *Alzheimer's & Dementia*; n/a. Epub ahead of print 12 December 2022. DOI: https://doi.org/10.1002/alz.12827.
14. Metoki A, Brookes RL, Zeestraten E, et al. Mnemonic function in small vessel disease and associations with white matter tract microstructure. *Neuropsychologia* 2017; 104: 1–7.
15. Biesbroek JM, Leemans A, den Bakker H, et al. Microstructure of Strategic White Matter Tracts and Cognition in Memory Clinic Patients with Vascular Brain Injury. *Dement Geriatr Cogn Disord* 2017; 44: 268–282.

16. Reijmer YD, Freeze WM, Leemans A, et al. The Effect of Lacunar Infarcts on White Matter Tract Integrity. *Stroke* 2013; 44: 2019–2021.
17. Maniega SM, Valdés Hernández MC, Clayden JD, et al. White matter hyperintensities and normal-appearing white matter integrity in the aging brain. *Neurobiol Aging* 2015; 36: 909–918.
18. Tuladhar AM, van Dijk E, Zwiers MP, et al. Structural network connectivity and cognition in cerebral small vessel disease. *Hum Brain Mapp* 2016; 37: 300–310.
19. Lawrence AJ, Chung AW, Morris RG, et al. Structural network efficiency is associated with cognitive impairment in small-vessel disease. *Neurology* 2014; 83: 304 LP – 311.
20. Reijmer YD, Fotiadis P, Martinez-Ramirez S, et al. Structural network alterations and neurological dysfunction in cerebral amyloid angiopathy. *Brain* 2015; 138: 179–188.
21. Tuladhar AM, van Dijk E, Zwiers MP, et al. Structural network connectivity and cognition in cerebral small vessel disease. *Hum Brain Mapp* 2016; 37: 300–310.
22. Jokinen H, Schmidt R, Ropele S, et al. Diffusion changes predict cognitive and functional outcome: The LADIS study. *Ann Neurol* 2013; 73: 576–583.
23. Tuladhar AM, Van Uden IWM, Rutten-Jacobs LCA, et al. Structural network efficiency predicts conversion to dementia. *Neurology* 2016; 86: 1112–1119.
24. Dewenter A, Gesierich B, ter Telgte A, et al. Systematic validation of structural brain networks in cerebral small vessel disease. *Journal of Cerebral Blood Flow & Metabolism* 2021; 42: 1020–1032.
25. De Luca A, Kuijf H, Exalto L, et al. Multimodal tract-based MRI metrics outperform whole brain markers in determining cognitive impact of small vessel disease-related brain injury. *Brain Struct Funct* 2022; 227: 2553–2567.
26. Caballero MÁA, Suárez-Calvet M, Duering M, et al. White matter diffusion alterations precede symptom onset in autosomal dominant Alzheimer's disease. *Brain* 2018; 141: 3065–3080.
27. Bendlin BB, Ries ML, Canu E, et al. White matter is altered with parental family history of Alzheimer's disease. *Alzheimer's & Dementia* 2010; 6: 394–403.
28. Barry DM, Stevenson W, Bober BG, et al. Expansion of Neurofilament Medium C Terminus Increases Axonal Diameter Independent of Increases in Conduction Velocity or Myelin Thickness. *The Journal of Neuroscience* 2012; 32: 6209 LP – 6219.
29. Rao M V, Campbell J, Yuan A, et al. The neurofilament middle molecular mass subunit carboxyl-terminal tail domains is essential for the radial growth and cytoskeletal architecture of axons but not for regulating neurofilament transport rate . *Journal of Cell Biology* 2003; 163: 1021–1031.
30. Meeker KL, Butt OH, Gordon BA, et al. Cerebrospinal fluid neurofilament light chain is a marker of aging and white matter damage. *Neurobiol Dis* 2022; 166: 105662.
31. Schultz SA, Strain JF, Adedokun A, et al. Serum neurofilament light chain levels are associated with white matter integrity in autosomal dominant Alzheimer's disease. *Neurobiol Dis*; 142. Epub ahead of print 2020. DOI: 10.1016/j.nbd.2020.104960.
32. Braak H, Braak E. Neuropathological stageing of Alzheimer-related changes. *Acta Neuropathol* 1991; 82: 239–259.
33. Thal DR, Rüb U, Orantes M, et al. Phases of Aβ-deposition in the human brain and its relevance for the development of AD. *Neurology* 2002; 58: 1791 LP – 1800.

34. Buckner RL, Sepulcre J, Talukdar T, et al. Cortical Hubs Revealed by Intrinsic Functional Connectivity: Mapping, Assessment of Stability, and Relation to Alzheimer's Disease. *The Journal of Neuroscience* 2009; 29: 1860 LP – 1873.

35. Seeley WW, Crawford RK, Zhou J, et al. Neurodegenerative Diseases Target Large-Scale Human Brain Networks. *Neuron* 2009; 62: 42–52.

36. Kantarci K, Murray ME, Schwarz CG, et al. White-matter integrity on DTI and the pathologic staging of Alzheimer's disease. *Neurobiol Aging* 2017; 56: 172–179.

37. Mito R, Raffelt D, Dhollander T, et al. Fibre-specific white matter reductions in Alzheimer's disease and mild cognitive impairment. *Brain* 2018; 141: 888–902.

38. Daianu M, Mezher A, Mendez MF, et al. Disrupted rich club network in behavioral variant frontotemporal dementia and early-onset Alzheimer's disease. *Hum Brain Mapp* 2016; 37: 868–883.

39. Daianu M, Jahanshad N, Nir TM, et al. Rich club analysis in the Alzheimer's disease connectome reveals a relatively undisturbed structural core network. *Hum Brain Mapp* 2015; 36: 3087–3103.

40. Sun Y, Bi Q, Wang X, et al. Prediction of Conversion From Amnestic Mild Cognitive Impairment to Alzheimer ' s Disease Based on the Brain Structural Connectome. *Front Neurol* 2019; 9: 1–15.

41. Lee WJ, Han CE, Aganj I, et al. Distinct Patterns of Rich Club Organization in Alzheimer's Disease and Subcortical Vascular Dementia: A White Matter Network Study. *Journal of Alzheimer's Disease* 2018; 63: 977–987.

42. Griffa A, Van den Heuvel MP. Rich-club neurocircuitry: function, evolution, and vulnerability. *Dialogues Clin Neurosci* 2018; 20: 121–132.

43. Power MC, Su D, Wu A, et al. Association of white matter microstructural integrity with cognition and dementia. *Neurobiol Aging* 2019; 83: 63–72.

44. Reijmer YD, Leemans A, Caeyenberghs K, et al. Disruption of cerebral networks and cognitive impairment in Alzheimer disease. *Neurology* 2013; 80: 1370–1377.

45. Kantarci K, Schwarz CG, Reid RI, et al. White matter integrity determined with diffusion tensor imaging in older adults without dementia: Influence of amyloid load and neurodegeneration. *JAMA Neurol* 2014; 71: 1547–1554.

46. Ukmar M, Makuc E, Onor ML, et al. Evaluation of white matter damage in patients with Alzheimer's disease and in patients with mild cognitive impairment by using diffusion tensor imaging. *Radiol Med* 2008; 113: 915–922.

47. Hanseeuw BJ, Betensky RA, Jacobs HIL, et al. Association of Amyloid and Tau With Cognition in Preclinical Alzheimer Disease: A Longitudinal Study. *JAMA Neurol* 2019; 76: 915–924.

48. Jack CR, Knopman DS, Jagust WJ, et al. Hypothetical model of dynamic biomarkers of the Alzheimer's pathological cascade. *Lancet Neurol* 2010; 9: 119–128.

49. Maillard P, Lu H, Arfanakis K, et al. Instrumental validation of free water, peak-width of skeletonized mean diffusivity, and white matter hyperintensities: MarkVCID neuroimaging kits. *Alzheimer's & Dementia: Diagnosis, Assessment & Disease Monitoring* 2022; 14: e12261.

50. Lu H, Kashani AH, Arfanakis K, et al. MarkVCID cerebral small vessel consortium: II. Neuroimaging protocols. *Alzheimer's & Dementia* 2021; 17: 716–725.

51. de Brito Robalo BM, Biessels GJ, Chen C, et al. Diffusion MRI harmonization enables joint-analysis of multicentre data of patients with cerebral small vessel disease. *Neuroimage Clin* 2021; 32: 102886.
52. de Brito Robalo BM, de Luca A, Chen C, et al. Improved sensitivity and precision in multicentre diffusion MRI network analysis using thresholding and harmonization. *Neuroimage Clin* 2022; 36: 103217.
53. Teunissen CE, Verberk IMW, Thijssen EH, et al. Blood-based biomarkers for Alzheimer's disease: towards clinical implementation. *Lancet Neurol* 2022; 21: 66–77.
54. Duering M, Konieczny MJ, Tiedt S, et al. Serum Neurofilament Light Chain Levels Are Related to Small Vessel Disease Burden. *J Stroke* 2018; 20: 228–238.
55. Torso M, Bozzali M, Zamboni G, et al. Detection of Alzheimer's Disease using cortical diffusion tensor imaging. *Hum Brain Mapp* 2021; 42: 967–977.
56. Weston PSJ, Poole T, Nicholas JM, et al. Measuring cortical mean diffusivity to assess early microstructural cortical change in presymptomatic familial Alzheimer's disease. *Alzheimers Res Ther* 2020; 12: 112.

APPENDICES

A

Nederlandse samenvatting
About the author
List of publications
Dankwoord

NEDERLANDSE SAMENVATTING

De ziekte van Alzheimer (AD) en small vessel disease (SVD) zijn de meest voorkomende oorzaken van problemen in het denken (cognitie) en dementie bij ouderen. Zowel AD als SVD zorgen voor een cascade aan ziekteprocessen die uiteindelijk leiden tot hersenschade en problemen in het functioneren. Om deze ziekteprocessen beter te begrijpen is er voor beide ziekten een grote behoefte aan gevoelige markers van hersenschade. Toen ik begon aan mijn onderzoek in 2017 waren er aanwijzingen dat maten van witte stof integriteit – afgeleid van diffusie MRI – interessant zouden kunnen zijn als schade marker.

In SVD is er altijd veel aandacht geweest voor schade aan de witte stof, omdat de schade zich voornamelijk hier bevindt. Echter, kunnen de standaard SVD maten voor schade slechts een deel van de schade vangen en zijn ze zwak gerelateerd met cognitie. Aan het begin van mijn onderzoek waren er al aanwijzingen dat diffusie MRI gevoeliger zou zijn voor de totale schade dan de standaard SVD maten en dat op diffusie MRI gebaseerde maten sterker samenhangen met cognitie. In AD is er over het algemeen weinig aandacht voor de witte stof. De focus ligt met name op de primair aangedane grijze stof. Echter waren er wel degelijk aanwijzingen dat ook de witte stof integriteit is aangedaan in AD.

Voor beide ziekten waren er meerdere open vragen met betrekking tot diffusie MRI als marker zoals: 1) zijn de veranderingen in het diffusie signaal specifiek voor AD en/of SVD? 2) Leidt AD en/of SVD-pathologie tot bepaalde patronen in witte stof schade? 3) Welke diffusie veranderingen kunnen het best cognitieve problemen verklaren? In dit proefschrift heb ik ingezoomd op deze nog onbekende factoren van diffusie MRI in AD en SVD. Mijn overkoepelende doel was om de integriteit van de witte stof in AD en SVD te onderzoeken om daarmee hersenschade en cognitieve achteruitgang in beide ziekten beter te begrijpen.

Diffusie MRI als marker van witte stof schade in SVD en AD

Een van de vragen die ik heb beantwoord in mijn proefschrift is of het diffusie signaal onderscheid kan maken tussen AD en SVD-pathologie. Een uitdaging in het onderzoek naar AD en SVD is dat deze ziekten bij ouderen veelal samen voorkomen, zogenaamde “mixed disease”. Dit maakt het lastig te bepalen welke schade door welke ziekte wordt veroorzaakt. In hoofdstuk 2 hebben we daarom

gekeken naar de bijdrage van zowel AD als SVD aan veranderingen in het diffusie signaal in zes verschillende groepen patiënten. Hierbij hebben we gevonden dat de huidige diffusie technieken niet in staat zijn om onderscheid te maken tussen deze twee ziekten. Diffusie MRI kan ons op dit moment informeren over de staat van de witte stof en veranderingen in de integriteit, maar niet over de onderliggende oorzaken van deze veranderingen.

Verder laten zowel mijn bevindingen in hoofdstuk 2, 3, 5, 6 en 7 als de recente literatuur consistent zien dat diffusie maten in SVD: 1) zeer gevoelig zijn voor SVD-gerelateerde witte stof schade 2) schade kunnen detecteren buiten de zichtbare laesies en 3) al zijn aangedaan in een vroeg stadium van de ziekte. Diffusie maten in AD zijn: 1) aangedaan in een vroeg stadium van de ziekte 2) over het algemeen slechts zwak gerelateerd aan andere schade- en ziekte markers van AD en 3) ook slechts zwak gerelateerd aan cognitie. Naar mijn mening zijn er daarom maten die beter passen om iets te zeggen over AD-gerelateerde schade en die maten zijn daarnaast ook nog specifieker voor AD.

Vinden van spatiele patronen van de ziekte

Het onderzoeken van spatiele patronen van schade is naar mijn mening belangrijk omdat het ervoor kan zorgen dat we beter begrijpen welke onderliggende ziekte mechanismen er een rol spelen. Daarnaast zouden we door middel van een schade patroon de ziekte sneller kunnen identificeren. Aan het begin van mijn onderzoek was echter niet bekend of er specifieke patronen van schade aan de witte stof waren in AD en/of SVD en wisten we ook niet hoe deze patronen er dan uit zou zien.

Voor SVD hebben we zowel op voxel niveau (een 3D pixel), het niveau van de witte stof banen en op het niveau van het structurele hersennetwerk gekeken naar eventuele patronen van schade. Daarbij hebben we gevonden dat de kleinste vaatjes door de gehele witte stof zijn aangedaan. SVD heeft dus een wijdverspreid effect heeft op de witte stof. Er is lokale schade, zoals te zien aan de variatie in het diffusie signaal door de witte stof heen (hoofdstuk 3) en aan dat verschillende witte stof banen verschillend zijn aangedaan. Echter, wanneer we uitzoomen zijn er geen specifieke subnetwerken aangedaan (hoofdstuk 6 en 7) en lijkt er geen duidelijk patroon van witte stof schade te zijn.

Voor AD werd mijn aandacht getrokken door de hypothese dat witte stof banen naast het overbrengen van informatie via neuronen ook als een soort pijpleiding zouden fungeren voor de verspreiding van ziekte. Deze hypothese hebben we onderzocht in hoofdstuk 4. We hebben geen bewijs kunnen vinden voor zo'n rol voor de structurele witte stof banen.

Daarnaast heb ik de hypothese onderzocht dat hersengebieden die een hoger-dan-gemiddeld aantal gebieden met elkaar verbinden, zogenaamde hubs, belangrijk zouden zijn voor het functioneren van het gehele netwerk. Deze hubs zouden tegelijkertijd ook kwetsbaarder zijn voor ziekteprocessen dan andere delen van het netwerk. In hoofdstuk 7 hebben we de impact van zowel AD als SVD op hub verbindingen onderzocht maar geen bewijs kunnen vinden voor een verhoogde kwetsbaarheid. Ook andere studies waren niet in staat om zo'n effect overtuigend te kunnen laten zien.

Verklaren van de functionele uitkomst

In 2017 werd de samenhang tussen SVD en cognitie slecht begrepen. Dit kwam mede doordat de zichtbare laesies slechts een zwakke relatie laten zien met cognitie. Er was daarom behoefte aan markers die cognitieve problemen beter kunnen verklaren. Destijds waren er al sterke aanwijzingen dat diffusie maten van witte stof integriteit gevoelig zouden zijn voor cognitie. In hoofdstuk 5 en 6 van dit proefschrift hebben we bijgedragen aan het -ondertussen - overtuigende bewijs dat in SVD diffusie maten consistent en sterk samenhangen met cognitie en hierbij tevens andere markers overtreffen. Ook hebben we in hoofdstuk 6 laten zien dat diffusie maten relateren aan cognitieve achteruitgang, dit is in lijn met andere literatuur waarin diffusie markers veelbelovend lijken als prognostische markers.

Hoewel ik cognitie in AD niet in detail heb bekeken in dit proefschrift, zijn er andere studies die een relatie laten zien tussen diffusie maten en cognitie. Deze relaties zijn echter vaak gevonden in groepen patiënten die leiden aan "mixed disease" en dit maakt het lastig te om de resultaten te interpreteren. In hoofdstuk 2 hebben we laten zien dat de aanwezigheid van SVD, ook in geringe mate, ervoor zorgt dat er een associatie is met diffusie maten. Hierdoor zou het zo kunnen zijn dat de gevonden associaties tussen diffusie maten en cognitieve problemen in patiëntengroepen met "mixed disease", eigenlijk meer zeggen over SVD-gerelateerde cognitieve problemen dan AD-gerelateerde cognitieve problemen.

Klinische implicaties en toekomstperspectieven

Er was een grote behoefte aan een marker die de effecten van AD en SVD-pathologie uit elkaar kon halen, mede zodat we beter zouden begrijpen wat er onderliggend is aan de diffusie veranderingen. Zoals gezien in hoofdstuk 2 is dit met de huidige diffusie modellen niet mogelijk. Hoewel er nog steeds behoefte is aan het beter begrijpen van de onderliggende ziekteprocessen is er naar mijn mening op dit moment minder behoefte aan een indirecte marker zoals diffusie MRI. Dit vanwege de sinds kort beschikbare bloedmarkers. Deze bloedmarkers zijn in staat om ziekteprocessen in AD veel makkelijker vast te stellen. Ze zijn in tegenstelling tot MRI, goedkoop, minimaal invasief, toegankelijk voor de klinische praktijk en hebben een hoge acceptatiegraad bij patiënten. Ook voor SVD zijn er markers in het bloed die mogelijk interessant zijn, hier is echter nog meer onderzoek voor nodig.

Wanneer we kijken naar de waarde voor diffusie MRI in diagnostiek zijn er naar mijn mening opties die logischer zijn dan diffusie maten voor beide ziekten. In het geval van AD diagnostiek zijn dit bijvoorbeeld PET, CSF of bloed markers en in het geval van SVD volstaat een standaard MRI-scan.

In SVD zie ik wel een rol voor diffusie maten om ziekte ernst vast te stellen. Echter, voordat dit geïmplementeerd kan worden in de klinische praktijk moet er op verschillende gebieden nog werk worden verzet. Er zouden bijvoorbeeld normatieve scores ontwikkeld moeten worden, de prognostische en diagnostische waarde zal moeten worden vastgesteld in individuele patiënten, het verwerken van de MRI-beelden zou idealiter moeten worden geautomatiseerd maar in ieder geval versimpeld en data van meerdere centra zou makkelijk moeten kunnen worden samengevoegd.

In AD zie ik alleen in een onderzoek setting waarde voor diffusie MRI, met name voor corticale diffusie. Corticale diffusie detecteert veranderingen in de staat van de grijze stof, het primair aangedane gebied in AD. Het zou daarmee vroeg kunnen informeren over neurodegeneratie.

Conclusies

Voor SVD zijn diffusie maten sterke markers die in staat zijn om relevante informatie voor de ziekte te vangen. Wanneer er wordt gewerkt aan bijvoorbeeld normscores en het versimpelen van de verwerking zijn ze veelbelovend voor implementatie in klinische trials en mogelijk zelfs de klinische praktijk.

Voor AD zijn er alternatieve markers die beter informeren over relevante aspecten van de ziekte en schade en daarbij ook specifieker zijn voor AD dan diffusie maten. Daarom zie ik weinig potentie voor deze maten in AD in een klinische setting.

Voor de toekomst kijk ik uit naar het oplossen van de technische uitdagingen en de kansen die dit zal brengen voor een bredere toepassing van diffusie maten, ook in de klinische praktijk.

ABOUT THE AUTHOR

Naomi Vlegels was born on July 19 1993 in Haarlem, the Netherlands. She had a great enthusiasm for learning from a young age and obtained her high school degree in 2010. She first started a study in Marketing, soon realized that this was not her place and started her Bachelor in Psychology at Leiden University in 2012. During the bachelor Psychology, her interest in research and more specifically brain-related research started to grow. She was selected for the Honours Program, which gave her the opportunity to finish her bachelor with an extended research-project that further sparked her interests in pursuing an academic career. After obtaining her bachelor degree she started a Research Master in Neuroscience and Cognition at Utrecht University. Her interest in brain diseases led her to a research internship at the Neurology department of the University Medical Center Utrecht where she studied the disruption of the white matter in patients with small vessel disease. This was followed by a second internship focusing on the utility of a novel biomarker in patients with small vessel disease at the Institute of Stroke and Dementia Research in Munich.

Soon after obtaining her master degree in 2017 she started her PhD research on white matter integrity in patients with small vessel disease and Alzheimer's disease under supervision of Prof. Dr. Geert Jan Biessels and Dr. Yael Reijmer. A large part of her PhD consisted of collaborative projects, with one especially large one with partners in Munich. At the end of her PhD, she received an out-of-the-box young talent grant from the Heart-Brain Consortium which allowed her to investigate white matter structural integrity in patients with hereditary cerebral amyloing angiophaty at the Leiden University Medical Center under supervision of Prof. dr. Marieke Wermer and Prof. dr. Thijs van Osch.

Currently, she is working as a postdoc at the Insitute of Stroke and Dementia Research in Munich in the group of Dr. Steffen Tiedt where she works on the circulating metabolome after stroke. She lives together with her partner Bram and daughter Nora in Noordwijk and in her free time she enjoys walks on the beach, reading and making puzzles.

LIST OF PUBLICATIONS

In this thesis

Vlegels N, Ossenkoppele R, van der Flier W, Koek HL, Reijmer YD, Wisse LEM, Biessels GJ. Does loss of integrity of the Cingulum bundle link Amyloid Beta accumulation and neurodegeneration in Alzheimer's Disease? Journal of Alzheimer's disease. 2022. DOI: 10.3233/JAD-220024

Vlegels N*, Finsterwalder S*, Gesierich B, et al. Small vessel disease more than Alzheimer's disease determines diffusion MRI alterations in memory clinic patients. Alzheimer's Dement. 2020;16:1504–1514. DOI: 10.1002/alz.12150. * authors contributed equally to this work

Vlegels N*, Heinen R*, de Bresser J, Leemans A, Biessels GJ, Reijmer YD. The cumulative effect of small vessel disease lesions is reflected in structural brain networks of memory clinic patients. NeuroImage: Clinical 2018;19:963-969. * authors contributed equally to this work

Not in this thesis

de Brito Robalo BM, **Vlegels N**, Meier J, Leemans A, Biessels GJ, Reijmer YD. Effect of fixed-density thresholding on structural brain networks: a demonstration in small vessel disease. Brain Connectivity 2020. DOI: 10.1089/brain.2019.0686.

de Brito Robalo BM, **Vlegels N**, Leemans A, Reijmer YD, Biessels GJ. Impact of thresholding on the consistency and sensitivity of diffusion MRI-based brain networks in patients with cerebral small vessel disease. Brain Behav. 2022. DOI: 10.1002/brb3.2523

Conference abstracts

Vlegels N*, van den Brink H*, Kopczak A, Arts T, Siero J, Gesierich B, de Luca A, Duering M, Zwanenburg J, Dichgans M, Biessels G.J. on behalf of the SVDs@target group. The relation between small vessel reactivity and white matter integrity in CADASIL – The ZOOM@SVDs study. * authors contributed equally to this work *Poster presentation at European Stroke Organisation Conference, Lyon, 2021*

Vlegels N, de Brito Robalo BM, Koek HL, Biessels GJ, Reijmer YD. Cognitive declinein small vessel disease and neurodegeneration: a specific role for critical white matter connections? *Oral presentation at the ESO-WSO Joint Virtual meeting, 2020*

Vlegels N*, Finsterwalder S*, Gesierich B, et al. Small vessel disease more than Alzheimer's disease determines diffusion MRI alterations in memory clinic patients. Alzheimer's Dement. 2020;16:1504–1514. DOI: 10.1002/alz.12150. * authors contributed equally to this work *Poster presentation at the ESO-WSO Joint Virtual meeting, 2020*

Vlegels N, de Brito Robalo BM, Koek HL, Biessels GJ, Reijmer YD. Brain network disruption and cognitive decline: specific role for critical white matter connections? *Poster presentation at the annual meeting of the Organization for Human Brain Mapping, Rome, 2019*

Vlegels N*, Heinen R*, de Bresser J, Leemans A, Biessels GJ, Reijmer YD. The cumulative effect of small vessel disease lesions is reflected in structural brain networks of memory clinic patients.* authors contributed equally to this work *Poster presentation at VASCOG, Hong Kong, 2018*

Vlegels N, Heinen R, Kuijf HJ, de Bresser J, Reijmer YD, Biessels GJ. Automated cortical parcellation of the brain using FreeSurfer in patients with vascular cognitive impairment: challenges, tips and tricks. *Poster presentation at VASCOG, Amsterdam, 2016*

DANKWOORD

Promoveren doe je niet alleen. Tijdens mijn promotie heb ik samen mogen werken met een grote groep inspirerende collega's en coauteurs zonder wie dit proefschrift niet tot stand had kunnen komen. Daarnaast heb ik het grote geluk omringd te zijn door veel lieve vrienden en familie die de afgelopen jaren klaar stonden met een luisterend oor maar er vooral voor zorgen dat mijn leven ontzettend leuk is.

Ik wil daarom eenieder die betrokken is geweest bij dit proefschrift in de afgelopen jaren hartelijk bedanken. Graag richt ik mij in het bijzonder tot een aantal mensen.

Allereerst, beste **Geert Jan**, alweer 6,5 jaar geleden begon ik als master student bij jou in de groep. Wat ben ik blij dat ik destijds mijn eerste echte stapjes in het onderzoek onder jouw begeleiding mocht nemen. Jouw bevlogenheid in het onderzoek en de grote waarde die je hecht aan wetenschappelijke integriteit heb ik altijd gewaardeerd. Je scherpe analytische blik heeft mij gedurende de jaren wel eens het gevoel gegeven dat ik gedrild werd tot onderzoeker, omdat niks aan jouw aandacht ontsnapt. Hoewel dit in het moment wel eens frustrerend was, kan ik er achteraf alleen maar dankbaar voor zijn omdat het mij heeft gevormd tot de onderzoeker die ik nu ben.

Beste **Yael,** wat heb ik ontzettend veel van jou mogen leren. Uiteraard van jouw expertise op het gebied van diffusie MRI en netwerken, maar ook zeker als beginnend onderzoeker. Ik kon altijd op een laagdrempelige manier nog wat extra vragen te stellen en jouw deur stond altijd open om nog verder te brainstormen over dat ene resultaat of onderzoeksidee. Het was een plezier om met je te werken! Je bent voor mij een voorbeeld van wie ik zelf als onderzoeker wil zijn.

Dear **Marco**, my internship within your group really taught me about the methodological side of neuroimaging. I'm grateful for the opportunity to work together in the free water project, that I'm very proud of. Thank you for sharing all your expertise and your always quick responses to my e-mails. Dear **Sofia**, I don't think I could have had a better partner for our collaborative project. At one point I think we had daily phone calls and e-mail conversations, but I'm very proud of the end result. I hope we can meet up for coffee in Munich soon! Daarnaast wil ik graag **dr. Rik Ossenkoppele, dr. Laura Wisse** en **prof. dr. Wiesje van de Flier** bedanken voor hun samenwerking. I also cannot forget to thank the people of the **DIAN consortium, DELCODE** and **ADNI** for their valuable contributions to my projects.

In de laatste maanden van mijn promotie kreeg ik de kans om onderzoek te doen in het LUMC, graag wil ik de groep daar bedanken voor hun gastvrije welkom en leuke tijd! In het bijzonder wil ik **Prof. dr. Marieke Wermer, Prof. dr. Thijs van Osch en dr. Marianne van Walderveen** bedanken voor alles wat ik geleerd heb over CAA in deze periode en jullie geduld met die voor jullie toch wat vreemde diffusie MRI. **Manon en Ingeborg**, jullie wil ik in het bijzonder bedanken voor de plezierige samenwerking in onze projecten. Ik hoop dat we elkaar snel nog eens tegenkomen op een congres of in het LUMC!

Lieve VCI-groep, van de kamer op C3-oost, naar de bibliotheek in het W-gebouw en daarna verspreid over het UMC, gezellig was het altijd! Lunches, koffie, borrels, groepsuitjes en congressen waren altijd een feestje! **Rutger**, bedankt voor de begeleiding tijdens mijn eerste stappen in de wereld van het onderzoek in VCI, diffusie en netwerken! **Hugo,** in het begin trakteerde ik je op goede koffie zodat ik weer eens om een gunst kon vragen. Later vond ik het vooral gewoon heel erg gezellig! De Hong Kong trip, vooral ook de tour met Sunny en de hike naar Lantau peak zijn mede dankzij jou absolute hoogtepunten van mijn promotie. **Alberto** your expertise in diffusion MRI has been of great value for my research! It often felt as a real luxury to have both you and Bruno as a technical support team. But besides all of your technical knowledge, you are also an awesome guy and I have enjoyed working together.

Lieve **Angela,** de moeder gans van de VCI-groep! Altijd was jij daar om even mee te denken als ik een afspraak nodig had, als er weer eens administratieve problemen waren of gewoon voor een luisterend oor. Zonder jou was het allemaal niet gelukt.

Willem, Jurre, Matthijs, Laurien, Doeschka, Lieza, Sanne, Hugo A., Floor, Naomi S., Mirthe, Malin, Manja en Yoni, ontzettend bedankt voor het mede creëren van een heel leuke omgeving om mijn onderzoek in te kunnen doen. **Ioana Maria** and **Minou**, thank you for your work during your internships which have been valuable contributions to my thesis.

Lieve frietjes, wat ben ik dankbaar dat ik samen met jullie mocht promoveren! Binnen 6 maanden van elkaar starten met je promotie schept een band en ik vind het enorm bijzonder dat we zowel de diepte- als de hoogtepunten van elkaars onderzoek met elkaar konden delen. **Nick**, beide hadden we te maken met grote imaging datasets die niet altijd deden wat wij wilden en het was fijn om iemand te hebben die begreep wat de struggles daarmee waren. Jouw droge humor en

foute woordgrapjes gaven altijd lucht aan de situatie en meer dan eens bleek je een oplossing te hebben voor een probleem waar ik tijdens de lunch over klaagde. **Bruno**, my network buddy from day 1! We started our adventure together and I think we formed a great team. Coming from different backgrounds really was such a plus, I thoroughly enjoyed our brainstorms, but most of all the fun we had! A cola and kinderbueno to beat the afternoon dip will always remind me of the W-building days. **Chloë**, voor een koffie en een luisterend oor kon ik echt altijd bij jou terecht. Na samen even flink geklaagd te hebben, wist je ook snel weer de humor erin te brengen en dat heb ik altijd onwijs gewaardeerd. We blijken een voorkeur te delen voor slechte filmpjes en ondertussen begin ik al met lachen als ik zie dat je me ergens in getagd hebt. **Hilde,** van master buddy's naar een dierbare vriendin. Aan een blik hebben we vaak genoeg en samen hebben we echt alle hoogte- en dieptepunten met elkaar gedeeld in onze promoties maar ondertussen ook in ons persoonlijke leven. Ondertussen zit de Atlantische oceaan ertussen en zijn we allebei begonnen met ons volgende avontuur in de wetenschap maar ik ben ontzettend blij dat dit aan onze band niks veranderd heeft.

Lieve **vrienden en vriendinnen**, wat een enorme rijkdom is het om zo'n vriendengroep te hebben! Onze jaarlijkse weekenden weg en het bijna traditionele bezoek aan de Vrienden van Amstel Live zijn mij ontzettend dierbaar. Lieve meiden, **Anoek, Annet, Bibi, Elise, Lisa, Lisanne en Nienke,** wat ben ik blij met jullie! In de afgelopen 13 jaar hebben we aardig wat lief en leed met elkaar gedeeld en zijn we van wekelijkse stapavondjes gegaan naar bruiloften en baby's. Maar gelukkig kunnen we nog steeds enorm met elkaar lachen. Hoe bijzonder is het dat ook de mannen het zo goed met elkaar kunnen vinden en dat onze kleine vriendjes (al praktisch een elftal ondertussen!?) nu met elkaar opgroeien.

Lieve **Sascha**, in 2012 kwamen wij elkaar tegen op de eerste dag van de opleiding Psychologie en sindsdien heb ik er een dierbare vriendin bij. Ik ben ontzettend blij dat we onze vriendschap na de studie hebben doorgezet met vele koffie, lunch en wandeldates. Ik vind het fijn dat zelfs wanneer wij elkaar door soms nogal tegenstrijdige agenda's niet zo vaak zien, we altijd goede gesprekken kunnen hebben. En, gelukkig daarnaast ook heel veel kunnen lachen.

Lieve **Jan en Co**, er zijn denk ik weinig mensen zó gastvrij als jullie. Vanaf het moment dat ik voor het eerst bij jullie thuiskwam, toen nog als vriendin van Bibi,

heb ik mij altijd thuis gevoeld. Het is daarom misschien ook geen toeval dat juist die gastvrijheid ervoor zorgde dat de vonk tussen Bram en mij bij jullie thuis oversloeg. Hoewel mijn promotie voor jullie denk ik een ver-van-mijn-bed-show was, waren en zijn jullie altijd geïnteresseerd en meelevend over wat ik allemaal deed, en dit waardeer ik echt enorm!

Lieve **Bibi en Rob**, het is denk ik geen geheim dat ik ontzettend blij ben met jullie als schoonzus en zwager. Hoe fijn is het wanneer je zo'n fijne band hebt met je schoonfamilie, iets dat zeker niet vanzelfsprekend is! Jullie geluk wordt binnenkort bekroond met kleine Gerrit, ik kan nu al niet wachten! Lieve **Bieb**, niet alleen de beste schoonzus maar ook de beste vriendin. Every brownie needs a blondie en wat ben ik blij dat jij altijd voor mij klaar staat! Jij kent mij echt door en door en ik kan voor zowel de leuke- als minder leuke dingen altijd op jou bouwen. Gelukkig winnen de leuke momenten het en hebben we vooral de slappe lach samen. Hoe bijzonder is het dat we ook de volgende stap: het moederschap, samen gaan beleven.

Lieve **Maickel,** hoewel we elkaar vroeger achter het behang konden plakken ben ik heel blij dat jij mijn broertje bent. Jij vindt mij een oppernerd en plaagt me daar ook graag mee maar voor mij was dat altijd een goede reminder dat er echt belangrijkere dingen zijn in het leven dan werk. Ik weet dat je er zelf moe van wordt, maar ik zou graag een fractie van jou relaxte "komt wel goed" houding willen hebben. Dat zou mij een hoop stress schelen.

Lieve **Sas**, het voelt ondertussen alsof jij altijd al in mijn leven bent geweest, zo belangrijk ben jij voor mij. Ik denk dat dat mede komt doordat wij stiekem toch op elkaar lijken en dat had ik misschien wel een beetje nodig binnen ons gezin. Altijd heb ik mij door jou enorm gesteund gevoeld in mijn academische ambities, zelfs al begrepen jij en mama weinig meer van de inhoud.

Lieve **mama**, Ik weet dat je af en toe gedacht hebt: "kind, wat doe je jezelf allemaal aan" maar altijd steunde je mij in mijn ambities en was je mijn grootste supporter. Ik ben enorm dankbaar dat ik jouw dochter mag zijn. Dankzij de kracht die jij hebt getoond na het overlijden van papa, ben ik wie ik nu ben. Lieve **papa**, ik kan alleen maar hopen dat je van boven mee kijkt en trots bent op wie ik geworden ben.

Lieve **Micah**, alweer 6 jaar mag ik onderdeel uitmaken van jouw leven. Zonder dat je het doorhad was jij een goede afleiding van werk. Je bent een fantastische jongen met een enorm groot hart en ik kijk er naar uit om te zien wat je allemaal gaat doen in je leven.

Liefste **Bram**, precies 1 maand voordat ik begon met mijn promotie kregen wij een relatie en ik denk dat je geen idee had wat dat nou eigenlijk inhield. Dat jij in een totaal andere wereld zit qua werk helpt mij met relativeren van wat er nou echt belangrijk is. Ik ben enorm blij dat ik jou ondertussen al 6 jaar naast mij mag hebben. Samen vormen we een enorm goed team, al zeg ik het zelf, en ik kijk er heel erg naar uit om de rest van ons leven samen te delen. Samen met jou is alles leuker.

Lieve **Nora**, jij bent mijn allergrootste geluk. Ik kan niet wachten om je te zien opgroeien en hoop dat ik jou met deze promotie kan laten zien dat hard werken je een heel eind brengt. De wereld ligt aan jouw voeten.